
Electronic Thesis and Dissertation Repository

7-21-2023 2:00 PM

Functionalizing conjugative systems to deliver CRISPR nucleases for targeted bacterial killing

Thomas A. Hamilton, *The University of Western Ontario*

Supervisor: Edgell, David R., *The University of Western Ontario*

Co-Supervisor: Gloor, Gregory B., *The University of Western Ontario*

A thesis submitted in partial fulfillment of the requirements for the Doctor of Philosophy degree in Biochemistry

© Thomas A. Hamilton 2023

Follow this and additional works at: <https://ir.lib.uwo.ca/etd>

 Part of the [Biochemistry Commons](#), and the [Molecular Biology Commons](#)

Recommended Citation

Hamilton, Thomas A., "Functionalizing conjugative systems to deliver CRISPR nucleases for targeted bacterial killing" (2023). *Electronic Thesis and Dissertation Repository*. 9423.
<https://ir.lib.uwo.ca/etd/9423>

This Dissertation/Thesis is brought to you for free and open access by Scholarship@Western. It has been accepted for inclusion in Electronic Thesis and Dissertation Repository by an authorized administrator of Scholarship@Western. For more information, please contact wlsadmin@uwo.ca.

Abstract

The interactions between humans and microbes are intimately important to human health, with both commensal and pathogenic bacteria affecting homeostasis and disease. Increasing concern over antibiotic resistance in bacterial pathogens represents a significant threat to human health, and use of traditional antibiotics to treat infections can be detrimental to commensal bacteria as well as pathogens, demonstrating a need for more specific antibacterial reagents. RNA-guided CRISPR nucleases, which can target and cleave genomes of interest, are a potential tool for specific bacterial targeting. A key limitation to the use of CRISPR antimicrobials is effective and robust delivery to the target bacteria. My thesis addresses this key issue by functionalizing conjugative systems to deliver a CRISPR nuclease for bacterial killing. First, a plasmid containing an arabinose-inducible *TevCas9* nuclease that is mobilizable *in-trans* by an RK2-based conjugative system was constructed. Inclusion of the RK2-based conjugative system *in-cis* on the same plasmid was shown to greatly increase the conjugation frequency over time. Furthermore, when conjugating in liquid we observed that providing glass beads to increase surface area for biofilm development and cell-cell contact significantly improved conjugation frequency. Crucially, conjugated *TevCas9* was able to kill *Salmonella enterica* with up to 99% efficiency, depending on the sgRNA provided. Next, to explore the importance of conjugative systems for delivery, a database containing thousands of conjugative systems identified from gut metagenomic data was constructed. From this database, a conjugative system of 54 kb native to the *Citrobacter* genus was constructed *de novo*. This conjugative plasmid, p20298-15a, showed 30-fold increased conjugation frequency to *Citrobacter rodentium* than to *Escherichia coli*, and was capable of conjugation to several additional *Citrobacter* strains. The p20298-15a plasmid was then functionalized to clone the arabinose-inducible CRISPR-*TevCas9* system, which was able to target and kill *C. rodentium*. Importantly, the construction and engineering of p20298 shows that large genetic systems found in metagenomic data sets can be synthesized and functionalized. Overall, this thesis demonstrates the effective use of conjugative systems as a delivery mechanism for CRISPR-based antimicrobials for the targeted killing of bacteria.

Keywords: Bacterial conjugation, CRISPR, *TevCas9*, microbiome, synthetic biology, functional metagenomics

Lay Summary

Bacteria are present in ecosystems throughout the world and are intimately linked to human health. Many bacteria in the human body are beneficial and required for health, whereas other bacteria are pathogenic. To conventionally treat infections of pathogenic bacteria, patients are typically given antibiotics, however, a growing concern in medicine is the rise of antibiotic resistant bacteria. Furthermore, these same antibiotics can have a detrimental impact on healthy, commensal bacteria. To continue to treat pathogenic bacteria, novel methods of specific bacteria killing are required. To address this problem, this thesis utilizes two key technologies. The first is bacterial conjugation, which is a naturally occurring mechanism that bacteria use to share genetic information. The second is CRISPR (clustered regularly interspaced short palindromic repeats) technology, which allows for the targeting of genomes at specific DNA sequences. Importantly, CRISPR nucleases are proteins that are guided towards the bacterial genome and cleave the DNA leading to cell death.

First a plasmid was constructed that contained a CRISPR nuclease that could specifically target bacterial DNA for cleavage. This plasmid was capable of being mobilized from a donor bacterial strain to a recipient bacterial strain. Importantly, including the conjugative machinery on the same plasmid allowed for better spread to recipient bacteria. A variety of plasmids were then constructed to target *Salmonella enterica* and were capable of killing up to 99% of the recipient cells.

Next, new conjugative systems were identified computationally in a gut metagenomic data set. These data represent the cumulative microbial DNA that is found in the human gut, from which thousands of different conjugative systems were identified. I proceeded to construct one of these conjugative systems synthetically to target a bacterium that the system was native to and showed that it could be transferred between bacteria. The CRISPR nuclease was then added to the new functional plasmid, and it was delivered to kill bacteria from the genus the original conjugative system was identified from.

Overall, this thesis describes an approach for the delivery of CRISPR nucleases via bacterial conjugation to target and kill specific bacteria of interest.

Co-Authorship Statement

For the published work presented in Chapter 2 and the unpublished work presented in Chapter 3, Thomas Hamilton performed the research with exceptions noted below. Thomas Hamilton, David Edgell and Gregory Gloor conceived and designed the experiments and analyzed the data. Thomas Hamilton, David Edgell, and Gregory Gloor wrote a majority of the manuscripts.

Chapter 2: Bogumil Karas helped conceive the project. Jasmine Therrien helped assemble plasmids and test conjugative function. Gregory Pellegrino and Peter Bartlett helped design, clone and test sgRNAs targeting the *Salmonella enterica* genome. Dalton Ham helped test liquid conjugation conditions and cloned, tested and analyzed the data for the TevSaCas9 variant of the pNuc plasmid. David Edgell designed the off-target prediction model and modeled the sgRNA killing efficiencies.

Chapter 3: Bogumil Karas helped conceive the project. Tyler Browne and Benjamin Joris designed and implemented the model to identify and construct a database of conjugative systems in gut microbiome data. The full extent of these methodologies are included in Benjamin Joris's PhD thesis. Arina Shrestha constructed p20298-15a and p20298-15a-M and validated their function.

Dedication

This thesis is dedicated to my teachers, mentors, friends, and family, who through their continual support made it possible to reach this point.

“Science, my lad, is made up of mistakes, but they are mistakes which it is useful to make, because they lead little by little to the truth.” - Jules Verne, Journey to the Center of the Earth

Acknowledgments

The completion of this thesis would have not been possible without the involvement and support of many individuals. First and foremost, I must thank Dr. David Edgell, who through his supervision taught me how to approach science, think critically, and to never forget anything. The environment of your lab enabled me to be creative in my science and continually learn throughout my time here. I also must thank my advisory committee members Dr. Greg Gloor and Dr. Bogumil Karas, who provided ideas and encouragement, and challenged my thoughts to make me think about experiments and data in different ways.

Next I must thank all my past and current labmates. I suspect I learned more throughout the cumulative discussions in hallways and offices than from anywhere else. Thank you also to those who collaborated with me on my projects. Greg, Dalton, Jasmine, Ben, Tyler, and Arina were instrumental in completing the research shown in this thesis. This also wouldn't have been possible without Dan, Matt, Chris, Ryan, and Stephanie, whose friendship and support greatly improved my PhD experience both inside and outside of the lab.

Most importantly I need to thank my family. To my parents, your support and encouragement throughout this process made this possible. To Alysia, I can not imagine anyone else to have by my side during this process. You were my biggest support, and a big part of how I made it to this point. I am extremely grateful to have all of your encouragement.

Table of Contents

Abstract	ii
Lay Summary	iii
Co-Authorship Statement	iv
Dedication	v
Acknowledgments	vi
Table of Contents	vii
List of Figures	x
List of Tables	xvi
List of Appendices	xvii
List of Abbreviations, Symbols, and Nomenclaturexviii
1 Introduction	1
1.1 Human health and the microbiome	1
1.1.1 On the interface of humans and microbes	1
1.1.2 Bacterial pathogens and antimicrobial resistance	2
1.1.3 Microbiome dysbioses and human health	3
1.2 Metagenomics	4
1.2.1 Metagenomes and Metagenome-assembled genomes (MAGs)	4
1.2.2 Functionalizing biological systems from microbial communities	5
1.3 Bacterial conjugation	6
1.3.1 Methods of horizontal gene transfer in bacteria	6
1.3.2 Conjugation - a history	8
1.3.3 Biology of conjugative systems	8
1.3.4 Diversity and classification of conjugative systems	10
1.3.5 Applications of bacterial conjugative systems	12
1.4 Plasmids	14
1.4.1 What is a plasmid?	14
1.4.2 Plasmid replication	14

1.4.3	Plasmid genetics	15
1.5	CRISPR-based antimicrobials	16
1.5.1	Clustered regularly interspaced short palindromic repeats (CRISPR) systems	16
1.5.2	CRISPR-Cas9 - a programmable endonuclease	17
1.5.3	CRISPR as a sequence-specific antimicrobial	18
1.5.4	Alternative applications of CRISPR in bacteria	20
1.6	Scope of the thesis	21
1.7	References	24
2	Efficient inter-species conjugative transfer of a CRISPR nuclease for targeted bacterial killing	39
2.1	Introduction	39
2.2	Methods	42
2.2.1	Bacterial and yeast strains	42
2.2.2	Plasmid construction	42
2.2.3	Quantitative PCR	44
2.2.4	Filter mating conjugation	44
2.2.5	<i>S. enterica</i> to <i>S. enterica</i> conjugation	45
2.2.6	Liquid and bead-supplemented conjugation assays	45
2.2.7	Killing efficiency assays	46
2.2.8	Escape mutant analyses	46
2.2.9	sgRNA off-target predictions in <i>E. coli</i>	47
2.2.10	Modelling <i>S. enterica</i> killing efficiency	47
2.3	Results	49
2.3.1	Increased conjugation frequency with a <i>cis</i> -conjugative plasmid	49
2.3.2	Cell-to-cell contact significantly increases conjugation	53
2.3.3	<i>S. enterica</i> killing by conjugative delivery of Cas9 and sgRNAs	56
2.4	Discussion	67
2.5	References	69
3	Functionalizing conjugative systems from metagenomic data for targeted delivery of a CRISPR nuclease	74
3.1	Introduction	74
3.2	Methods and Materials	76
3.2.1	Bacterial and yeast strains	76
3.2.2	Identifying conjugative systems from gut metagenome data	76
3.2.3	Molecular cloning	77
3.2.4	sgRNA cloning	77
3.2.5	Bacterial conjugation assays	78
3.2.6	RNA-seq	78
3.2.7	Plasmid stability assays	79
3.2.8	<i>C. rodentium</i> killing assays	79
3.3	Results	80
3.3.1	Identifying conjugative systems from metagenomic data	80
3.3.2	Constructing a conjugative system <i>de novo</i>	84

3.3.3	Conjugation of p20298-15a	85
3.3.4	Conjugation in <i>trans</i> of a mobilizable plasmid containing the putative <i>oriT</i> from p20298	89
3.3.5	p20298-15a stability in <i>C. rodentium</i> transconjugants	89
3.3.6	RNA-seq of p20298-15a in <i>E. coli</i> Epi300 and <i>E. coli</i> to <i>C. rodentium</i> . . .	91
3.3.7	Functionalizing p20298 to kill <i>C. rodentium</i> with CRISPR-TevCas9	96
3.4	Discussion	98
3.5	References	101
4	Discussion	105
4.1	Manipulating bacteria with CRISPR nucleases	105
4.2	On the future of conjugative delivery to bacteria	106
4.3	Functionalizing metagenomic sequencing data	108
4.4	Techniques and challenges for the synthesis and construction of large plasmids . .	109
4.5	Conclusions	111
4.6	References	112
A	Supplemental Material for Chapter 2	115
B	Supplemental Material for Chapter 3	138
C	Copyright permission for Chapter 2 - no copyright permission required	147

List of Figures

1.1	Mechanisms of horizontal gene transfer in bacteria. a. Transformation. Bacteria take up DNA from the extracellular environment. b. Conjugation. DNA is transferred cell-to-cell using a type 4 secretion system. Conjugation can be initiated by either an integrative conjugative element or a conjugative plasmid. c. Transduction. Bacteriophage transduction can result in horizontal gene transfer when prophages excise themselves from the chromosome of a host. Assembled bacteriophage virions are then able to infect new hosts and integrate into their chromosome.	9
1.2	Mechanism of bacterial conjugation of plasmid DNA in bacteria. Conjugation is initiated by donor pilus attachment to a potential recipient cell. A DNA relaxase nicks a single strand of the plasmid at the <i>oriT</i> and becomes covalently bound to the strand (the T-strand). The relaxase-T-strand complex is coupled to the T4SS by a T4CP where it is transferred to the recipient cell. Once in the recipient, re-ligation and second strand synthesis of the plasmid occurs.	11
1.3	Targeted cleavage of DNA by TevCas9. TevCas9 is a dual endonuclease fusing the I-TevI nuclease and linker domains to <i>S. pyogenes</i> Cas9. TevCas9 can cleave at both the I-TevI and Cas9 cleavage sites facilitating a 33-35 bp deletion with non-compatible overhangs.	19
1.4	Process of constructing and functionalizing conjugative plasmids. The first component is identifying and constructing conjugative systems. The second component is functionalizing conjugative systems for applications, such as engineering plasmids to deliver CRISPR systems to target and kill bacteria.	23
2.1	Plasmid maps of pNuc- <i>cis</i> and pNuc- <i>trans</i>	50

2.2 Impact of *cis* or *trans* localization of conjugative machinery on conjugation frequency. **a.** Schematic view of the pNuc-*cis* and pNuc-*trans* plasmids. *oriT*, conjugative origin of transfer; *oriV*, vegetative plasmid origin; Gm^R, gentamicin resistance gene; Cm^R, chloramphenicol resistance gene; TevSpCas9/sgRNA, coding region for TevSpCas9 nuclease gene and sgRNA; Conjugative machinery, genes required for conjugation derived from the IncP RK2 conjugative system. **b.**(Top) The TevSpCas9 and sgRNA cassette (not to scale) highlighting the arabinose regulated pBAD and constitutive pTet promoters. (Below) The modular TevSpCas9 protein and DNA-binding site. Interactions of the functional TevSpCas9 domains with the corresponding region of substrate are indicated. **c.** Model of pNuc spread after conjugation with the *cis* and *trans* setups. Cell growth overtime will account for increase of pNuc-*trans*. **d.** Filter mating assays performed over 24 hr demonstrate that pNuc-*cis* has a higher conjugation frequency than pNuc-*trans*. Points represent independent experimental replicates, and the 95% confidence intervals are indicated as the shaded areas. Conjugation frequency is reported as the number of transconjugants (Gm^R, Kan^R) per total recipient *S. enterica* cells (Kan^R). **e.** Conjugation frequency of *S. enterica* transconjugants harbouring either pNuc-*cis* or pNuc-*trans* to naive *S. enterica* recipients. Data are shown as boxplots with points representing individual replicate experiments **f.** pNuc-*cis* and pNuc-*trans* copy number determined by quantitative PCR in either *E. coli* or *S. enterica*. Data are shown as boxplots with solid lines indicating the median of the data, the rectangle the interquartile bounds, and the whiskers the range of the data. Points are individual experiments. **g.** pNuc-*cis* and pNuc-*trans* stability in *E. coli* or *S. enterica* determined as the ratio of cells harbouring the plasmid after 24 hrs growth without antibiotic selection over total cells. 52

2.3 Optimizing liquid culture conditions for *E. coli* to *S. enterica* conjugation. **a.** Conjugation frequency for different sodium chloride (NaCl) media conditions. **b.** Conjugation frequency measured with different *E. coli* donor to *S. enterica* recipient ratios at the start of conjugation. **c.** Effect of culture agitation on conjugation frequency (RPM - revolutions per minute). For each plot, points indicate conjugation frequency for independent biological replicates. 54

2.4 Influence of enhanced cell-to-cell contact on conjugation frequency. **a.** Schematic of experimental design. Liquid conjugation experiments in culture tubes with **b.** pNuc-*cis* and **c.** pNuc-*trans* were performed with 0.5 mm glass beads or without glass beads over 72 hrs at the indicated shaking speed (in revolutions per minute). Conjugations were performed with (filled circles) or without (filled diamonds) sgRNA targeting the STM1005 locus cloned into pNuc-*cis* and pNuc-*trans*. Both plasmids encoded the TevSpCas9 nuclease. Data are plotted on a log10 as boxplots with data points from independent biological replicates. The solid line represents the median of data, the rectangle represents the interquartile range of the data, and the whiskers represent the maximum and minimum of the data. 55

2.5	Killing of <i>S. enterica</i> by conjugative delivery of TevSaCas9. a. Schematic of TevSaCas9 target site in the <i>fepB</i> gene of <i>S. enterica</i> , with the I-TevI cleavage motif, DNA spacer, sgRNA binding site and PAM motif indicated. b. Plot of <i>S. enterica</i> killing efficiency with no sgRNA cloned in pNuc, or the <i>fepB</i> sgRNA cloned in pNuc. Points are independent biological replicates.	57
2.6	Killing efficiency of multiplexed pairs of sgRNAs, with single sgRNAs plotted for comparison. Data are plotted on log10 scale as the mean of at least three independent biological replicates, with vertical lines representing the standard error of the mean. A Mann-Whitney Wilcoxon test comparing if multiplexed sgRNAs had a significantly higher killing efficiency as a group than their single sgRNA constituents yielded a p-value=0.003.	58
2.7	Examples of <i>S. enterica</i> escape mutants. a. Nucleotide sequence of the TevSpCas9 target site in the Gifsy prophage. Nucleotide substitutions in the seed region of the sgRNA are indicated and underlined. b. Example of an agarose gel of pNuc DNA isolated from EM30 or from wild-type pNuc (+ve) incubated with (+) or without (-) a mixture of FspI and MslII restriction enzymes. Size standards in kilobase pairs (kb) are indicated to the right of the gel image. c. Example of multiplex PCR with pNuc DNA isolated from EM19, EM20 or wild-type pNuc (+ve) with primers specific for the Cm ^R and TevSpCas9 coding regions.	59
2.8	Killing efficiency of sgRNAs targeted to the <i>S. enterica</i> genome. a. Ranked killing efficiency of individual sgRNAs coded as to whether the target site is found in an essential gene (blue filled circles), non-essential gene (orange diamonds), or unknown if the gene is essential (inverted red triangles). Vertical lines represent the standard error of the data from at least 3 biological replicates. b. Killing efficiency of each sgRNA plotted relative to their position in the <i>S. enterica</i> genomes, color-coded as in panel a . The terminator region (<i>ter</i>) and origin of replication (<i>ori</i>) are indicated by vertical red and green lines, respectively.	61
2.9	Summary of generalized linear model of sgRNA parameters that are indicative of killing efficiency with P-values indicated (left), and a graphical representation of the confidence intervals associated with each parameter. Note that parameters with confidence intervals that pass over the 0 line are not considered significant.	62
2.10	Example of agarose gel of diagnostic restriction digest of different guideRNAs cloned into pNuc- <i>trans</i> . Each plasmid was digested with EcoRI and KpnI and compared to the pNuc- <i>trans</i> backbone (CTL). Asterisks indicate unexpected digestion patterns. The size of the ladder is indicated in kilobase pairs (kb) to the left of the gel image.	64

2.11	Effect of sgRNA targeting parameters on killing efficiency. a. Plot of predicted sgRNA activity versus <i>S. enterica</i> killing efficiency for all 65 sgRNAs. The shaded area is the 95% confidence interval of the line of best fit. Boxplots of sgRNAs targeting different strands for b. transcriptional (S, sense strand; AS, anti-sense strand) and c. replication, and d. sgRNAs targeting genes with essential (Ess), non-essential (NEss) or unresolved phenotypes (Un) versus killing efficiency. e. Plot of relative position of sgRNAs within genes versus average killing efficiency for the sense strand and f. anti-sense strand of targeted genes. For each plot, points are filled according to their predicted sgRNA activity. Killing efficiency is plotted on a log10 scale.	66
3.1	Identifying conjugative systems from gut metagenomic data. a. Conjugative systems were identified from a near-complete non-redundant gut database containing both reference genomes and metagenome-assembled genomes (MAGs). Relaxase families were predicted using MOBScan (16). The outer region represents all 1598 contigs containing putative conjugative systems. The inner region is a focused section of conjugative systems identified in the Proteobacteria clade. The highlighted system, 20298 is a conjugative system with a MOBPI relaxase that was chosen for synthesis. b. Predicted conjugative contig “20298” showing the trimmed part of the contig containing the predicted conjugative elements and which was then synthesized. The predicted relaxase is coloured orange, while the predicted <i>oriT</i> (29) is coloured pink.	83
3.2	Synthesis and assembly of p20298-AGE. a. Schematic of assembly. 11 tiles were synthesized as clonal DNA fragments from TWIST Bioscience. Tile 9 could not be synthesized in this manner and was instead synthesized in 4 fragments by a Telesis Bio BioXP 3200. b. TAE-agarose gel showing fragments used for yeast assembly of p20298-AGE. Bands marked by astericks represent the plasmid backbone the clonal fragments were excised from with PmeI. c. Diagnostic digest of yeast assembly clones that have been transformed into <i>E. coli</i> , isolated, and digested with NcoI-HF and NotI-HF. Checks indicate colonies with the correct expected banding pattern.	86

3.3	Conjugation of p20298. a. Diagram of conjugative plasmids p20298-AGE and p20298-15a showing the region of synthesis error and the difference in backbones. Deleterious mutations were present in both <i>traV</i> and <i>traY</i> in p20298-AGE that were repaired in 20298-15a. The plasmid backbone was simultaneously swapped from a pAGE backbone to a p15a backbone. b. Conjugation of p20298-15a, and p20298-AGE from an <i>E. coli</i> donor to an <i>E. coli</i> recipient. Five biological replicates were performed for each. c. Conjugation of p20298-15a from an <i>E. coli</i> donor (left) to <i>E. coli</i> (Ec), <i>C. rodentium</i> (Cr), and <i>Salmonella enterica</i> Typhimurium (St). Five biological replicates were performed for each. d. Conjugation from a <i>C. rodentium</i> donor (right) to <i>E. coli</i> (Ec), <i>C. rodentium</i> (Cr), and <i>Salmonella enterica</i> Typhimurium (St) (St). Three biological replicates were performed for each. e. Time-course conjugation from 30 minutes to 24 hours of p20298-15a from an <i>E. coli</i> Epi300 donor to an <i>E. coli</i> and a <i>C. rodentium</i> recipient. Three biological replicates were performed at each timepoint for each recipient strain. Shaded regions indicate the 95 % confidence interval. f. Conjugation of p20298-15a from <i>E. coli</i> to seven additional <i>Citrobacter</i> strains, with <i>C. rodentium</i> as a control. Three biological replicates were performed for each recipient strain.	87
3.4	Evaluating p20298-15a function. a. Re-conjugation of <i>C. rodentium</i> transconjugants. Six <i>C. rodentium</i> transconjugants of p20298-15a were isolated and conjugated to a rifampin-resistant strain of <i>C. rodentium</i> . b. Conjugation of p298-oriT <i>in trans</i> . The p20298-15a oriT was predicted using oriTfinder (29), and cloned into a plasmid compatible with p20298-15a.	90
3.5	<i>C. rodentium</i> native plasmids. Plasmids were prepared and digested with NotI-HF and NcoI-HF (NEB) and ran on a 0.8% TAE-agarose gel. Digested bands indicate expected background bands when digesting p20298-15a plasmids that were isolated from <i>C. rodentium</i>	92
3.6	Diagnostic digests of p20298-15a isolated from <i>C. rodentium</i> after being passaged. Colonies were passaged twice on plates before being diluted and grown to saturation overnight for plasmid extraction. Extracted plasmids were digested with NotI-HF and NcoI-HF. This contains the complete digests that are partially shown in Figure 2. Asterisks indicate bands which result from digestion of native <i>C. rodentium</i> plasmids (see Figure 3.5).	93
3.7	Nucleotide coverage from RNA-seq analysis of p20298-15a expression in a. <i>E. coli</i> Epi300 (DAP-) or b. <i>C. rodentium</i> . Coloured data represents nucleotide frequency on a given strand of the plasmid. Shaded regions indicate the orientation of reading frames on the plasmid.	94
3.8	Volcano plot showing differential gene expression effect size of p20298 genes in <i>E. coli</i> compared to <i>C. rodentium</i> , with both axes on a log scale. Genes with 2-fold differential expression, and p-values less than 0.01 are located in the upper left and upper right quadrants and are coloured red. Genes in the upper right quadrant have higher relative expression in <i>C. rodentium</i> , genes in the upper left quadrant have higher relative express in <i>E. coli</i>	95

3.9 Functionalizing p20298 to kill *C. rodentium*. **a.** p20298 was modified to include a gateway destination cassette for cargo insertion to create p20298-dest. pENTR-TC9 was constructed to facilitate the recombination of CRISPR-TevCas9 with various sgRNAs into the p20298-dest plasmid. **b.** Schematic of chromosomal targeting by a conjugated p20298-TC9 plasmid. p20298-TC9 is conjugated from *E. coli* to *C. rodentium*. CRISPR-TevCas9 targeting the *C. rodentium* genome is either induced with arabinose, or repressed with glucose and allowed to outgrow for 2 hours to kill. The remaining transconjugants are grown overnight on plates, and killing efficiency is calculated by comparing these conditions. **c.** Killing efficiency of *C. rodentium* with p20298-TC9. 8 sgRNAs targeting the *C. rodentium* genome (blue circle), a non-targeted sgRNA (red triangle), and an empty sgRNA cassette control (black diamond) were tested in three biological replicates each. Killing efficiencies were calculated as described above and expressed as a percent. 97

C.1 Proof of copyright permission not being required for chapter 2. 147

List of Tables

1.1	Conjugative relaxase MOB types and their mechanisms of catalyzing relaxation and joining at the conjugative <i>oriT</i>	13
3.1	Identified mutations by full plasmid Nanopore sequencing in p20298-AGE clones isolated from <i>E. coli</i>	85
3.2	Identified mutations by full plasmid nanopore sequencing in p20298-15a.	85
A.1	Table of primers used in chapter 2.	115
B.1	Table of primers used in chapter 3.	138

List of Appendices

Appendix A - Supplemental Material for Chapter 2	115
Appendix B - Supplemental Material for Chapter 3	138
Appendix C - Copyright permission for Chapter 2 - no copyright permission required	147

List of Abbreviations, Symbols, and Nomenclature

%	percent
°C	degrees Celcius
~	approximately
AMR	antimicrobial resistance
ARSH4	autonomous replication sequence
ATP	adenosine triphosphate
BLAST	basic local alignment search tool
bp	base pair
Cas9	CRISPR associated protein 9
cat	chloramphenicol acetyltransferase
CEN6	chromosome 6 centromere
Cm	chloramphenicol
CRISPR	clustered regularly interspaced short palindromic repeats
CRISPRa	CRISPR activation
CRISPRi	CRISPR interference
DAP	Diaminopimelic acid
dCas9	dead (catalytically inactive) Cas9
ddH ₂ O	double-distilled H ₂ O
DNA	deoxyribonucleic acid
del	deletion
dtr	DNA transfer and replication
EDTA	ethylenediaminetetraacetic acid
FMT	fecal microbiota transplant
Gm	gentamycin
HE	homing endonuclease
HGT	horizontal gene transfer

his	histidine
ICE	integrative conjugative element
Kan	kanamycin
kb	kilobase
LB	lysogeny broth
LSLB	low salt lysogeny broth
M	Molar concentration
MAG	metagenome-assembled genome
Mb	megabase
min	minute
mg	milligram
mL	millileter
mpf	mating pair formation
OD	optical density
ORF	open reading frame
oriT	origin of transfer
oriV	origin of vegetative replication
PAM	protospacer adjacent motif
PEG	polyethylene glycol
PCR	polymerase chain reaction
pH	potential of hydrogen
qPCR	quantitative real time PCR
RCF	relative centrifugal force
RCR	rolling circle replication
Rif	rifampin
RNA	ribonucleic acid
RNAP	RNA polymerase
RNA-seq	RNA sequencing
RPM	revolutions per minute
s	second

SDS	sodium dodecyl sulfate
SNP	single-nucleotide polymorphism
SOC	super optimal broth with catabolite repression
sgRNA	single guide ribonucleic acid
TALEN	transcription activator-like effector nucleases
T4SS	type 4 secretion system
T4CP	type 4 coupling protein
TevCas9	I-TevI nuclease domain and Cas9 fusion protein
TRIS-HCl	tris(hydroxymethyl)aminomethane hydrochloride
T-strand	transfer DNA strand
w/v	weight per volume
ZFN	Zinc-finger nuclease
μg	microgram
μL	microliter

Chapter 1

Introduction

1.1 Human health and the microbiome

1.1.1 On the interface of humans and microbes

The relationship between humans and microbes is a remarkable factor in our lives, and crucially important for homeostasis. In fact, the human body is home to numerous diverse ecosystems of microbes that have key roles in human health (3, 39, 135, 173). For instance, research on gut microbiome dysbiosis has suggested important involvement in diseases including obesity (166), cancer (151) and inflammatory bowel disease (68). While the gut microbiome is perhaps the most extensively studied, other commensal microbial communities have critical health implications when dysbiosis occurs including the oral (50), vaginal (30), and skin (23) microbiomes. With estimates for the ratio of the number of bacterial to human cells in the body ranging between 10:1 (150) and 1:1 (153) it is evident that the human body is more than just one organism, highlighting the significance of our symbiosis with microbes. While healthy interactions between humans and microbes are essential, not all of our relationships are symbiotic in nature. Throughout human history, we have observed and been affected by the negative interactions that can exist between humans and microbes, facing pandemics caused by bacterial agents such as the plague (*Yersinia pestis*) (138), cholera (*Vibrio cholera*) (48), and tuberculosis (*Mycobacterium tuberculosis*) (145). While modern medicine has allowed us to face the challenges associated with bacterial diseases through the use of traditional antibiotics, we continue to face significant health consequences as a result of bacterial infections and growing antimicrobial resistance (AMR) in pathogenic species (125).

Taken together, the relationship between humans and bacteria is a delicate balance of symbiosis and pathogenesis which has a critical impact on human health.

1.1.2 Bacterial pathogens and antimicrobial resistance

Bacterial pathogenesis is a major contributor to human disease. In fact, a recent study indicated that globally in 2019, 7.7 million deaths were linked to infections from 33 clinically significant pathogens (76). The majority of these deaths were caused by five bacteria: *Staphylococcus aureus*, *Escherichia coli*, *Streptococcus pneumoniae*, *Klebsiella pneumoniae*, and *Pseudomonas aeruginosa*. In addition to the risk of mortality, each of these bacteria demonstrated resistance to traditional antibiotic therapies (36, 56, 129, 133, 137). Furthermore, tuberculosis continues to be a bacterial disease of concern. In 2019, 10 million people developed tuberculosis, 1.4 million deaths were associated with infection, and approximately 4.7% of patients were infected with multidrug-resistant or rifampicin-resistant strains (57). The growing prevalence of resistance to antibiotics is a major threat to human health that requires diverse solutions to generate effective treatments. Generally, the development of AMR bacteria is somewhat paradoxical, as overuse of traditional antibiotics selects for resistant variants (169). Therefore, the more we utilize life-saving antibiotics, the higher the risk of not being able to treat the same bacterial targets later on. Beyond their use in healthcare, large-scale use of antibiotics in agriculture significantly contributes to the generation of resistant bacteria (169, 181). These combined pressures continue to drive evolution of new AMR strains of potential human pathogens, illustrating the need to develop novel and diverse solutions to target these strains. While methods for identifying new antibiotic compounds continue to be explored (120, 158), the development of novel solutions to combat AMR is imperative to diversify the ability to target bacteria of concern. One solution is phage therapy, which utilizes bacteriophages that natively kill bacteria (96). Phage therapy is not a novel treatment idea, having first been used a century ago, but growing concern over AMR has led to renewed interest for targeting bacteria (72, 96). Furthermore, sequence-specific antimicrobials that take advantage of modern biological tools to target bacterial DNA for cleavage also provoke significant interest (17, 40, 64). The ability for phage therapy and sequence-specific antimicrobials to more precisely target microbes is a potential advantage over many broad-range antibiotics. Ultimately, having

diverse solutions to combat current and future AMR bacteria is necessary to help combat the continuing evolution of bacterial pathogens. While continued development of traditional therapies is necessary, novel solutions are also required to diversify the way we target and treat these microbial infections.

1.1.3 Microbiome dysbioses and human health

Beyond the challenges that are presented from pathogenic bacteria, dysbioses of native human microbial ecosystems influence human health. Perhaps the most well studied microbiome with respect to human health is the human gut microbiome. Although gut microbiomes contain diverse bacteria, and can vary between different individuals (53), specific perturbations and balances of normally commensal bacteria have been implicated in various diseases. Perhaps the most obvious example of this occurs with gut diseases such as inflammatory bowel disease and ulcerative colitis, which have both been linked with low gut microbiota diversity (107, 164). In fact, fecal microbiota transplant (FMT) to restore a healthy microbiome has been demonstrated as a successful treatment procedure for ulcerative colitis (44). The ability to fix diversity-related gut diseases with healthy community replacement illustrates the importance of healthy and balanced microbial ecosystems to human gut health.

Another example of the role of the gut microbiome in disease is with obesity. Two studies showed that genetically obese mice have an increased abundance of *Bacteroidetes* and a corresponding decreased abundance of *Firmicutes* (108, 167), although these conclusions have been criticized in future analyses (162). Nevertheless, literature suggests an association may exist between microbiome composition and obesity related-factors, even if the link is not yet completely clear (166). It has also recently been suggested that the human gut microbiome impacts the efficacy of immune checkpoint inhibitor therapy treatment for cancer (106, 184), although the precise differences are not fully understood and appear to vary greatly between individuals. Interestingly, co-treatment with FMT from healthy donors was shown to improve immune checkpoint inhibitor-associated colitis (174), further supporting the link between gut microbiome health and treatment efficacy. Overall, while yet to be fully understood, it is evident that gut microbiome health is intricately related to the health of the human host in a symbiotic manner.

While the gut microbiome is essential to human health, other microbial communities use the human body as a host, and dysbioses in these systems have also been implicated in disease. For example, dysbiosis of the human skin microbiome has been associated with atopic dermatitis (180), a chronic inflammatory skin disorder. Likewise, the vaginal microbiome appears to have different compositional changes when affected by various diseases (30), indicating important relationships between microbes and vaginal health. Additionally, the oral microbiome is another complex ecosystem where overabundance of certain pathogens has been linked to oral disease (50). Poor oral hygiene has also been associated with cardiovascular health, suggesting the possibility of a deeper interaction between the oral microbiome and general human health (86). Ultimately, though there remains much left to be understood about the relationship between humans and our bacterial symbiotes, it is evident that this relationship is vital to human health.

1.2 Metagenomics

1.2.1 Metagenomes and Metagenome-assembled genomes (MAGs)

The study of the functional impact that microbial communities have on both human health and the environment has been advanced by the development and innovation of molecular biology and DNA sequencing technologies. These advances made way for the study of metagenomes, which were first described as the collection of genomes in a microbial community, originally being applied to soil microflora (69). The field of metagenomics has since expanded to encompass the study of microbial systems across environmental and health-related samples. In particular, the evolution of next-generation sequencing technology has enabled the shotgun metagenomics approach to rapidly generate data from complex microbial communities (141). Furthermore, long-read sequencing technologies such as the Oxford Nanopore MinION can be used to study low-complexity microbial populations (101). Combining long-read and short-read sequencing data for hybrid metagenomic assemblies can also enable higher resolution assembly of metagenomes (15).

Studying microbial communities by analyzing their metagenomes is particularly useful as it can generate functional information for both culturable and non-culturable organisms (51). This is important as traditional microbiological techniques limit functional study to bacteria that can

be readily isolated. Advanced methodologies for binning metagenomic data allow for genomes to be recovered from the information, known as metagenome-assembled genomes (MAGs) (2, 149). This strategy has been applied to metagenomic data where it was used to recover microbial genomes from public metagenome data, greatly increasing the known diversity of archaeal and bacterial genome trees by more than 30% (131). Furthermore, it has been specifically applied to gut microbiome data to generate a genomic blueprint of the gut microbiome by constructing MAGs, including those from nearly 2000 uncultured candidate bacteria (3). MAGs are generally less complete and lower quality than isolate genomes (119), although circularized genomes can be recovered from long-read sequencing metagenomic data (47). A further limitation with MAGs is that plasmids are generally under-represented in the binned sequences. This under-representation occurs due to difficulty in successfully recovering and binning plasmid sequences (1). Overall, metagenomic sequencing expands the ability to study both taxonomy and function of microbes in diverse communities.

1.2.2 Functionalizing biological systems from microbial communities

An important function of metagenomic data is the ability to identify key functional systems from diverse microbial communities (1). Functional metagenomics can identify genes and systems with interesting activities in microbial ecosystems. This method typically uses DNA isolated from microbial communities which is then used to generate a library of genetic material in host cloning vectors (99). These libraries can then be screened to identify desired functions of interest from the community and clones that exhibit desired activities can then be sequenced and analyzed further. Functional metagenomics can help elucidate the unique functions of complex microbial communities. For instance, functional metagenomics can be used to study extremophiles in harsh environments (121) and antibiotic resistance in environmental samples (165). In human samples, antibiotic resistance has been further studied to identify novel resistance genes in the human gut microbiome (35).

Importantly, using functional metagenomics to identify genes and systems can be exploited to identify biological activities with applications in biotechnology. Through functional metagenomics, various novel enzymes have been isolated including thermostable polymerases (124), Cas9

inhibitors (55), and genes for naphthalene degradation (175). From human microbiome data, genes for bile salt hydrolase activity have also been identified (84). Additionally, systems that generate antimicrobial molecules have been identified through functional studies (113). Ultimately, functional metagenomics is capable of identifying genes and systems from microbial communities which would be difficult or impossible to discover by isolate-based approaches. Importantly, advancements in DNA synthesis technologies have made DNA synthesis from sequence possible at scale (97). While functional metagenomics traditionally uses a function-to-sequence approach to identify genetic systems, these advancements provide the groundwork for a sequence-to-function approach for the synthetic construction of genes and pathways that are identified directly from metagenomic sequencing data. For example, libraries of bacterial regulatory elements have been constructed from metagenomic data (82, 157) and enzyme sequences have been used to design primers for PCR amplification of genes from isolated metagenomic DNA (185).

1.3 Bacterial conjugation

1.3.1 Methods of horizontal gene transfer in bacteria

One of the principal mechanisms that drives evolution in bacteria is horizontal gene transfer (HGT) (22, 98). HGT is the lateral movement of genetic information between organisms, and has been observed in bacteria, archaea, and eukaryotes (89, 98, 170). In bacteria there are three major natural processes by which HGT occurs: transformation, transduction and conjugation (Figure 1.1). Furthermore, HGT is a causative mechanism in the development of antimicrobial resistance (25, 118). Importantly, these mechanisms of DNA transfer can be readily exploited for molecular biology and synthetic biology applications.

The first of these three methods of HGT to be discovered was transformation (Figure 1.1a), which was identified serendipitously by Frederick Griffith in 1928 when he observed that mixing non-virulent strains of *Streptococcus pneumoniae* with heat-killed virulent strains of *S. pneumoniae*, caused non-virulent strains to be "transformed" into the virulent type (65). Bacterial transformation involves the direct uptake of exogenous DNA from the environment by the bacterial cell (33). In the case of natural transformation, uptake of DNA is an active process which utilizes

enzymes to facilitate the transfer of DNA across cell membranes (33). Artificial transformation is often used in laboratories and uses either chemical preparation, or electroporation to force the transfer of DNA through pores in the membrane (6). In either case, transformation is a popular tool for introducing exogenous DNA into a bacterial cell, and has been crucial in the advancement of molecular and synthetic biology.

The second major process by which HGT occurs in bacteria is through bacteriophage transduction (Figure 1.1c). Bacteriophages (phages) are viruses that target and infect bacteria. Lysogenic phages are capable of inserting themselves into the host chromosome, becoming prophages (26). Under certain conditions, prophages are able to excise themselves from the chromosome, sometimes taking portions of the host DNA with them (26). When host DNA is repackaged into a new virion, it can then be transferred to a new cell upon subsequent infection. Generalized transduction has also been observed where fragments of the host chromosome, not immediately adjacent to the prophage, are packaged into new phage particles and can be mobilized (21, 26). The multiple mechanisms by which host DNA can be packaged into virions and transferred to a new cell highlights how phages facilitate the transfer of genetic material between bacteria. Bacteriophages have been a noted cause of HGT, such as in the case of *Vibrio cholerae* where the cholera toxin itself is phage-encoded (171). Additionally, antibiotic resistance genes have been found in collected bacteriophage samples (42), and the transfer of resistance genes from bacteriophages to host bacteria has been observed (117, 179). The ability for phages to introduce foreign DNA into new cells has made them a desirable delivery tool in synthetic biology across a range of applications (152).

The final HGT process to discuss is bacterial conjugation (Figure 1.1b), which involves the cell-to-cell transfer of genetic material in bacteria (25). Typically bacterial conjugative systems encode for two key processes: DNA relaxation caused by strand nicking at the origin of transfer (*oriT*) by a DNA relaxase, and a type IV secretion system (T4SS) which facilitates the transfer of DNA between cells (25). Generally, these systems are found encoded either as a conjugative plasmid, or on the bacterial chromosome itself as an integrated conjugative element (ICE) (25, 183). Bacterial conjugative systems are perhaps the most common method of HGT transfer within microbial communities, and frequently carry genes that confer antimicrobial resistance (25, 118). For this reason, a significant amount of research has aimed to study the persistence and evolution of these plasmids (10, 52, 54, 146). Furthermore, their ability to carry large genetic loads (102)

makes conjugative plasmids of great interest for synthetic biology.

1.3.2 Conjugation - a history

The process of bacterial conjugation was discovered throughout a series of papers from Joshua Lederberg and his collaborators (29, 103–105), for which he would ultimately be awarded the Nobel prize in 1958 (123). Lederberg's work with Edward Tatum identified a "sexual process" in *E. coli* when mixing cultures of different mutants (104), which would later be recognized as bacterial conjugation. Eventually, this work alongside other key scientists including Esther Lederberg, and Luigi Luca Cavalli-Sforza would lead to the discovery of a fertility factor or "F" (105), later identified as the F conjugative plasmid (29, 103). At this time, very little was understood about the underlying molecular mechanisms of the transfer, beyond the idea that extra-chromosomal elements were involved, and that cell-to-cell contact seemed necessary for transfer (29). Overall, this series of experiments was foundational for understanding the biology of bacterial conjugation.

1.3.3 Biology of conjugative systems

Bacterial conjugation is perhaps most easily understood as a two-step process that unites the system for rolling-circle DNA replication with secretion of DNA through a T4SS (111) (Figure 1.2). Rolling-circle replication of plasmids is initiated by the nicking of a plasmid DNA strand at the origin of replication (90). In the same manner, initiation of conjugation occurs when the conjugative relaxase nicks a single strand of the plasmid (known as the transferred strand, or T-strand) at the origin of transfer (*oriT*) (111). A protein complex known as the relaxosome, which includes the conjugative relaxase, is formed on the DNA substrate where the nick occurs (25). A nucleophilic tyrosine residue in the relaxase attacks a 5' phosphate on the T-strand causing nicking of the plasmid. This reaction results in the relaxase being covalently bound to the T-strand of the DNA substrate (25, 66). The second step in the conjugative process is the transfer of the T-strand through a type 4 secretion system (T4SS) (111). Type 4 secretion systems are versatile, and known to serve several functions in bacterial cells including conjugation, DNA-exchange with the environment, and secretion of effector proteins (28). In the case of bacterial conjugation systems, T4SS are composed of mating pair formation proteins which generate a conjugative pilus and a

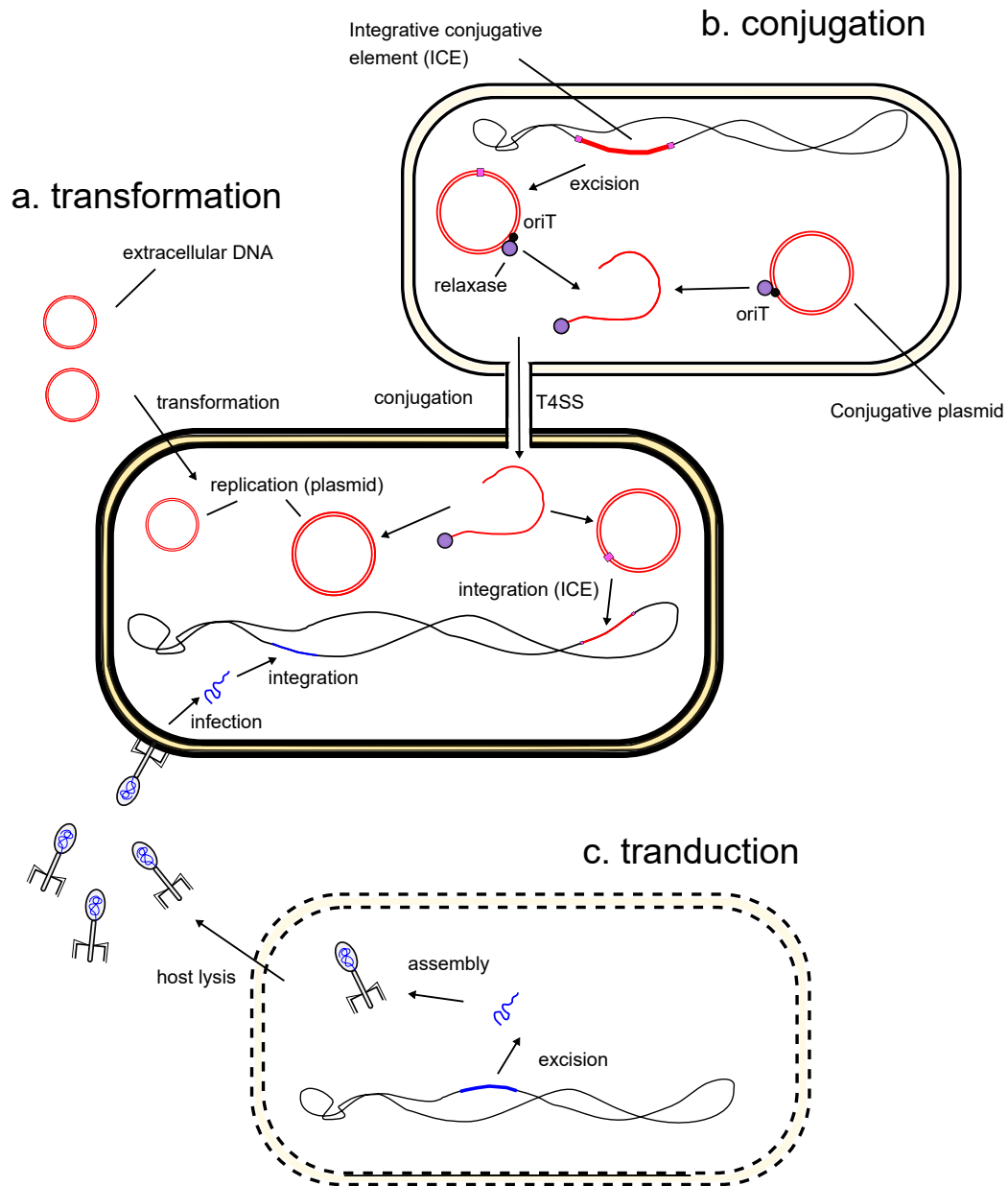


Figure 1.1: Mechanisms of horizontal gene transfer in bacteria. **a.** Transformation. Bacteria take up DNA from the extracellular environment. **b.** Conjugation. DNA is transferred cell-to-cell using a type 4 secretion system. Conjugation can be initiated by either an integrative conjugative element or a conjugative plasmid. **c.** Transduction. Bacteriophage transduction can result in horizontal gene transfer when prophages excise themselves from the chromosome of a host. Assembled bacteriophage virions are then able to infect new hosts and integrate into their chromosome.

transenvelope complex that facilitates the transfer of the T-strand to the recipient cell (25, 28). The important molecular link between DNA relaxation and secretion from the T4SS is the interaction with a coupling protein (T4CP), which associates with both the relaxosome and the T4SS, and is required to mobilize the relaxosome complex to the T4SS (4, 24, 28, 111). While this view simplifies conjugation to two key functional systems, conjugative DNA transfer requires the coordination of a multitude of proteins to successfully mobilize a plasmid. In the case of the IncP α conjugative plasmids, which includes the RK2/RP4 conjugative system, this organization has been studied and reviewed in great detail (130). This system has conjugative machinery encoded in two separate gene clusters, identified as Tra1 and Tra2, which together encode at least 27 genes that are responsible for mating pair formation and DNA transfer and replication (130). More specifically, genes in the Tra1 region encode products that are required for DNA transfer and replication function, such as relaxosome formation, whereas genes in Tra2 are required for mating pair functions, which importantly includes the formation of the conjugative pilus (130). This conjugative system has been of particular interest as it is capable of conjugation to a diverse range of gram-negative bacteria, which has led to various attempts to improve its conjugative frequency and minimize its coding size through genetic engineering, including the generation of plasmids such as pTA-Mob and pTA-Mob 2.0 (8, 156, 159). The RK2/RP4 conjugative system is an example of a well-studied conjugative system, although several others have also been well-characterized including the aforementioned F plasmid (95).

1.3.4 Diversity and classification of conjugative systems

Conjugative systems are diverse and their classification can be approached from a number of directions. A primary method of classifying conjugative systems sorts conjugative relaxases into MOB families based upon relaxase homology (31, 59, 60). Most relaxase MOB families are cation-dependent HUH (histidine-hydrophobe-histidine) endonucleases which have a conserved active site motif containing two histidine residues separated by a hydrophobic residue. This family of endonucleases uses a catalytic tyrosine to cleave single-stranded DNA, and result in a covalent phosphotyrosine bond forming between the HUH endonuclease and the DNA strand, as is the case with conjugative relaxases (31, 59). Three of the MOB relaxase super families (MOB_T, MOB_C,

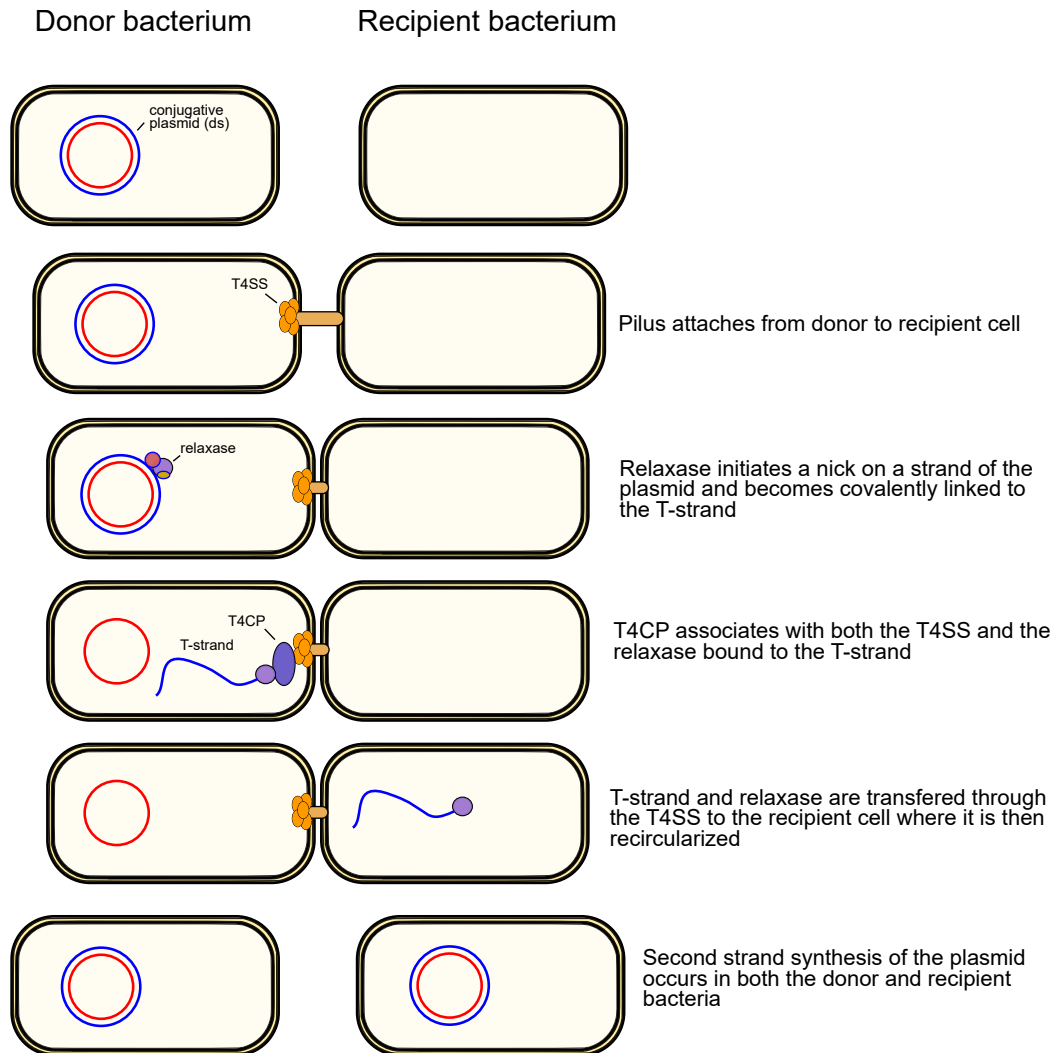


Figure 1.2: Mechanism of bacterial conjugation of plasmid DNA in bacteria. Conjugation is initiated by donor pilus attachment to a potential recipient cell. A DNA relaxase nicks a single strand of the plasmid at the *oriT* and becomes covalently bound to the strand (the T-strand). The relaxase-T-strand complex is coupled to the T4SS by a T4CP where it is transferred to the recipient cell. Once in the recipient, re-ligation and second strand synthesis of the plasmid occurs.

and MOB_M) appear to engage in alternative biochemical processes to the HUH endonuclease MOB families. MOB_T conjugative relaxases utilize a rep_{trans} rolling circle replication mechanism without an HUH motif, MOB_C contain a C-terminal catalytic domain similar to PD-(D/E)XK restriction endonucleases, and MOB_M are most similar to tyrosine recombinases (59). Furthermore, some members of the MOB_V family appear to use a catalytic histidine for the nucleophilic attack of the DNA strand at the *oriT* instead of a catalytic tyrosine (59, 136). These varying mechanisms of catalysis demonstrate the diversity of how conjugative systems have evolved to function.

Ultimately, MOB-type classification sorts conjugative relaxases into 9 superfamilies (Table 1.1), from which further phylogenetic analysis has been performed (59). This classification system is effective for sorting and providing a basic phylogeny of conjugative systems. A comprehensive review suggests it to be a useful means of classification, as much can be understood about a conjugative system simply by sequencing the relaxase gene (60). It is perhaps a more applicable method of separating conjugative systems into clades than by incompatibility groups, which is another way conjugative plasmids are commonly sorted. Although, incompatibility groups still provide critical information regarding plasmid division and replication (127), they do not directly address the conjugative system. However, incompatibility groups do seem to often cluster into relaxase clades (60). Ultimately, conjugative systems are widespread and can be readily separated on the basis of relaxase homology, providing a basis for considering the evolution and classification of conjugative systems.

1.3.5 Applications of bacterial conjugative systems

The use of conjugative systems in molecular biology and biotechnology has been diverse and innovative. For instance, one of the earliest applications of conjugative systems involved utilizing interrupted conjugative mating to effectively map the location of genes on bacterial chromosomes (9). Critically, conjugation is a useful tool for delivering plasmids to bacteria that are difficult to transform by other methods, such as *Deinococcus radiodurans* (20) and *Lactobacillus* spp. (148). Beyond this, the use of bacterial conjugation as a delivery mechanism for sequence-specific antimicrobials has been explored (40, 126), a concept that will be discussed in greater detail later on in this chapter.

Table 1.1: Conjugative relaxase MOB types and their mechanisms of catalyzing relaxation and joining at the conjugative *oriT*.

Mob Type	Endonuclease superfamily	Notes
MOB _P	HUH endonuclease	Includes the RK2/RP4 conjugative system
MOB _B	HUH endonuclease	Includes the F and R1 plasmids Some members (pMV158) utilize a catalytic histidine instead of tyrosine for the nicking and joining reaction
MOB _F	HUH endonuclease	
MOB _Q	HUH endonuclease	
MOB _V	HUH endonuclease	
MOB _H	HUH endonuclease	
MOB _T	Rep_trans RCR	
MOB _C	PD(D/E)XK restriction endonuclease	
MOB _M	Tyr recombinase	

Additionally, *trans*-kingdom conjugation has been observed in a number of situations between bacteria and eukaryotes. An example of this observed in nature is transfer of the Ti plasmid from *Agrobacterium tumefaciens* to dicotyledonous plants, resulting in the formation of crown gall tumors (38). Furthermore, conjugation between bacteria and mammalian cells has been observed (176), indicating the potential for this to occur both naturally, and be applied to synthetic biology. Together, these provide evidence for the potential versatility of conjugative systems outside of classic bacterium-to-bacterium transfer providing new potential applications for conjugation technology. For example, bacterial conjugation has been demonstrated between bacteria and several fungal species with the intent to serve as an antifungal reagent (41). It has also proven to be an effective tool in the delivery of DNA to microalgae, providing improved methods for biotechnology applications (88, 154). Overall, this highlights the vast potential of bacterial conjugation as a tool in biotechnology.

1.4 Plasmids

1.4.1 What is a plasmid?

The term "plasmid" was first conceived by Joshua Lederberg as "any extra-chromosomal hereditary determinant" after his co-discovery of the F plasmid (103). A modern definition describes plasmids as DNA elements that can replicate autonomously in the host cell, and are typically circular and double-stranded (45). Plasmids are extremely diverse and can be found across most prokaryotic phyla (146). Plasmids are a well established vessel for HGT, including the spread of AMR genes (146), and can be introduced into bacteria by various mechanisms including bacterial conjugation (25) and transformation (33). Furthermore, phagemids contain the the required plasmid replication and selection machinery, however, can be introduced to cells via transduction (178). The diversity and abundance of plasmids in nature makes them of great interest to study due to the impact they have on host cells. The ability to engineer them and easily introduce them to bacterial cells by multiple mechanisms makes them a fundamental tool in molecular biology.

1.4.2 Plasmid replication

When utilizing plasmids in molecular and synthetic biology, it is crucial to consider the mechanism of replication for several reasons. In general, plasmids replicate either through rolling-circle replication (RCR) (90) or theta replication (110), the latter of which has multiple subtypes. Copy number of plasmids is regulated through multiple mechanisms including iteron sequences, anti-sense RNAs, and protein inhibitors in conjunction with antisense RNAs (49). As bacterial plasmids replicate autonomously from the chromosome, copy number varies plasmid to plasmid. Copy control as plasmids replicate is important to consider, not just due to its impact on gene dosage, but also due to its impact on plasmid partitioning, the mechanism by which plasmid copies are separated to daughter cells during cell division (7). While high copy plasmids can generally successfully partition to both daughter cells during replication by diffusion in the cell, lower copy plasmids require more complex partitioning systems to ensure successful passage to both daughter cells during division (7). Plasmid partitioning is therefore important for the overall stability of plasmid existence in a bacterial cell lineage, particularly for low copy plasmids.

The stable separation of plasmid copies to two daughter cells during replication is also vital for plasmid incompatibility - the inability for two plasmids to be stably inherited as bacterial cells divide (127). Generally speaking, when two plasmids share the same origins and mechanisms of plasmid partitioning, they are likely to be incompatible with each other (127), meaning that as bacteria divide, both plasmids are unlikely to be maintained through generations. Plasmid incompatibility has been a common method of sorting and identifying plasmids, as grouping can easily be identified by PCR-based replicon typing (27). Plasmid incompatibility is a critical consideration for synthetic biology, as any engineered plasmid needs to be compatible with native plasmids in the bacterial strain of interest, as well as with other engineered plasmids in the system.

1.4.3 Plasmid genetics

Beyond the scope of replication and partitioning, there are other major genetic features that plasmids may have. Of course, one of the most established of these features is their conjugative machinery which allows them to spread between different cells. While this affects the evolution of host strains, it also contributes towards evolution of the plasmid itself, often in a co-evolutionary manner (70). Another key set of elements that plasmids often include are addiction systems. For example, the *ccdA/ccdB* system from the F plasmid (128) and the *hok/sok* system from the R1 plasmid (163), which prevent survival of daughter cells that do not successfully retain the plasmid during segregation. These systems ensure that the plasmid is successfully maintained throughout a bacterial cell line, as any cells that do not successfully obtain a copy of the plasmid during division will die. Plasmids have also been shown to encode for genes that alter the extracellular environment, for instance by increasing the formation of biofilms (63), and stabilizing mating pair formation during conjugation (112). They also often carry genes that increase virulence in many pathogens including *E. coli* (83), *Salmonella* spp. (147) and *Yersinia* spp. (43). This direct impact of pathogenesis on human health makes plasmids an area of consequential research interest. Further contributing to plasmid impact on human health is their demonstrated ability to carry and spread antibiotic resistance genes (13), facilitating the development of AMR bacteria. The diversity of genes encoded by plasmids makes them a key consideration in disease, but also demonstrates the capacity to carry genetic cargo that can be readily exploited for the development

of plasmid-based delivery tools.

1.5 CRISPR-based antimicrobials

1.5.1 Clustered regularly interspaced short palindromic repeats (CRISPR) systems

Where humans are in a constant evolutionary battle with pathogenic bacteria, bacteria themselves are in an ongoing evolutionary arms race with bacteriophages that can infect and kill them (177). One of the primary methods of defense against bacteriophages used by bacteria is CRISPR (clustered regularly interspaced short palindromic repeats), a form of bacterial adaptive immune system (73, 94).

The discovery of CRISPR systems in microbial genomes dates back to 1987 when researchers identified the unusual repetitive sequence when attempting to sequence the *iap* gene in *E. coli*, although, at the time they did not understand what precisely they were observing (77). CRISPR systems would eventually be observed in diverse bacteria and archaea, although their function was yet to be discovered (79). CRISPR systems were indicated by their characteristic direct repeats which are separated by unique spacer sequences and importantly, CRISPR-associated genes (*cas* genes) were found to be present in these prokaryotes (79). It was eventually recognized that spacer sequences were derived from bacteriophage DNA and other extra-chromosomal elements (18) and proven that DNA spacers were being inserted into the CRISPR array as a result of bacteriophage challenge (12). The CRISPR locus is expressed as an RNA molecule that is processed into small CRISPR RNAs which guide the targeting of foreign DNA in prokaryotes (19). Crucially, it was found that Cas effectors in *S. thermophilus* cleaved both plasmid and bacteriophage DNA through endonucleolytic activity of effector Cas proteins at the site of the protospacer (the foreign sequence matching the spacer in the CRISPR array) (61). Additionally, a protospacer adjacent motif (PAM) in the target sequence is required for immune function (61, 74, 122). Furthermore, CRISPR effector proteins have been shown to cleave both RNA and single-stranded DNA targets (109, 160). Taken together, these observations indicate the nature of CRISPR systems as bacterial adaptive immune systems which acquire and integrate foreign spacers into their arrays, and utilize Cas ef-

effector proteins to cleave the foreign DNA on subsequent infection. CRISPR systems are diverse and widespread in nature, and can be generally classified into two classes. Class 1 CRISPR systems utilize multi-protein effector complexes, whereas class 2 systems utilize single, multi-domain effector proteins. Systems are further classified into types 1-6 based on phylogeny of Cas effector proteins and genetic architecture of the CRISPR systems (94).

1.5.2 CRISPR-Cas9 - a programmable endonuclease

The utilization of the Cas9 effector protein from the *S. pyogenes* CRISPR system as a programmable RNA-guided DNA endonuclease (81) had immediate implications in genetic engineering. Coming from a class 2 CRISPR system, Cas9 can function as an endonuclease in the absence of other Cas proteins. Crucially, Jinek *et al.* engineered the single guide RNA (sgRNA), which can be easily programmed to target sequences of interest provided that a PAM motif is present (81). This was revolutionary for genome engineering as previous tools including homing endonucleases (HEs) (67), zinc finger nucleases (ZFNs) (168), and transcription activator-like effector nucleases (TALENs) (87) required more laborious engineering to target specific sequences. It was quickly shown that Cas9 could be readily programmed to facilitate editing at specific sites in both bacterial (80) and human genomes (116, 143). Alternative Cas proteins from other class 2 systems were also adapted to expand sequence targeting and grow the CRISPR-Cas toolbox, such as *Staphylococcus aureus* Cas9 (144) and Cas12a/Cpf1 (34). Rational mutations were made to Cas9 proteins to enable high specificity of cleavage against the desired target site with fewer off target effects (93, 155). This is crucial, in particular, for genome editing applications where off-target effects are detrimental to effective and desired outcomes.

The development of the sgRNA (81) for the *Streptococcus pyogenes* Cas9 (SpCas9) facilitated the ability to rapidly generate and clone sgRNAs against specific target sites in the genome. This specificity is dictated by both the targeted protospacer and the PAM. Without the presence of a PAM, Cas9 is unable to cleave. Significant engineering of Cas9 has been done to expand the library of PAM motifs to broaden the range of potential target sites (91, 92, 172). Provided there is a PAM motif, the targeting of the ~20nt protospacer by Cas9 provides the site-directed specificity, although mismatches are tolerated to a degree, particularly when they are distal to the PAM (5,

75, 132). For SpCas9 protospacers, the 7-12 nt proximal region to the PAM where mismatches are less tolerated is referred to as the seed region. If a perfectly matched sequence is recognized, Cas9 generates a double-strand break of the DNA through two separate nuclease domains, each of which cleaves a strand (81).

The nature of the separate nuclease domains in SpCas9 allows for the generation of Cas9 nickase variants which cut only one strand of the target site through inactivation of either the HNH or the RuvC nuclease domains (115, 142). Inactivation of both catalytic nuclease domains of Cas9 generates dCas9, which associates with the DNA target but can not catalyze cleavage (100). When properly targeted towards genes of interest, this can be used to cause transcriptional interference, facilitating RNA-guided targeted knockdown of gene expression (CRISPRi) (100, 139). Furthermore, Cas9 can be modified by the addition of other protein domains to provide additional functions. Fusion of transcription activation domains to dCas9 can generate transcriptional gene activator variants (CRISPRa) (114). Additionally, fusion of deaminases to dCas9 can be used to generate CRISPR base editors, capable of directed base pair sequence conversion (62).

Importantly for this thesis, the fusion of additional nuclease domains to Cas9 can generate dual-endonucleases which are capable of generating multiple DNA cleavage events at the target site simultaneously (182). TevCas9 is a fusion of the I-TevI nuclease domain and linker region to the N-terminus of the SpCas9 molecule (Figure 1.3). This dual-endonuclease can be readily targeted to DNA substrates by an sgRNA, where both nuclease domains are capable of catalyzing a double-stranded break on the target molecule. Importantly, if both the Cas9 and I-TevI nuclease domains successfully cleave, TevCas9 generates a 33-36 bp deletion at the target and generates non-compatible overhangs, challenging DNA repair (182).

1.5.3 CRISPR as a sequence-specific antimicrobial

While the initial applications for CRISPR-Cas9 were focused towards genome editing, alternative applications for easily-programmable endonucleases were quickly explored. Applying Cas9 as a sequence-specific antimicrobial was an innovation of the technology that yielded significant promise in addressing the issue of antibiotic resistance, and was rapidly shown by multiple groups (17, 40, 64), each contributing significant information to the field. Gomma *et al.* found that

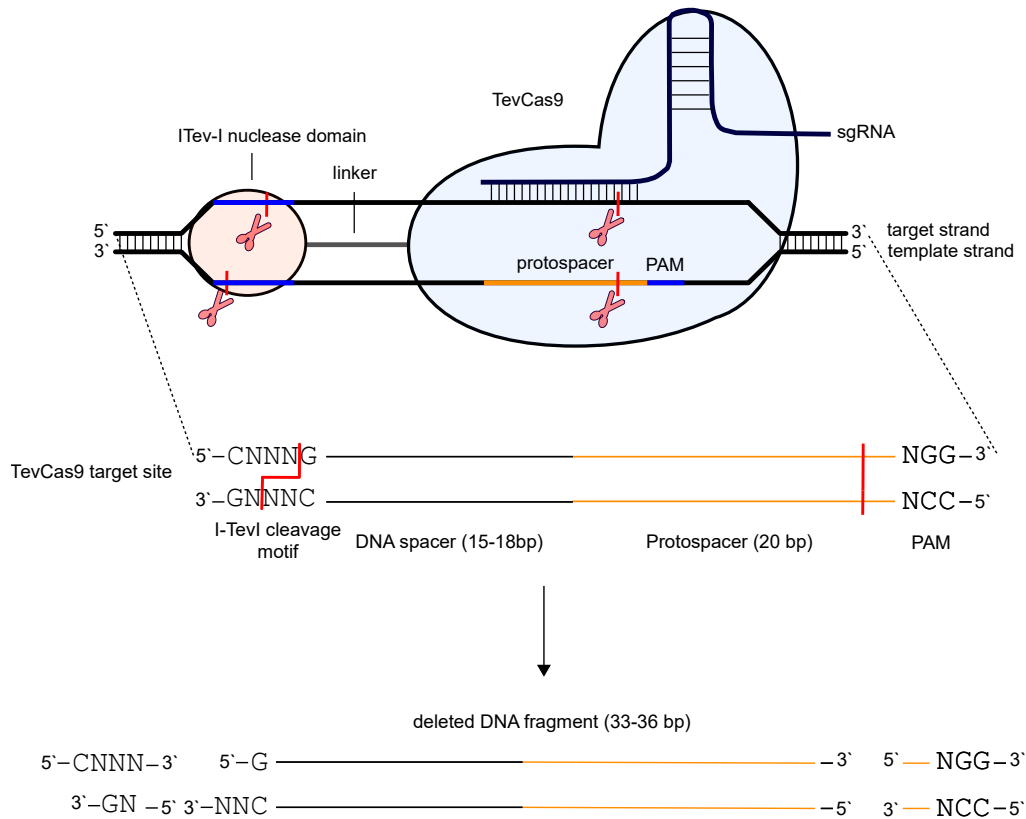


Figure 1.3: Targeted cleavage of DNA by TevCas9. TevCas9 is a dual endonuclease fusing the I-TevI nuclease and linker domains to *S. pyogenes* Cas9. TevCas9 can cleave at both the I-TevI and Cas9 cleavage sites facilitating a 33-35 bp deletion with non-compatible overhangs.

targeting anywhere on the *E. coli* chromosome was sufficient to kill *E. coli*, and simultaneously demonstrated that sgRNAs were specific enough to distinguish between bacterial strains (64). Bacterial death as a result of chromosomal targeting by Cas9 is likely a consequence of the inability for bacteria to successfully undergo homologous recombination while all chromosomal copies are actively being attacked by Cas9 in the cell (46).

Delivery of CRISPR nucleases is a limiting factor to the success of CRISPR-based systems for targeted removal of bacteria. Citorik *et al.* attempted delivery using both conjugative plasmids and bacteriophage transduction (40). In their particular system, they observed low efficiency of conjugation, and preferred the bacteriophage method of delivery for its higher observed delivery efficiency. Bikard *et al.* also utilized phage transduction for delivery with a phagemid containing the CRISPR system (17). Both bacterial conjugation and phage transduction have their own strengths and limitations for delivery of genetic material to bacteria. Bacteriophages are limited by the host-range of bacteria they can infect, and by acquired resistance in the targeted bacteria (32). Furthermore, native gut flora may have other protective characteristics that protect bacteria against phage infection (37). Phages tend to have a much lower carrying capacity than plasmids (102), limiting the ability to package genetic cargo on specific phages. Conjugative plasmids have their own limitations to consider, including host-range of replicative origins, incompatibility with host plasmids, and entry exclusion in different recipients (14, 58, 78). Conjugative plasmids, however, can carry sizeable genetic loads (11), which greatly improves their utility for encoding additional genetic elements. In conclusion, the diversity of conjugative systems provides a plethora of potential delivery vessels to different bacteria (60).

1.5.4 Alternative applications of CRISPR in bacteria

While using Cas9 as a sequence-specific antimicrobial is an attractive use of the technology, it is far from the only utility in bacteria. CRISPRi is an attractive tool for gene regulation in bacteria, initially being shown possible in *E. coli* (16, 139), although many other examples have since been explored. For instance, CRISPRi has been used to repress a virulence gene in *Pseudomonas aeruginosa*, attenuating the virulence in a murine model (140), and for targeting glucuronide-utilization enzymes (GUS) in Gammaproteobacteria (134). CRISPRi has also been used in bacteria to help

tune biosynthetic pathways in *E. coli* by regulating gene expression to help increase product yield of 5-aminolevulinic acid (5-ALA), an intermediate in the production of heme (161). Beyond repression, dCas9 fusions can be used in *E. coli* to activate gene expression. Examples of this include fusing the omega subunit of RNA polymerase (RNAP) to dCas9 (16), and fusing of phage protein AsiA to dCas9 (71), generating transcriptional activator variants. These examples demonstrate the vast and diverse potential for CRISPR technology in bacteria. Importantly, the successful implementation of all of these technologies is reliant upon robust and efficient delivery tools.

1.6 Scope of the thesis

The focus of this thesis is on utilizing conjugative plasmids as delivery vectors for the targeted killing of bacteria with the TevCas9 nuclease. Bacterial conjugation is a robust method of DNA delivery that naturally occurs in bacteria. Conjugative plasmids in particular are widespread in nature and have been found to carry a vast range of genetic material that they spread throughout microbial communities. I initially hypothesized that conjugative systems could be optimized for the efficient delivery of cargo to bacteria of interest. Furthermore, I hypothesized that a TevCas9 dual-endonuclease system would be an effective tool for targeted bacterial elimination. Together these concepts present an efficient method for the targeted killing of bacteria.

The first objective of this thesis, presented in chapter 2, is to utilize an established conjugative system to deliver an inducible TevCas9 nuclease to *Salmonella enterica* LT2, and subsequently kill the recipient. The first challenge in this was optimizing the conjugative delivery of the plasmid, as I quickly identified that *in-trans* mobilization of the pNuc plasmid was highly inefficient. I proceeded to construct a version of the plasmid that could self-mobilize, which yielded a large increase in conjugation frequency. I also identified that conjugation of this plasmid in a liquid-phase was improved by providing additional surface area to facilitate increased biofilm formation. While optimizing the conjugation of this plasmid, we simultaneously designed and tested 65 sgRNAs and demonstrated that they were able to kill the targeted *Salmonella enterica* with varying effectiveness, with some sgRNAs approaching 100% killing efficiency. Ultimately, this system presented critical evidence that bacterial conjugation could be used as an effective delivery tool for a TevCas9 nuclease, and that targeted elimination was possible.

The second objective of this thesis, presented in chapter 3, focuses on identifying native conjugative systems in metagenomic data, and engineering them to target bacteria of interest. This takes advantage of a database constructed by Dr. Benjamin Joris (85), which contains thousands of conjugative systems identified in metagenomic data from the human gut microbiome. This represents a "sequence-to-synthesis" approach to functional metagenomics based on our foundational understanding of conjugative systems. Within this database, we identified a contig sourced from a *Citrobacter* isolate that appeared to encode a complete conjugative system. I proceeded to have the conjugative portion of this contig synthesized in fragments, and assembled it into a plasmid (p20298-AGE). The first iteration of this plasmid was non-conjugative, and non-replicative in *Citrobacter rodentium*. To approach this challenge, we re-assembled the plasmid into a new backbone which was known to replicate in *C. rodentium*, while simultaneously repairing mutations that occurred during the original synthesis of the plasmid, generating p20298-15a. Successful conjugation of this plasmid proved that we could synthesize functional conjugative systems identified in microbiome data. I proceeded to functionalize this plasmid to allow for rapid cloning of TevCas9 with different sgRNAs. I subsequently tested multiple sgRNAs to prove that p20298-15a could successfully deliver a TevCas9 nuclease for the targeted elimination of *C. rodentium*. These results demonstrate that conjugative systems can be identified from metagenomic data sets, and subsequently functionalized for the delivery of cargo to bacteria of interest. Perhaps more importantly, it serves as a proof-of-principle for the functionalization of large genetic systems in metagenomic data for use in synthetic biology through a DNA synthesis based approach.

Overall this thesis covers two key concepts that are crucial for the targeted elimination of bacteria in communities (Figure 1.2). Firstly, it addresses the problem of targeted delivery via conjugation. Second, it shows that conjugative plasmids can be functionalized to kill by adding a TevCas9 system as cargo. Together, this demonstrates the power of conjugative plasmids as a delivery vector for targeted nucleases to kill bacteria.

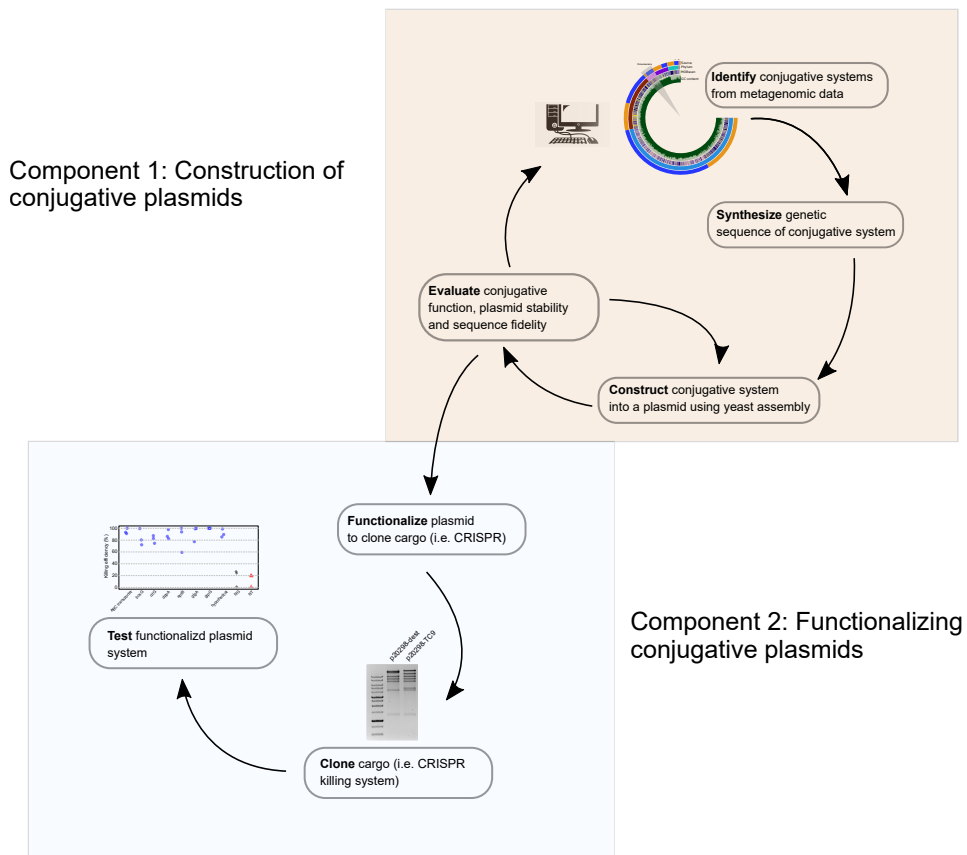


Figure 1.4: Process of constructing and functionalizing conjugative plasmids. The first component is identifying and constructing conjugative systems. The second component is functionalizing conjugative systems for applications, such as engineering plasmids to deliver CRISPR systems to target and kill bacteria.

1.7 References

- [1] Sahar Abubucker, Nicola Segata, Johannes Goll, Alyxandria M Schubert, Jacques Izard, Brandi L Cantarel, Beltran Rodriguez-Mueller, Jeremy Zucker, Mathangi Thiagarajan, Bernard Henrissat, et al. Metabolic reconstruction for metagenomic data and its application to the human microbiome. *PLoS Computational Biology*, 8(6):e1002358, 2012.
- [2] Mads Albertsen, Philip Hugenholtz, Adam Skarshewski, Kåre L Nielsen, Gene W Tyson, and Per H Nielsen. Genome sequences of rare, uncultured bacteria obtained by differential coverage binning of multiple metagenomes. *Nature Biotechnology*, 31(6):533–538, 2013.
- [3] Alexandre Almeida, Alex L Mitchell, Miguel Boland, Samuel C Forster, Gregory B Gloor, Aleksandra Tarkowska, Trevor D Lawley, and Robert D Finn. A new genomic blueprint of the human gut microbiota. *Nature*, 568(7753):499–504, 2019.
- [4] Itxaso Álvarez-Rodríguez, Begoña Ugarte-Uribe, Igor De la Arada, José Luis R Arrondo, Carlos Garbisu, and Itziar Alkorta. Conjugative coupling proteins and the role of their domains in conjugation, secondary structure and *in vivo* subcellular location. *Frontiers in Molecular Biosciences*, 7:185, 2020.
- [5] Emily M Anderson, Amanda Haupt, John A Schiel, Eldon Chou, Hidevaldo B Machado, Žaklina Strezoska, Steve Lenger, Shawn McClelland, Amanda Birmingham, Annaleen Vermeulen, et al. Systematic analysis of CRISPR-Cas9 mismatch tolerance reveals low levels of off-target activity. *Journal of Biotechnology*, 211:56–65, 2015.
- [6] Trond Erik Vee Aune and Finn Lillelund Aachmann. Methodologies to increase the transformation efficiencies and the range of bacteria that can be transformed. *Applied Microbiology and Biotechnology*, 85:1301–1313, 2010.
- [7] Stuart Austin and Kurt Nordström. Partition-mediated incompatibility of bacterial plasmids. *Cell*, 60(3):351–354, 1990.
- [8] Ana Babic, Anne-Marie Guérout, and Didier Mazel. Construction of an improved RP4 (RK2)-based conjugative system. *Research in Microbiology*, 159(7-8):545–549, 2008.
- [9] Barbara J Bachmann, K Brooks Low, and Austin L Taylor. Recalibrated linkage map of *Escherichia coli* k-12. *Bacteriological Reviews*, 40(1):116–167, 1976.
- [10] Martin Iain Bahl, Lars Hestbjerg Hansen, and Søren J Sørensen. Persistence mechanisms of conjugative plasmids. *Horizontal Gene Transfer: Genomes in Flux*, pages 73–102, 2009.
- [11] Bhakti Bajpai. High capacity vectors. *Advances in Biotechnology*, pages 1–10, 2014.
- [12] Rodolphe Barrangou, Christophe Fremaux, H el ene Deveau, Melissa Richards, Patrick Boyaval, Sylvain Moineau, Dennis A Romero, and Philippe Horvath. CRISPR provides acquired resistance against viruses in prokaryotes. *Science*, 315(5819):1709–1712, 2007.
- [13] Pauline M Bennett. Plasmid encoded antibiotic resistance: acquisition and transfer of antibiotic resistance genes in bacteria. *British Journal of Pharmacology*, 153(S1):S347–S357, 2008.

- [14] Fabienne Benz, Jana S Huisman, Erik Bakkeren, Joana A Herter, Tanja Stadler, Martin Ackermann, Médéric Diard, Adrian Egli, Alex R Hall, Wolf-Dietrich Hardt, et al. Plasmid- and strain-specific factors drive variation in ESBL-plasmid spread *in vitro* and *in vivo*. *The ISME journal*, 15(3):862–878, 2021.
- [15] Denis Bertrand, Jim Shaw, Manesh Kalathiyappan, Amanda Hui Qi Ng, M Senthil Kumar, Chenhao Li, Mirta Dvornicic, Janja Paliska Soldo, Jia Yu Koh, Chengxuan Tong, et al. Hybrid metagenomic assembly enables high-resolution analysis of resistance determinants and mobile elements in human microbiomes. *Nature Biotechnology*, 37(8):937–944, 2019.
- [16] David Bikard, Wenyan Jiang, Poulami Samai, Ann Hochschild, Feng Zhang, and Luciano A Marraffini. Programmable repression and activation of bacterial gene expression using an engineered CRISPR-Cas system. *Nucleic Acids Research*, 41(15):7429–7437, 2013.
- [17] David Bikard, Chad W Euler, Wenyan Jiang, Philip M Nussenzweig, Gregory W Goldberg, Xavier Duportet, Vincent A Fischetti, and Luciano A Marraffini. Exploiting CRISPR-Cas nucleases to produce sequence-specific antimicrobials. *Nature Biotechnology*, 32(11):1146, 2014.
- [18] Alexander Bolotin, Benoit Quinquis, Alexei Sorokin, and S Dusko Ehrlich. Clustered regularly interspaced short palindrome repeats (CRISPRs) have spacers of extrachromosomal origin. *Microbiology*, 151(8):2551–2561, 2005.
- [19] Stan JJ Brouns, Matthijs M Jore, Magnus Lundgren, Edze R Westra, Rik JH Slijkhuis, Ambrosius PL Snijders, Mark J Dickman, Kira S Makarova, Eugene V Koonin, and John Van Der Oost. Small CRISPR RNAs guide antiviral defense in prokaryotes. *Science*, 321(5891):960–964, 2008.
- [20] Stephanie L Brumwell, Katherine D Van Belois, Daniel J Giguere, David R Edgell, and Bogumil J Karas. Conjugation-based genome engineering in *Deinococcus radiodurans*. *ACS Synthetic Biology*, 11(3):1068–1076, 2022.
- [21] Julie Burke, David Schneider, and Janet Westpheling. Generalized transduction in *Streptomyces coelicolor*. *Proceedings of the National Academy of Sciences*, 98(11):6289–6294, 2001.
- [22] Alita R Burmeister. Horizontal gene transfer. *Evolution, Medicine, and Public Health*, 2015(1):193–194, 2015.
- [23] Allyson L Byrd, Yasmine Belkaid, and Julia A Segre. The human skin microbiome. *Nature Reviews Microbiology*, 16(3):143–155, 2018.
- [24] E Cabezón, J Ignacio Sastre, and F De La Cruz. Genetic evidence of a coupling role for the TraG protein family in bacterial conjugation. *Molecular and General Genetics MGG*, 254:400–406, 1997.
- [25] Elena Cabezón, Jorge Ripoll-Rozada, Alejandro Peña, Fernando De La Cruz, and Ignacio Arechaga. Towards an integrated model of bacterial conjugation. *FEMS Microbiology Reviews*, 39(1):81–95, 2015.

- [26] Carlos Canchaya, Ghislain Fournous, Sandra Chibani-Chennoufi, Marie-Lise Dillmann, and Harald Brüssow. Phage as agents of lateral gene transfer. *Current Opinion in Microbiology*, 6(4):417–424, 2003.
- [27] Alessandra Carattoli, Alessia Bertini, Laura Villa, Vincenzo Falbo, Katie L Hopkins, and E John Threlfall. Identification of plasmids by PCR-based replicon typing. *Journal of Microbiological Methods*, 63(3):219–228, 2005.
- [28] Eric Cascales and Peter J Christie. The versatile bacterial type IV secretion systems. *Nature Reviews Microbiology*, 1(2):137–149, 2003.
- [29] LL Cavalli, Joshua Lederberg, and Esther M Lederberg. An infective factor controlling sex compatibility in bacterium coli. *Microbiology*, 8(1):89–103, 1953.
- [30] Camilla Ceccarani, Claudio Foschi, Carola Parolin, Antonietta D’Antuono, Valeria Gaspari, Clarissa Consolandi, Luca Laghi, Tania Camboni, Beatrice Vitali, Marco Severgnini, et al. Diversity of vaginal microbiome and metabolome during genital infections. *Scientific Reports*, 9(1):1–12, 2019.
- [31] Michael Chandler, Fernando De La Cruz, Fred Dyda, Alison B Hickman, Gabriel Moncalian, and Bao Ton-Hoang. Breaking and joining single-stranded DNA: the HUH endonuclease superfamily. *Nature Reviews Microbiology*, 11(8):525–538, 2013.
- [32] Mai Huong Chatain-Ly. The factors affecting effectiveness of treatment in phages therapy. *Frontiers in Microbiology*, 5:51, 2014.
- [33] Inês Chen and David Dubnau. DNA uptake during bacterial transformation. *Nature Reviews Microbiology*, 2(3):241–249, 2004.
- [34] Janice S Chen, Enbo Ma, Lucas B Harrington, Maria Da Costa, Xinran Tian, Joel M Palefsky, and Jennifer A Doudna. CRISPR-Cas12a target binding unleashes indiscriminate single-stranded DNase activity. *Science*, 360(6387):436–439, 2018.
- [35] Gong Cheng, Yongfei Hu, Yeshe Yin, Xi Yang, Chunsheng Xiang, Baohong Wang, Yanfei Chen, Fengling Yang, Fang Lei, Na Wu, et al. Functional screening of antibiotic resistance genes from human gut microbiota reveals a novel gene fusion. *FEMS Microbiology Letters*, 336(1):11–16, 2012.
- [36] Regine Cherazard, Marcia Epstein, Thien-Ly Doan, Tanzila Salim, Sheena Bharti, and Miriam A Smith. Antimicrobial resistant *Streptococcus pneumoniae*: prevalence, mechanisms, and clinical implications. *American Journal of Therapeutics*, 24(3):e361–e369, 2017.
- [37] Sandra Chibani-Chennoufi, Josette Sidoti, Anne Bruttin, Elizabeth Kutter, Shafiq Sarker, and Harald Brüssow. *In vitro* and *in vivo* bacteriolytic activities of *Escherichia coli* phages: implications for phage therapy. *Antimicrobial Agents and Chemotherapy*, 48(7):2558–2569, 2004.

- [38] Mary-Dell Chilton, Martin H Drummond, Donald J Merlo, Daniela Sciaky, Alice L Montoya, Milton P Gordon, and Eugene W Nester. Stable incorporation of plasmid DNA into higher plant cells: the molecular basis of crown gall tumorigenesis. *Cell*, 11(2):263–271, 1977.
- [39] Ilseung Cho and Martin J Blaser. The human microbiome: at the interface of health and disease. *Nature Reviews Genetics*, 13(4):260, 2012.
- [40] Robert J Citorik, Mark Mimee, and Timothy K Lu. Sequence-specific antimicrobials using efficiently delivered RNA-guided nucleases. *Nature Biotechnology*, 32(11):1141, 2014.
- [41] Ryan R Cochrane, Arina Shrestha, Mariana M Severo de Almeida, Michelle Agyare-Tabbi, Stephanie L Brumwell, Samir Hamadache, Jordyn S Meaney, Daniel P Nucifora, Henry Heng Say, Jehoshua Sharma, et al. Superior conjugative plasmids delivered by bacteria to diverse fungi. *BioDesign Research*, 2022, 2022.
- [42] Marta Colomer-Lluch, Juan Jofre, and Maite Muniesa. Antibiotic resistance genes in the bacteriophage DNA fraction of environmental samples. *PloS One*, 6(3):e17549, 2011.
- [43] Guy R Cornelis, Anne Boland, Aoife P Boyd, Cecile Geuijen, Maite Iriarte, Cécile Neyt, Marie-Paule Sory, and Isabelle Stainier. The virulence plasmid of *Yersinia*, an antihost genome. *Microbiology and Molecular Biology Reviews*, 62(4):1315–1352, 1998.
- [44] SP Costello, W Soo, RV Bryant, V Jairath, AL Hart, and JM Andrews. Systematic review with meta-analysis: faecal microbiota transplantation for the induction of remission for active ulcerative colitis. *Alimentary Pharmacology & Therapeutics*, 46(3):213–224, 2017.
- [45] MARTINE Couturier, Françoise Bex, Peter L Bergquist, and Werner K Maas. Identification and classification of bacterial plasmids. *Microbiological Reviews*, 52(3):375–395, 1988.
- [46] Lun Cui and David Bikard. Consequences of Cas9 cleavage in the chromosome of *Escherichia coli*. *Nucleic Acids Research*, 44(9):4243–4251, 2016.
- [47] Anna Cuscó, Daniel Pérez, Joaquim Viñes, Norma Fàbregas, and Olga Francino. Long-read metagenomics retrieves complete single-contig bacterial genomes from canine feces. *BMC Genomics*, 22(1):330, 2021.
- [48] Jacqueline Deen, Martin A Mengel, and John D Clemens. Epidemiology of cholera. *Vaccine*, 38:A31–A40, 2020.
- [49] Gloria Del Solar and Manuel Espinosa. Plasmid copy number control: an ever-growing story. *Molecular Microbiology*, 37(3):492–500, 2000.
- [50] Floyd E Dewhirst, Tuste Chen, Jacques Izard, Bruce J Paster, Anne CR Tanner, Wen-Han Yu, Abirami Lakshmanan, and William G Wade. The human oral microbiome. *Journal of Bacteriology*, 192(19):5002–5017, 2010.
- [51] Elizabeth A Dinsdale, Robert A Edwards, Dana Hall, Florent Angly, Mya Breitbart, Jennifer M Brulc, Mike Furlan, Christelle Desnues, Matthew Haynes, Linlin Li, et al. Functional metagenomic profiling of nine biomes. *Nature*, 452(7187):629–632, 2008.

- [52] F Dionisio, IC Conceicao, ACR Marques, L Fernandes, and I Gordo. The evolution of a conjugative plasmid and its ability to increase bacterial fitness. *Biology Letters*, 1(2):250–252, 2005.
- [53] Paul B Eckburg, Elisabeth M Bik, Charles N Bernstein, Elizabeth Purdom, Les Dethlefsen, Michael Sargent, Steven R Gill, Karen E Nelson, and David A Relman. Diversity of the human intestinal microbial flora. *Science*, 308(5728):1635–1638, 2005.
- [54] Raúl Fernández-López, M Pilar Garcillán-Barcia, Carlos Revilla, Miguel Lázaro, Luis Vielva, and Fernando De La Cruz. Dynamics of the IncW genetic backbone imply general trends in conjugative plasmid evolution. *FEMS Microbiology Reviews*, 30(6):942–966, 2006.
- [55] Kevin J Forsberg, Ishan V Bhatt, Danica T Schmidtke, Kamyab Javanmardi, Kaylee E Dillard, Barry L Stoddard, Ilya J Finkelstein, Brett K Kaiser, and Harmit S Malik. Functional metagenomics-guided discovery of potent Cas9 inhibitors in the human microbiome. *elife*, 8:e46540, 2019.
- [56] Timothy J Foster. Antibiotic resistance in *Staphylococcus aureus*. Current status and future prospects. *FEMS Microbiology Reviews*, 41(3):430–449, 2017.
- [57] Rena Fukunaga, Philippe Glaziou, Jennifer B Harris, Anand Date, Katherine Floyd, and Tereza Kasaeva. Epidemiology of tuberculosis and progress toward meeting global targets—worldwide, 2019. *Morbidity and Mortality Weekly Report*, 70(12):427, 2021.
- [58] M Pilar Garcillán-Barcia and Fernando de la Cruz. Why is entry exclusion an essential feature of conjugative plasmids? *Plasmid*, 60(1):1–18, 2008.
- [59] M Pilar Garcillán-Barcia, Santiago Redondo-Salvo, Luis Vielva, and Fernando de la Cruz. MOBscan: automated annotation of MOB relaxases. *Horizontal Gene transfer: Methods and Protocols*, pages 295–308, 2020.
- [60] María Pilar Garcillán-Barcia, María Victoria Francia, and Fernando de La Cruz. The diversity of conjugative relaxases and its application in plasmid classification. *FEMS Microbiology Reviews*, 33(3):657–687, 2009.
- [61] Josiane E Garneau, Marie-Ève Dupuis, Manuela Villion, Dennis A Romero, Rodolphe Barrangou, Patrick Boyaval, Christophe Fremaux, Philippe Horvath, Alfonso H Magadán, and Sylvain Moineau. The CRISPR/Cas bacterial immune system cleaves bacteriophage and plasmid DNA. *Nature*, 468(7320):67, 2010.
- [62] Nicole M Gaudelli, Alexis C Komor, Holly A Rees, Michael S Packer, Ahmed H Badran, David I Bryson, and David R Liu. Programmable base editing of a•t to g•c in genomic dna without dna cleavage. *Nature*, 551(7681):464–471, 2017.
- [63] Jean-Marc Ghigo. Natural conjugative plasmids induce bacterial biofilm development. *Nature*, 412(6845):442, 2001.

- [64] Ahmed A Gomaa, Heidi E Klumpe, Michelle L Luo, Kurt Selle, Rodolphe Barrangou, and Chase L Beisel. Programmable removal of bacterial strains by use of genome-targeting CRISPR-Cas systems. *MBio*, 5(1):e00928–13, 2014.
- [65] Fred Griffith. The significance of pneumococcal types. *Epidemiology & Infection*, 27(2): 113–159, 1928.
- [66] Alicia Guasch, María Lucas, Gabriel Moncalián, Matilde Cabezas, Rosa Pérez-Luque, F Xavier Gomis-Rüth, Fernando De la Cruz, and Miquel Coll. Recognition and processing of the origin of transfer DNA by conjugative relaxase TrwC. *Nature Structural & Molecular Biology*, 10(12):1002–1010, 2003.
- [67] Mohamed Hafez and Georg Hausner. Homing endonucleases: DNA scissors on a mission. *Genome*, 55(8):553–569, 2012.
- [68] Jonas Halfvarson, Colin J Brislawn, Regina Lamendella, Yoshiki Vázquez-Baeza, William A Walters, Lisa M Bramer, Mauro D’amato, Ferdinando Bonfiglio, Daniel McDonald, Antonio Gonzalez, et al. Dynamics of the human gut microbiome in inflammatory bowel disease. *Nature Microbiology*, 2(5):1–7, 2017.
- [69] Jo Handelsman, Michelle R Rondon, Sean F Brady, Jon Clardy, and Robert M Goodman. Molecular biological access to the chemistry of unknown soil microbes: a new frontier for natural products. *Chemistry & Biology*, 5(10):R245–R249, 1998.
- [70] Ellie Harrison and Michael A Brockhurst. Plasmid-mediated horizontal gene transfer is a coevolutionary process. *Trends in Microbiology*, 20(6):262–267, 2012.
- [71] Hsing-I Ho, Jennifer R Fang, Jacky Cheung, and Harris H Wang. Programmable CRISPR-Cas transcriptional activation in bacteria. *Molecular Systems Biology*, 16(7):e9427, 2020.
- [72] Karen Ho. Bacteriophage therapy for bacterial infections: rekindling a memory from the pre-antibiotics era. *Perspectives in Biology and Medicine*, 44(1):1–16, 2001.
- [73] Philippe Horvath and Rodolphe Barrangou. CRISPR/Cas, the immune system of bacteria and archaea. *Science*, 327(5962):167–170, 2010.
- [74] Philippe Horvath, Dennis A Romero, Anne-Claire Coûté-Monvoisin, Melissa Richards, Hélene Deveau, Sylvain Moineau, Patrick Boyaval, Christophe Fremaux, and Rodolphe Barrangou. Diversity, activity, and evolution of crisper loci in streptococcus thermophilus. *Journal of bacteriology*, 190(4):1401–1412, 2008.
- [75] Patrick D Hsu, David A Scott, Joshua A Weinstein, F Ann Ran, Silvana Konermann, Vineeta Agarwala, Yinqing Li, Eli J Fine, Xuebing Wu, Ophir Shalem, et al. DNA targeting specificity of RNA-guided Cas9 nucleases. *Nature Biotechnology*, 31(9):827–832, 2013.
- [76] Kevin S Ikuta, Lucien R Swetschinski, Gisela Robles Aguilar, Fablina Sharara, Tomislav Mestrovic, Authia P Gray, Nicole Davis Weaver, Eve E Wool, Chieh Han, Anna Gershberg Hayoon, et al. Global mortality associated with 33 bacterial pathogens in 2019: a systematic analysis for the Global Burden of Disease Study 2019. *The Lancet*, 400(10369):2221–2248, 2022.

- [77] Yoshizumi Ishino, Hideo Shinagawa, Kozo Makino, Mitsuko Amemura, and Atsuo Nakata. Nucleotide sequence of the *iap* gene, responsible for alkaline phosphatase isozyme conversion in *Escherichia coli*, and identification of the gene product. *Journal of bacteriology*, 169(12):5429–5433, 1987.
- [78] Aayushi Jain and Preeti Srivastava. Broad host range plasmids. *FEMS Microbiology Letters*, 348(2):87–96, 2013.
- [79] Ruud Jansen, Jan DA van Embden, Wim Gaastra, and Leo M Schouls. Identification of genes that are associated with DNA repeats in prokaryotes. *Molecular Microbiology*, 43(6):1565–1575, 2002.
- [80] Wenyan Jiang, David Bikard, David Cox, Feng Zhang, and Luciano A Marraffini. RNA-guided editing of bacterial genomes using CRISPR-Cas systems. *Nature Biotechnology*, 31(3):233–239, 2013.
- [81] Martin Jinek, Krzysztof Chylinski, Ines Fonfara, Michael Hauer, Jennifer A Doudna, and Emmanuelle Charpentier. A programmable dual-RNA-guided DNA endonuclease in adaptive bacterial immunity. *Science*, page 1225829, 2012.
- [82] Nathan I Johns, Antonio LC Gomes, Sung Sun Yim, Anthony Yang, Tomasz Blazejewski, Christopher S Smillie, Mark B Smith, Eric J Alm, Sriram Kosuri, and Harris H Wang. Metagenomic mining of regulatory elements enables programmable species-selective gene expression. *Nature Methods*, 15(5):323–329, 2018.
- [83] Timothy J Johnson and Lisa K Nolan. Pathogenomics of the virulence plasmids of *Escherichia coli*. *Microbiology and Molecular Biology Reviews*, 73(4):750–774, 2009.
- [84] Brian V Jones, Máire Begley, Colin Hill, Cormac GM Gahan, and Julian R Marchesi. Functional and comparative metagenomic analysis of bile salt hydrolase activity in the human gut microbiome. *Proceedings of the National Academy of Sciences*, 105(36):13580–13585, 2008.
- [85] Benjamin R Joris. *Towards more complete metagenomic analyses through circularized genomes and conjugative elements*. PhD thesis, The University of Western Ontario, 2022.
- [86] K Jv Joshipura, EB Rimm, CW Douglass, D Trichopoulos, A Ascherio, and WC Willett. Poor oral health and coronary heart disease. *Journal of Dental Research*, 75(9):1631–1636, 1996.
- [87] J Keith Joung and Jeffry D Sander. TALENs: a widely applicable technology for targeted genome editing. *Nature Reviews Molecular Cell Biology*, 14(1):49–55, 2013.
- [88] Bogumil J Karas, Rachel E Diner, Stephane C Lefebvre, Jeff McQuaid, Alex PR Phillips, Chari M Noddings, John K Brunson, Ruben E Valas, Thomas J Deerinck, Jelena Jablanovic, et al. Designer diatom episomes delivered by bacterial conjugation. *Nature Communications*, 6:6925, 2015.

- [89] Patrick J Keeling and Jeffrey D Palmer. Horizontal gene transfer in eukaryotic evolution. *Nature Reviews Genetics*, 9(8):605–618, 2008.
- [90] Saleem A Khan. Plasmid rolling-circle replication: highlights of two decades of research. *Plasmid*, 53(2):126–136, 2005.
- [91] Benjamin P Kleinstiver, Michelle S Prew, Shengdar Q Tsai, Nhu T Nguyen, Ved V Topkar, Zongli Zheng, and J Keith Joung. Broadening the targeting range of staphylococcus aureus crisper-cas9 by modifying pam recognition. *Nature Biotechnology*, 33(12):1293–1298, 2015.
- [92] Benjamin P Kleinstiver, Michelle S Prew, Shengdar Q Tsai, Ved V Topkar, Nhu T Nguyen, Zongli Zheng, Andrew PW Gonzales, Zhuyun Li, Randall T Peterson, Jing-Ruey Joanna Yeh, et al. Engineered crisper-cas9 nucleases with altered pam specificities. *Nature*, 523(7561):481–485, 2015.
- [93] Benjamin P Kleinstiver, Vikram Pattanayak, Michelle S Prew, Shengdar Q Tsai, Nhu T Nguyen, Zongli Zheng, and J Keith Joung. High-fidelity CRISPR–Cas9 nucleases with no detectable genome-wide off-target effects. *Nature*, 529(7587):490–495, 2016.
- [94] Eugene V Koonin, Kira S Makarova, and Feng Zhang. Diversity, classification and evolution of CRISPR-Cas systems. *Current Opinion in Microbiology*, 37:67–78, 2017.
- [95] Günther Koraimann. Spread and persistence of virulence and antibiotic resistance genes: a ride on the F plasmid conjugation module. *EcoSal Plus*, 8(1), 2018.
- [96] Kaitlyn E Kortright, Benjamin K Chan, Jonathan L Koff, and Paul E Turner. Phage therapy: a renewed approach to combat antibiotic-resistant bacteria. *Cell Host & Microbe*, 25(2): 219–232, 2019.
- [97] Sriram Kosuri and George M Church. Large-scale *de novo* DNA synthesis: technologies and applications. *Nature Methods*, 11(5):499–507, 2014.
- [98] Victor Kunin and Christos A Ouzounis. The balance of driving forces during genome evolution in prokaryotes. *Genome Research*, 13(7):1589–1594, 2003.
- [99] Kathy N Lam, JiuJun Cheng, Katja Engel, Josh D Neufeld, and Trevor C Charles. Current and future resources for functional metagenomics. *Frontiers in Microbiology*, 6:1196, 2015.
- [100] Matthew H Larson, Luke A Gilbert, Xiaowo Wang, Wendell A Lim, Jonathan S Weissman, and Lei S Qi. Crispr interference (crispr) for sequence-specific control of gene expression. *Nature protocols*, 8(11):2180–2196, 2013.
- [101] Adriel Latorre-Pérez, Pascual Villalba-Bermell, Javier Pascual, and Cristina Vilanova. Assembly methods for nanopore-based metagenomic sequencing: a comparative study. *Scientific Reports*, 10(1):13588, 2020.
- [102] Sébastien Leclercq, Clément Gilbert, and Richard Cordaux. Cargo capacity of phages and plasmids and other factors influencing horizontal transfers of prokaryote transposable elements. *Mobile Genetic Elements*, 2(2):115–118, 2012.

- [103] Joshua Lederberg. Cell genetics and hereditary symbiosis. *Physiological Reviews*, 32(4): 403–430, 1952.
- [104] Joshua Lederberg and Edward L Tatum. Gene recombination in *Escherichia coli*. *Nature*, 158(4016):558, 1946.
- [105] Joshua Lederberg, Luigi L Cavalli, and Esther M Lederberg. Sex compatibility in *Escherichia coli*. *Genetics*, 37(6):720, 1952.
- [106] Karla A Lee, Andrew Maltez Thomas, Laura A Bolte, Johannes R Björk, Laura Kist de Ruijter, Federica Armanini, Francesco Asnicar, Aitor Blanco-Miguez, Ruth Board, Neus Calbet-Llopart, et al. Cross-cohort gut microbiome associations with immune checkpoint inhibitor response in advanced melanoma. *Nature Medicine*, 28(3):535–544, 2022.
- [107] Patricia Lepage, Robert Häslér, Martina E Spehlmann, Ateequr Rehman, Aida Zvirbliene, Alexander Begun, Stephan Ott, Limas Kupcinskis, Joël Doré, Andreas Raedler, et al. Twin study indicates loss of interaction between microbiota and mucosa of patients with ulcerative colitis. *Gastroenterology*, 141(1):227–236, 2011.
- [108] Ruth E Ley, Fredrik Bäckhed, Peter Turnbaugh, Catherine A Lozupone, Robin D Knight, and Jeffrey I Gordon. Obesity alters gut microbial ecology. *Proceedings of the National Academy of Sciences*, 102(31):11070–11075, 2005.
- [109] Shi-Yuan Li, Qiu-Xiang Cheng, Jia-Kun Liu, Xiao-Qun Nie, Guo-Ping Zhao, and Jin Wang. CRISPR-Cas12a has both *cis*- and *trans*-cleavage activities on single-stranded DNA. *Cell Research*, 28(4):491–493, 2018.
- [110] Joshua Lilly and Manel Camps. Mechanisms of theta plasmid replication. *Plasmids: Biology and Impact in Biotechnology and Discovery*, pages 33–44, 2015.
- [111] Matxalen Llosa, F Xavier Gomis-Rüth, Miquel Coll, and Fernando de la Cruz. Bacterial conjugation: a two-step mechanism for DNA transport. *Molecular Microbiology*, 45(1): 1–8, 2002.
- [112] Wen Wen Low, Joshua LC Wong, Leticia C Beltran, Chloe Seddon, Sophia David, Hok-Sau Kwong, Tatiana Bizeau, Fengbin Wang, Alejandro Peña, Tiago RD Costa, et al. Mating pair stabilization mediates bacterial conjugation species specificity. *Nature Microbiology*, 7(7): 1016–1027, 2022.
- [113] IA MacNeil, CL Tiong, C Minor, PR August, TH Grossman, KA Loiacono, BA Lynch, T Phillips, S Narula, R Sundaramoorthi, et al. Expression and isolation of antimicrobial small molecules from soil dna libraries. *Journal of Molecular Microbiology and Biotechnology*, 3(2):301–308, 2001.
- [114] Morgan L Maeder, Samantha J Linder, Vincent M Cascio, Yanfang Fu, Quan H Ho, and J Keith Joung. Crispr rna-guided activation of endogenous human genes. *Nature Methods*, 10(10):977–979, 2013.

- [115] Prashant Mali, John Aach, P Benjamin Stranges, Kevin M Esvelt, Mark Moosburner, Sri-ram Kosuri, Luhan Yang, and George M Church. Cas9 transcriptional activators for target specificity screening and paired nickases for cooperative genome engineering. *Nature Biotechnology*, 31(9):833–838, 2013.
- [116] Prashant Mali, Luhan Yang, Kevin M Esvelt, John Aach, Marc Guell, James E DiCarlo, Julie E Norville, and George M Church. RNA-guided human genome engineering via Cas9. *Science*, 339(6121):823–826, 2013.
- [117] R Mazaheri Nezhad Fard, MD Barton, and MW Heuzenroeder. Bacteriophage-mediated transduction of antibiotic resistance in enterococci. *Letters in Applied Microbiology*, 52(6):559–564, 2011.
- [118] D Mazel and J Davies. Antibiotic resistance in microbes. *Cellular and Molecular Life Sciences CMLS*, 56:742–754, 1999.
- [119] Alexandra Meziti, Luis M Rodriguez-R, Janet K Hatt, Angela Peña-Gonzalez, Karen Levy, and Konstantinos T Konstantinidis. The reliability of metagenome-assembled genomes (MAGs) in representing natural populations: insights from comparing MAGs against isolate genomes derived from the same fecal sample. *Applied and Environmental Microbiology*, 87(6):e02593–20, 2021.
- [120] Marcus Miethke, Marco Pieroni, Tilmann Weber, Mark Brönstrup, Peter Hammann, Ludovic Halby, Paola B Arimondo, Philippe Glaser, Bertrand Aigle, Helge B Bode, et al. Towards the sustainable discovery and development of new antibiotics. *Nature Reviews Chemistry*, 5(10):726–749, 2021.
- [121] Salvador Mirete, Veronica Morgante, and José Eduardo González-Pastor. Functional metagenomics of extreme environments. *Current Opinion in Biotechnology*, 38:143–149, 2016.
- [122] Francisco JM Mojica, César Díez-Villaseñor, Jesús García-Martínez, and Cristóbal Almendros. Short motif sequences determine the targets of the prokaryotic CRISPR defence system. *Microbiology*, 155(3):733–740, 2009.
- [123] Stephen S Morse. Joshua Lederberg (1925-2008). *Science*, 319(5868):1351–1351, 2008.
- [124] Michael J Moser, Robert A DiFrancesco, Krishne Gowda, Audrey J Klingele, Darby R Sugar, Stacy Stocki, David A Mead, and Thomas W Schoenfeld. Thermostable DNA polymerase from a viral metagenome is a potent RT-PCR enzyme. *PLoS One*, 7(6):e38371, 2012.
- [125] Christopher JL Murray, Kevin Shunji Ikuta, Fablina Sharara, Lucien Swetschinski, Gisela Robles Aguilar, Authia Gray, Chieh Han, Catherine Bisignano, Puja Rao, Eve Wool, et al. Global burden of bacterial antimicrobial resistance in 2019: a systematic analysis. *The Lancet*, 399(10325):629–655, 2022.

- [126] Kevin Neil, Nancy Allard, Patricia Roy, Frédéric Grenier, Alfredo Menendez, Vincent Burrus, and Sébastien Rodrigue. High-efficiency delivery of CRISPR-Cas9 by engineered probiotics enables precise microbiome editing. *Molecular Systems Biology*, 17(10):e10335, 2021.
- [127] Richard P Novick. Plasmid incompatibility. *Microbiological Reviews*, 51(4):381–395, 1987.
- [128] Teru Ogura and Sota Hiraga. Mini-F plasmid genes that couple host cell division to plasmid proliferation. *Proceedings of the National Academy of Sciences*, 80(15):4784–4788, 1983.
- [129] Preeti Pachori, Ragini Goyal, and Puneet Gandhi. Emergence of antibiotic resistance *Pseudomonas aeruginosa* in intensive care unit; a critical review. *Genes & Diseases*, 6(2): 109–119, 2019.
- [130] Werner Pansegrau, Erich Lanka, Peter T Barth, David H Figurski, Donald G Guiney, Dieter Haas, Donald R Helinski, Helmut Schwab, Vilma A Stanisich, and Christopher M Thomas. Complete nucleotide sequence of birmingham IncP α plasmids: compilation and comparative analysis. *Journal of Molecular Biology*, 239(5):623–663, 1994.
- [131] Donovan H Parks, Christian Rinke, Maria Chuvochina, Pierre-Alain Chaumeil, Ben J Woodcroft, Paul N Evans, Philip Hugenholtz, and Gene W Tyson. Recovery of nearly 8,000 metagenome-assembled genomes substantially expands the tree of life. *Nature Microbiology*, 2(11):1533–1542, 2017.
- [132] Vikram Pattanayak, Steven Lin, John P Guilinger, Enbo Ma, Jennifer A Doudna, and David R Liu. High-throughput profiling of off-target DNA cleavage reveals RNA-programmed Cas9 nuclease specificity. *Nature Biotechnology*, 31(9):839–843, 2013.
- [133] Gisele Peirano, Liang Chen, Barry N Kreiswirth, and Johann DD Pitout. Emerging antimicrobial-resistant high-risk *Klebsiella pneumoniae* clones ST307 and ST147. *Antimicrobial Agents and Chemotherapy*, 64(10):e01148–20, 2020.
- [134] Gregory M Pellegrino, Tyler S Browne, Keerthana Sharath, Khaleda A Bari, Sarah J Van-curen, Emma Allen-Vercoe, Gregory B Gloor, and David R Edgell. Metabolically-targeted dCas9 expression in bacteria. *Nucleic Acids Research*, 2023.
- [135] Kathryn J Pflughoeft and James Versalovic. Human microbiome in health and disease. *Annual Review of Pathology: Mechanisms of Disease*, 7:99–122, 2012.
- [136] Radoslaw Pluta, D Roeland Boer, Fabián Lorenzo-Díaz, Silvia Russi, Hansel Gómez, Cris Fernández-López, Rosa Pérez-Luque, Modesto Orozco, Manuel Espinosa, and Miquel Coll. Structural basis of a histidine-DNA nicking/joining mechanism for gene transfer and promiscuous spread of antibiotic resistance. *Proceedings of the National Academy of Sciences*, 114(32):E6526–E6535, 2017.
- [137] Laurent Poirel, Jean-Yves Madec, Agnese Lupo, Anne-Kathrin Schink, Nicolas Kieffer, Patrice Nordmann, and Stefan Schwarz. Antimicrobial resistance in *Escherichia coli*. *Microbiology Spectrum*, 6(4):6–4, 2018.

- [138] Michael B Prentice and Lila Rahalison. Plague. *The Lancet*, 369(9568):1196–1207, 2007.
- [139] Lei S Qi, Matthew H Larson, Luke A Gilbert, Jennifer A Doudna, Jonathan S Weissman, Adam P Arkin, and Wendell A Lim. Repurposing CRISPR as an RNA-guided platform for sequence-specific control of gene expression. *Cell*, 152(5):1173–1183, 2013.
- [140] Jiuxin Qu, Neha K Prasad, Michelle A Yu, Shuyan Chen, Amy Lyden, Nadia Herrera, Melanie R Silvis, Emily Crawford, Mark R Looney, Jason M Peters, et al. Modulating pathogenesis with mobile-CRISPRi. *Journal of Bacteriology*, 201(22):e00304–19, 2019.
- [141] Christopher Quince, Alan W Walker, Jared T Simpson, Nicholas J Loman, and Nicola Segata. Shotgun metagenomics, from sampling to analysis. *Nature Biotechnology*, 35(9):833–844, 2017.
- [142] F Ann Ran, Patrick D Hsu, Chie-Yu Lin, Jonathan S Gootenberg, Silvana Konermann, Alexandro E Trevino, David A Scott, Azusa Inoue, Shogo Matoba, Yi Zhang, et al. Double nicking by RNA-guided CRISPR Cas9 for enhanced genome editing specificity. *Cell*, 154(6):1380–1389, 2013.
- [143] F Ann Ran, Patrick D Hsu, Jason Wright, Vineeta Agarwala, David A Scott, and Feng Zhang. Genome engineering using the CRISPR-Cas9 system. *Nature Protocols*, 8(11):2281–2308, 2013.
- [144] F Ann Ran, Le Cong, Winston X Yan, David A Scott, Jonathan S Gootenberg, Andrea J Kriz, Bernd Zetsche, Ophir Shalem, Xuebing Wu, Kira S Makarova, et al. *In vivo* genome editing using *Staphylococcus aureus* Cas9. *Nature*, 520(7546):186, 2015.
- [145] Michael JA Reid, Nimalan Arinaminpathy, Amy Bloom, Barry R Bloom, Catharina Boehme, Richard Chaisson, Daniel P Chin, Gavin Churchyard, Helen Cox, Lucica Ditiu, et al. Building a tuberculosis-free world: The Lancet Commission on tuberculosis. *The Lancet*, 393(10178):1331–1384, 2019.
- [146] Jerónimo Rodríguez-Beltrán, Javier DelaFuente, Ricardo Leon-Sampedro, R Craig MacLean, and Alvaro San Millan. Beyond horizontal gene transfer: the role of plasmids in bacterial evolution. *Nature Reviews Microbiology*, 19(6):347–359, 2021.
- [147] Rafael Rotger and Josep Casadesús. The virulence plasmids of *Salmonella*. *International Microbiology*, 2:177–184, 1999.
- [148] Sara Samperio, Dolores L Guzmán-Herrador, Rigoberto May-Cuz, Maria Cruz Martín, Miguel A Álvarez, and Matxalen Llosa. Conjugative DNA transfer from *e. coli* to transformation-resistant *Lactobacilli*. *Frontiers in Microbiology*, 12:606629, 2021.
- [149] Naseer Sangwan, Fangfang Xia, and Jack A Gilbert. Recovering complete and draft population genomes from metagenome datasets. *Microbiome*, 4(1):1–11, 2016.
- [150] Dwayne C Savage. Microbial ecology of the gastrointestinal tract. *Annual Review of Microbiology*, 31(1):107–133, 1977.

- [151] Robert F Schwabe and Christian Jobin. The microbiome and cancer. *Nature Reviews Cancer*, 13(11):800–812, 2013.
- [152] Cory Schwarz, Jacques Mathieu, Jenny A Laverde Gomez, Pingfeng Yu, and Pedro JJ Alvarez. Renaissance for phage-based bacterial control. *Environmental Science & Technology*, 56(8):4691–4701, 2021.
- [153] Ron Sender, Shai Fuchs, and Ron Milo. Revised estimates for the number of human and bacteria cells in the body. *PLoS Biology*, 14(8):e1002533, 2016.
- [154] Samuel S Slattery, Andrew Diamond, Helen Wang, Jasmine A Therrien, Jeremy T Lant, Teah Jazey, Kyle Lee, Zachary Klassen, Isabel Desgagné-Penix, Bogumil J Karas, et al. An expanded plasmid-based genetic toolbox enables Cas9 genome editing and stable maintenance of synthetic pathways in *Phaeodactylum tricornutum*. *ACS Synthetic Biology*, 7(2): 328–338, 2018.
- [155] Ian M Slaymaker, Linyi Gao, Bernd Zetsche, David A Scott, Winston X Yan, and Feng Zhang. Rationally engineered cas9 nucleases with improved specificity. *Science*, 351(6268): 84–88, 2016.
- [156] Maximillian PM Soltysiak, Rebecca S Meaney, Samir Hamadache, Preetam Janakirama, David R Edgell, and Bogumil J Karas. Trans-kingdom conjugation within solid media from *Escherichia coli* to *Saccharomyces cerevisiae*. *International Journal of Molecular Sciences*, 20(20):5212, 2019.
- [157] Brynne C Stanton, Alec AK Nielsen, Alvin Tamsir, Kevin Clancy, Todd Peterson, and Christopher A Voigt. Genomic mining of prokaryotic repressors for orthogonal logic gates. *Nature Chemical Biology*, 10(2):99–105, 2014.
- [158] Jonathan M Stokes, Kevin Yang, Kyle Swanson, Wengong Jin, Andres Cubillos-Ruiz, Nina M Donghia, Craig R MacNair, Shawn French, Lindsey A Carfrae, Zohar Bloom-Ackermann, et al. A deep learning approach to antibiotic discovery. *Cell*, 180(4):688–702, 2020.
- [159] Trine Aakvik Strand, Rahmi Lale, Kristin Fløgstad Degnes, Malin Lando, and Svein Valla. A new and improved host-independent plasmid system for RK2-based conjugal transfer. *PloS One*, 9(3):e90372, 2014.
- [160] Steven C Strutt, Rachel M Torrez, Emine Kaya, Oscar A Negrete, and Jennifer A Doudna. RNA-dependent RNA targeting by CRISPR-Cas9. *elife*, 7:e32724, 2018.
- [161] Tianyuan Su, Qi Guo, Yi Zheng, Quanfeng Liang, Qian Wang, and Qingsheng Qi. Fine-tuning of hemb using CRISPRi for increasing 5-aminolevulinic acid production in *Escherichia coli*. *Frontiers in Microbiology*, 10:1731, 2019.
- [162] Marc A Sze and Patrick D Schloss. Looking for a signal in the noise: revisiting obesity and the microbiome. *MBio*, 7(4):e01018–16, 2016.

- [163] Thomas Thisted and Kenn Gerdes. Mechanism of post-segregational killing by the hok/sok system of plasmid R1: Sok antisense RNA regulates hok gene expression indirectly through the overlapping mok gene. *Journal of Molecular Biology*, 223(1):41–54, 1992.
- [164] Maomeng Tong, Xiaoxiao Li, Laura Wegener Parfrey, Bennett Roth, Andrew Ippoliti, Bo Wei, James Borneman, Dermot PB McGovern, Daniel N Frank, Ellen Li, et al. A modular organization of the human intestinal mucosal microbiota and its association with inflammatory bowel disease. *PLoS One*, 8(11):e80702, 2013.
- [165] Gloria Torres-Cortés, Vicenta Millán, Hugo C Ramírez-Saad, Rafael Nisa-Martínez, Nicolás Toro, and Francisco Martínez-Abarca. Characterization of novel antibiotic resistance genes identified by functional metagenomics on soil samples. *Environmental Microbiology*, 13(4): 1101–1114, 2011.
- [166] Ching-Hung Tseng and Chun-Ying Wu. The gut microbiome in obesity. *Journal of the Formosan Medical Association*, 118:S3–S9, 2019.
- [167] Peter J Turnbaugh, Ruth E Ley, Michael A Mahowald, Vincent Magrini, Elaine R Mardis, and Jeffrey I Gordon. An obesity-associated gut microbiome with increased capacity for energy harvest. *Nature*, 444(7122):1027–1031, 2006.
- [168] Fyodor D Urnov, Edward J Rebar, Michael C Holmes, H Steve Zhang, and Philip D Gregory. Genome editing with engineered zinc finger nucleases. *Nature Reviews Genetics*, 11(9): 636–646, 2010.
- [169] C Lee Ventola. The antibiotic resistance crisis: part 1: causes and threats. *Pharmacy and Therapeutics*, 40(4):277, 2015.
- [170] Alexander Wagner, Rachel J Whitaker, David J Krause, Jan-Hendrik Heilers, Marleen Van Wolferen, Chris Van Der Does, and Sonja-Verena Albers. Mechanisms of gene flow in archaea. *Nature Reviews Microbiology*, 15(8):492–501, 2017.
- [171] Matthew K Waldor and John J Mekalanos. Lysogenic conversion by a filamentous phage encoding cholera toxin. *Science*, 272(5270):1910–1914, 1996.
- [172] Russell T Walton, Kathleen A Christie, Madelynn N Whittaker, and Benjamin P Kleinstiver. Unconstrained genome targeting with near-PAMless engineered CRISPR-Cas9 variants. *Science*, 368(6488):290–296, 2020.
- [173] Baohong Wang, Mingfei Yao, Longxian Lv, Zongxin Ling, and Lanjuan Li. The human microbiota in health and disease. *Engineering*, 3(1):71–82, 2017.
- [174] Yinghong Wang, Diana H Wiesnoski, Beth A Helmink, Vancheswaran Gopalakrishnan, Kati Choi, Hebert L DuPont, Zhi-Dong Jiang, Hamzah Abu-Sbeih, Christopher A Sanchez, Chia-Chi Chang, et al. Fecal microbiota transplantation for refractory immune checkpoint inhibitor-associated colitis. *Nature Medicine*, 24(12):1804–1808, 2018.

- [175] Yun Wang, Yin Chen, Qian Zhou, Shi Huang, Kang Ning, Jian Xu, Robert M Kalin, Stephen Rolfe, and Wei E Huang. A culture-independent approach to unravel uncultured bacteria and functional genes in a complex microbial community. *PLoS One*, 7(10):e47530, 2012.
- [176] Virginia L Waters. Conjugation between bacterial and mammalian cells. *Nature Genetics*, 29(4):375–376, 2001.
- [177] Joshua S Weitz, Hyman Hartman, and Simon A Levin. Coevolutionary arms races between bacteria and bacteriophage. *Proceedings of the National Academy of Sciences*, 102(27):9535–9540, 2005.
- [178] Caroline Westwater, David A Schofield, Michael G Schmidt, James S Norris, and Joseph W Dolan. Development of a P1 phagemid system for the delivery of DNA into gram-negative bacteria. *Microbiology*, 148(4):943–950, 2002.
- [179] K Willi, H Sandmeier, EM Kulik, and J Meyer. Transduction of antibiotic resistance markers among *Actinobacillus actinomycetemcomitans* strains by temperate bacteriophages aa ϕ 23. *Cellular and Molecular Life Sciences*, 53:904–910, 1997.
- [180] Michael R Williams and Richard L Gallo. The role of the skin microbiome in atopic dermatitis. *Current Allergy and Asthma Reports*, 15:1–10, 2015.
- [181] Wolfgang Witte. Medical consequences of antibiotic use in agriculture. *Science*, 279(5353):996–997, 1998.
- [182] Jason M Wolfs, Thomas A Hamilton, Jeremy T Lant, Marcon Laforet, Jenny Zhang, Louisa M Salemi, Gregory B Gloor, Caroline Schild-Poulter, and David R Edgell. Biasing genome-editing events toward precise length deletions with an RNA-guided TevCas9 dual nuclease. *Proceedings of the National Academy of Sciences*, 113(52):14988–14993, 2016.
- [183] Rachel AF Wozniak and Matthew K Waldor. Integrative and conjugative elements: mosaic mobile genetic elements enabling dynamic lateral gene flow. *Nature Reviews Microbiology*, 8(8):552–563, 2010.
- [184] Ming Yi, Shengnan Yu, Shuang Qin, Qian Liu, Hanxiao Xu, Weiheng Zhao, Qian Chu, and Kongming Wu. Gut microbiome modulates efficacy of immune checkpoint inhibitors. *Journal of Hematology & Oncology*, 11:1–10, 2018.
- [185] Dimitra Zarafeta, Danai Moschidi, Efthymios Ladoukakis, Sergey Gavrilov, Evangelia D Chrysina, Aristotelis Chatziioannou, Ilya Kublanov, Georgios Skretas, and Fragiskos N Kolisis. Metagenomic mining for thermostable esterolytic enzymes uncovers a new family of bacterial esterases. *Scientific Reports*, 6(1):1–16, 2016.

Chapter 2

Efficient inter-species conjugative transfer of a CRISPR nuclease for targeted bacterial killing

The work presented in this chapter is adapted from:

Thomas A. Hamilton, Gregory M Pellegrino, Jasmine A Therrien, Dalton T Ham, Peter C Bartlett, Bogumil J Karas, Gregory B Gloor, and David R Edgell. Efficient inter-species conjugative transfer of a CRISPR nuclease for targeted bacterial killing. *Nature Communications*. 10:4544, 2019.

2.1 Introduction

Microbial ecosystems are essential for human health and proper development, and disturbances of the ecosystem correlate with a multitude of diseases (9, 12, 15, 33, 38, 47, 49, 52). A central problem is the lack of specific tools to selectively control pathogenic species, or to otherwise alter the composition of the human microbiome and other microbial communities. Traditional methods such as antibiotic treatment suffer from a number of limitations that preclude selective control in a defined and efficient manner, and are becoming less effective because of overuse and the development of multi-drug resistant bacteria (48). Phage-based therapy is limited by host range and the rapid development of phage-resistant bacteria (8). Probiotics and prebiotics are effective but of use in only a few defined conditions (40). Stool transplants are effective treatments for gastrointestinal dysbioses, but can result in wide-spread alterations in the composition of the gut

microbiome with unknown long-term effects (26, 30, 37). These limitations highlight an increasing need for effective and selective tools for the targeted modulation of microbiomes.

The CRISPR (clustered regularly interspaced short palindromic repeats) system is a bacterial immune system that targets invading DNA for elimination (2, 13, 14, 23). The Cas9 protein (CRISPR-associated protein 9) has been adapted for genome-editing applications in a wide range of organisms (24). Cas9 and related proteins can also be used as anti-microbial agents because the sequence of the guide RNA can be changed to target Cas9 to specific sequences in bacterial genomes. The introduction of double-strand breaks in bacterial chromosomes by Cas9 causes replication fork collapse and subsequent cell death (3, 10, 18). A critical component of studies adapting CRISPR as sequence-specific antimicrobial was the testing of different delivery vectors, including well-studied conjugation systems that would mobilize CRISPR-containing plasmids. However, the low frequency of conjugation was found to be a limiting factor in CRISPR-mediated killing, whereas phagemid- or bacteriophage-mediated delivery was found to be much more efficient. Nonetheless, conjugative plasmid delivery of CRISPR nucleases remains an attractive option because conjugative plasmids have broad-host ranges (22), are resistant to restriction-modification systems (32), are easy to engineer with large coding capacities (44), and do not require a cellular receptor (35) that would provide a facile mechanism for bacterial resistance. Conjugative plasmids are known to encode factors that promote biofilm formation (16) presumably because enhanced cell-to-cell contact increases rates of conjugative plasmid transfer (21). Conjugative plasmids may thus be well suited for delivery of molecular tools for modulating composition of human microbial communities (5, 29, 36, 42), many of which exist as biofilms.

Here, we show that conjugative plasmids are an efficient delivery system to deliver CRISPR nucleases to bacteria. We develop a *cis*-conjugative system where the plasmid encodes both the conjugative machinery and CRISPR nuclease (51), as opposed to previously tested *trans* setups where the conjugative machinery and nuclease were encoded on separate DNA molecules (10) (Figure 2.2). Bacteria that receive the *cis*-conjugative plasmid become potential donors for subsequent rounds of conjugation, potentially leading to exponentially increasing numbers of conjugative donor bacteria in the population. We test the *cis*-conjugative plasmid in a two-species co-culture system, finding high frequency of conjugative transfer of plasmids from *Escherichia coli* to *Salmonella enterica* under conditions that enhance cell-to-cell contact. Our results high-

light the promise of conjugative delivery of CRISPR nucleases as an effective tool for modification of microbiomes.

2.2 Methods

2.2.1 Bacterial and yeast strains

Escherichia coli EPI300 (F' λ *mcrA* Δ (*mrr-hsdRMS-mcrBC*) ϕ 80*dlacZ* Δ *M15* Δ (*lac*)*X74* *recA1* *endA1* *araD139* Δ (*ara, leu*)7697 *galU galK rpsL* (Str^R) *nupG trfA dhfr*) (Epicentre) was used for cloning and as a conjugative donor. *Salmonella typhimurium* sub. species *enterica* LT2 (Δ *hilA::Kan*^R) (acquired from Dr. David Haniford at Western University) was used as a conjugative recipient strain. *Saccharomyces cerevisiae* VL6-48 cells (*MATa, his3* Δ 200, *trp* Δ 1, *ura3-52, ade2-101, lys2, psi+cir*^o) was used for yeast assembly of conjugative plasmids.

2.2.2 Plasmid construction

Plasmids were constructed using a modified yeast assembly(17, 31). A detailed protocol can be found below and a list of primers in Appendix A. Briefly, the pNuc-*trans* plasmid was constructed by PCR amplifying fragments with 60-120 bp homology overlaps from pre-existing plasmids. The *oriT* fragment was amplified from pPtGE30(43) using primers DE-3302 and DE-3303. The p15A origin, chloramphenicol acetyl-transferase gene, and sgRNA cassette was amplified using primers DE-3308 and DE-3309 from a modified pX458 plasmid containing the TevCas9 coding region (51). The TevCas9 gene was amplified from the modified pX458 plasmid using primers DE-3306 and DE-3307. The *araC* gene and pBAD promoter were amplified from pBAD-24 (20) using primers DE-3304 and DE-3305. The CEN6-ARSH4-HIS3 yeast element was amplified from pPtGE30(43) using primers DE-3316 and DE-3317. *S. cerevisiae* VL6-48 was grown from a single colony to an OD₆₀₀ of 2.5-3, centrifuged at 2500 xg for 10 mins and washed in 50 mL sterile ddH₂O and centrifuged. Cells were resuspended in 50 mL of 1 M sorbitol, centrifuged, and spheroplasting initiated by resuspending the pellet in 20 mL SPE solution (1 M sorbitol, 10 mM sodium phosphate buffer pH 7, 10 mM Na₂EDTA pH 7.5) and by adding 30 μ L 12M 2-mercaptoethanol and 40 μ L zymolyase 20T solution (200 mg zymolyase 20 T (USB), 9 mL H₂O, 1 mL 1 M Tris pH 7.5, 10 mL 50% glycerol) and incubated at 30°C with shaking at 75 RPM. The yeast was considered spheroplasted once the ratio of the OD₆₀₀ in sorbitol to the A600 of yeast in ddH₂O reached 1.8-2. Spheroplasts were centrifuged at 1000 xg for 5 mins before being gently resuspended in

50 mL 1 M sorbitol, and centrifuged again. Spheroplasts were then resuspended in 2 mL STC solution (1 M sorbitol, 10 mM Tris-HCl pH 7, 10 mM CaCl₂) and incubated at room temperature for 10 minutes. Pooled DNA fragments at equimolar ratio for each plasmid assembly were gently mixed with 200 μ L of spheroplasted yeast and incubated at room temperature for 10 minutes. A volume of 1 mL of PEG-8000/CaCl₂ solution (20% (w/v) PEG 8000, 10 mM CaCl₂, 10 mM Tris-HCl, pH 7.5) was added and incubated at room temperature for 20 mins before being centrifuged at 1500 xg for 7 mins. Yeast was resuspended in 1 mL of SOS solution (1 M sorbitol, 6.5 mM CaCl₂, 0.25% (w/v) yeast extract, 0.5% (w/v) peptone) and incubated at 30°C for 30 mins. The spheroplast solution was added to 8 mL of histidine-deficient regenerative agar (Teknova), poured into a petri dish, and incubated overnight at 30°C. A volume of 8 mL histidine-deficient liquid regenerative media was then added on top of the solidified regenerative agar and grown at 30°C for 2-5 days. Total DNA was isolated from 1.5-3 mL *S. cerevisiae* using 250 μ L buffer P1 (50 mM Tris-HCl pH 8.0, 10 mM EDTA, 100 μ g/mL RNase A), 12.5 μ L zymolyase 20T solution and 0.25 μ L 12 M 2-mercaptoethanol and incubated at 37 °C for 1 hr. 250 μ L buffer P2 (200 mM NaOH, 1% SDS) was added, incubated at room temperature for 10 mins, followed by 250 μ L buffer P3 (3.0 M CH₃CO₂K pH 5.5) was added. DNA was precipitated with 700 μ L ice-cold isopropanol, washed with 70% ethanol, briefly dried and resuspended in 50 μ L ddH₂O. The plasmid pool was subsequently electroporated into *E. coli* EPI300. Individual colonies were screened by diagnostic digest (Figure 2.10) and sequencing, and one clone for each sgRNA selected for further use. TevSpCas9 sgRNAs targeting *S. enterica* genes were predicted as previously described (51). A TevSpCas9 site consists of (in the 5' to 3' direction) an I-TevI cleavage motif (5'-CNNNG-3'), a DNA spacer region of 14-19 bp separating the I-TevI cleavage site and the SpCas9 sgRNA binding site, and a SpCas9 PAM site (5'-NGG-3'). Putative sites in the *S. enterica* LT2 genome were ranked according to the predicted activity of the identified I-TevI cleavage site (relative to the I-TevI cognate 5'-CAACG-3' cleavage site) and the fit of the DNA spacer region to nucleotide tolerances of I-TevI. Oligonucleotides corresponding to the guide RNA were cloned into a BsaI cassette site present in pNuc-*trans*. To construct the pNuc-*cis* plasmid, the *oriT*, *araC*, TevCas9, sgRNA, and CEN6-ARSH4-HIS3 elements were amplified from pNuc-*trans* using primers DE-3024 and DE-3025 that possessed 60 bp homology to both sides of the AvrII restriction site in pTA-Mob. The pTA-Mob plasmid was linearized by AvrII (New England Biolabs), combined with the PCR am-

plified fragment from pNuc-*trans* and transformed into *S. cerevisiae* VL6-48 spheroplasts. Correct pNuc-*cis* clones were identified as above for pNuc-*trans*. Both pNuc-*trans* and pNuc-*cis* were completely sequenced to confirm assembly. A detailed plasmid map of each plasmid is found in Figure 2.1.

2.2.3 Quantitative PCR

E. coli EPI300 donors and *S. enterica* transconjugants harbouring pNuc-*trans* and pTA-Mob (*trans* helper plasmid) or pNuc-*cis* were grown overnight under selection. sgRNAs were absent from the *cis* and *trans* plasmids. Overnight cultures were diluted 1:50 in selective media and grown to an A_{600} of ~ 0.5 . Each culture was diluted, plated on selective LSLB plates (10 g/L tryptone, 5 g/L yeast extract, and 5 g/L sodium chloride, 1% agar), and grown overnight. Colonies were counted manually to determine the CFUs/mL of each culture. At the same time, 500 μ L of each culture was pelleted and resuspended in 500 μ L 1x PBS and incubated at 95 °C for 10 minutes before immediate transfer to -20 °C. Quantitative real-time PCR was performed on boil-lysed samples using SYBR Select Master Mix (Applied Biosystems) using primers DE-4635 and DE-4636 that amplified a DNA fragment present on both pNuc-*trans* and pNuc-*cis*. Purified pNuc-*trans* was used as a copy number standard.

2.2.4 Filter mating conjugation

Saturated cultures of donor *E. coli* EPI300 and recipient *S. enterica* LT2 were diluted 1:50 into 50 mL non-selective LSLB media. The diluted cultures were grown to an A_{600} of ~ 0.5 and concentrated 100-fold by centrifugation at 4000xg for 10 minutes. A volume of 200 μ L of concentrated donors were mixed with 200 μ L concentrated recipients on polycarbonate filters adhered to conjugation plates (LSLB supplemented with 1.5% agar). Conjugation proceeded at 37 °C from 5 minutes to 24 hours. Following conjugation, filters were placed in conical tubes containing 30 mL of 1x phosphate buffer saline (PBS) (8 g/L NaCl, 0.2 g/L KCl, 1.42 g/L Na₂HPO₄, 0.24 g/L KH₂PO₄) and vortexed for 1 minute to remove the bacteria from the filter. The supernatant was serially diluted and plated on LSLB plates with selection for donor *E. coli* EPI300 (gentamicin 40 μ g/mL for the *cis* setup and gentamicin 40 μ g/mL, chloramphenicol 25 μ g/mL for the *trans* setup), recipient *S.*

enterica LT2 (kanamycin 50 $\mu\text{g}/\text{mL}$), and transconjugants (kanamycin 50 $\mu\text{g}/\text{mL}$, chloramphenicol 25 $\mu\text{g}/\text{mL}$, 0.2% D-glucose for pNuc-*trans* transconjugants or kanamycin 50 $\mu\text{g}/\text{mL}$, gentamicin 40 $\mu\text{g}/\text{mL}$, 0.2% D-glucose for pNuc-*cis* transconjugants). D-glucose represses the expression of TevCas9 in transconjugants. Plates were incubated overnight at 37 °C for 16-20 hours. Colonies were counted manually.

2.2.5 *S. enterica* to *S. enterica* conjugation

S. enterica LT2 transconjugants harbouring pNuc-*cis* or pNuc-*trans* with no sgRNA encoded were obtained from plate conjugation experiments described in detail below. Transconjugant colonies were grown overnight in LSLB supplemented with kanamycin 50 $\mu\text{g}/\text{mL}$, gentamicin 40 $\mu\text{g}/\text{mL}$ and 0.2% D-glucose for pNuc-*cis*, or kanamycin 50 $\mu\text{g}/\text{mL}$, chloramphenicol 25 $\mu\text{g}/\text{mL}$ and 0.2% D-glucose for pNuc-*trans*. *S. enterica* LT2 was transformed with pUC19 to confer ampicillin resistance for use as a recipient and was grown overnight in LSLB supplemented with kanamycin 50 $\mu\text{g}/\text{mL}$ and ampicillin 100 $\mu\text{g}/\text{mL}$. All donor and recipient *S. enterica* cultures were diluted 1:50 into LSLB and grown to an A_{600} of 0.5 before spreading 200 μL of each on a conjugation plate supplemented with 0.2% w/v D-glucose to repress TevCas9 expression. Conjugations proceeded for 2 hours at 37 °C before cells were scraped into 500 μL SOC with a cell spreader. Resulting cell suspensions were serially diluted and plated to select for donors (kanamycin 50 $\mu\text{g}/\text{mL}$, gentamicin 25 $\mu\text{g}/\text{mL}$ for pNuc-*cis* or kanamycin 50 $\mu\text{g}/\text{mL}$, chloramphenicol 25 $\mu\text{g}/\text{mL}$ for pNuc-*trans*), recipient (kanamycin 50 $\mu\text{g}/\text{mL}$, ampicillin 100 $\mu\text{g}/\text{mL}$), and transconjugant (kanamycin 50 $\mu\text{g}/\text{mL}$, gentamicin 40 $\mu\text{g}/\text{mL}$, ampicillin 100 $\mu\text{g}/\text{mL}$ for pNuc-*cis*, chloramphenicol 25 $\mu\text{g}/\text{mL}$, ampicillin 100 $\mu\text{g}/\text{mL}$ for pNuc-*trans*). Plates were incubated at 37 °C for 16-20 hours and colonies were counted manually.

2.2.6 Liquid and bead-supplemented conjugation assays

E. coli EPI300 and recipient *S. enterica* LT2 were grown overnight to saturation. Tubes containing 5 mL LSLB supplemented with 0.2 % D-glucose were inoculated with 180 μL saturated *E. coli* and 18 μL saturated *S. enterica*. Bead-supplemented conjugations were prepared similarly with the addition of 1 mL soda lime glass beads (0.5 mm diameter). Conjugations proceeded by incubating

at 37 °C with 0 or 60 RPM agitation for 72 hours. Cultures were homogenized by vortexing, serially diluted and spot-plated in 10 μ L spots on plates containing appropriate antibiotic selection for donors, recipients and transconjugants. Plates were incubated at 37 °C for 16-20 hours. Colonies were counted manually. Alterations to this protocol were made to determine the effect of donor to recipient ratio (50:1, 10:1, 1:1, 1:10, 1:50), NaCl concentration (2.5 g/L, 5 g/L, 10 g/L) and shaking speed (0 RPM, 60 RPM, 120 RPM) on conjugation frequency.

2.2.7 Killing efficiency assays

Saturated cultures of *E. coli* EPI300 donors harbouring pNuc-*trans* plasmids encoding sgRNAs and recipient *S. enterica* LT2 were diluted 1:50 into LSLB supplemented with 0.2 % D-glucose. The diluted cultures were grown to an A_{600} of \sim 0.5. 200 μ L of each donor was mixed with 200 μ L of recipient on a conjugation plate supplemented with 0.2 % D-glucose to repress expression of TevCas9. Conjugations proceeded for 1 hour at 37 °C before cells were scraped into 500 μ L SOC (20 g/L tryptone, 5 g/L yeast extract, 0.5 g/L NaCl, 2.5 mM KCl, 10 mM MgCl₂, and 20 mM D-glucose) with a cell spreader. Resulting cell suspensions were serially diluted and plated on selection for donors and recipients in addition to selection for transconjugants with CRISPR repression (kanamycin 50 μ g/mL, chloramphenicol 25 μ g/mL, 0.2 % D-glucose) and transconjugants with CRISPR activation (kanamycin 50 μ g/mL, chloramphenicol 25 μ g/mL, 0.2 % L-arabinose). Plates were incubated overnight at 37 °C for 16-20 hours. Killing efficiency is the ratio of cells on selective to non-selective plates.

2.2.8 Escape mutant analyses

Escape mutant colonies were picked from plates selecting for exconjugant *S. enterica* cells with TevSpCas9 activated after conjugation. These colonies were grown overnight to saturation and plasmids were extracted using the BioBasic miniprep kit. The isolated plasmids were then transformed into *E. coli* EPI300 cells to increase plasmid expression for analysis and re-isolated for analysis. The plasmids were analyzed by diagnostic restriction digest with FspI and MsiI, and by multiplex PCR for the chloramphenicol resistance marker, and a TevSpCas9 gene fragment. Total DNA was isolated using a standard alkaline lysis protocol followed by isopropanol precipitation

of the DNA. Potential target sites were PCR amplified from the total DNA sample using Amplitaq 360 (Thermofisher Scientific) and subsequently sequenced.

2.2.9 sgRNA off-target predictions in *E. coli*

To predict sgRNA off-target sites, we searched the *E. coli* genome for sites with less than 6 mismatches to each sgRNA using a Perl script with an XOR bit search. A mismatch score was calculated that indicates the likelihood of a stable sgRNA/DNA heteroduplex using the formula:

$$mm_score = \sum_{mismatch} 0.5^{non_seed} + 1.2^{seed}$$

where *non_seed* is a mismatch in the non-seed region of the sgRNA (positions 1-12 from the 5' end of the target site) and *seed* is a mismatch in the seed regions (positions 13-20 from the 5' end of the target site). By this method, mismatches in the 5' end of sgRNA/DNA heteroduplex are more tolerated than mismatches closer to the PAM sequence. For each sgRNA, we also added a correction for if the adjacent three nucleotides matched the consensus SpCas9 PAM sequence 5'-NGG-3'. Off-target sites with perfect match PAMs were given more weight than off-target sites with 1 or 2 mismatches.

2.2.10 Modelling *S. enterica* killing efficiency

To model sgRNA parameters that were predictive of *S. enterica* killing efficiency, we used a generalized linear model in the R statistical language with the formula:

$$sgRNA_{KE} \sim sgRNA_{score} + sgRNA_{targetstrand} + sgRNA_{repstrand} + sgRNA_{genefunc} + sgRNA_{reldist}$$

where $sgRNA_{KE}$ is the average killing efficiency for a given sgRNA, $sgRNA_{score}$ is the predicted sgRNA activity score using the algorithm of Guo et al., $sgRNA_{targetstrand}$ is the transcription strand

targeted by the sgRNA (sense or anti-sense), $sgRNA_{repstrand}$ is whether the sgRNA targets the leading or lagging strand, $sgRNA_{genefunc}$ is whether the sgRNA targets an essential or non-essential gene in *S. enterica*, and $sgRNA_{reldist}$ is the position of the sgRNA relative to the AUG codon of the targeted gene. A summary table and graphical output of the model parameters is shown in Figure 2.9.

2.3 Results

2.3.1 Increased conjugation frequency with a *cis*-conjugative plasmid

We constructed a conjugative plasmid, pNuc, based on the IncP RK2 (46) plasmid to examine parameters that contributed to conjugation (Figure 2.2a). The pNuc plasmid encoded the TevSp-Cas9 nuclease (I-TevI nuclease domain fused to *Streptococcus pyogenes* Cas9) controlled by an arabinose-inducible pBAD promoter (20), and a single guide RNA (sgRNA) cassette driven by a constitutive promoter derived from the tetracycline resistance gene (pTet) into which we cloned oligonucleotides corresponding to predicted target sites in the *S. enterica* genome (Figure 2.2b). Two forms of the plasmid were constructed (Figure 2.1, Figure 2.2a). First, a *cis* configuration (pNuc-*cis*) where the origin of transfer (*oriT*) and CRISPR system were cloned into the pTA-Mob backbone that encodes the genes necessary for conjugation (46). The second setup employed a plasmid *trans* configuration (pNuc-*trans*) that included only the CRISPR system, *oriT* and chloramphenicol resistance. The *oriT* sequence on pNuc-*trans* is recognized by the relaxase expressed in *trans* from the pTA-Mob helper plasmid to facilitate conjugation. The pNuc-*trans* setup mimics the plasmids used in previous studies that examined conjugative delivery of CRISPR nucleases in an *E. coli* donor/recipient system (3, 10, 18).

We used the pNuc-*cis* and pNuc-*trans* plasmids to test the hypothesis that the *cis* setup would support higher levels of conjugation relative to the *trans* setup in a time-course filter-mating assay using *E. coli* as the donor and *S. enterica* as the recipient (Figure 2.2c). As shown in Figure 2.2d, conjugation frequency (transconjugants/total recipients) for pNuc-*cis* continually increased over the time of the experiment reaching a maximum of 1×10^{-2} by 24 hrs. In contrast, conjugation frequency for pNuc-*trans* peaked at early time points with a maximal frequency of $\sim 1 \times 10^{-3}$, declining to $\sim 1 \times 10^{-5}$ by 24 hrs. We isolated 5 *S. enterica* transconjugants each from experiments with the pNuc-*cis* or pNuc-*trans* plasmids and showed that the transconjugants were viable donors for subsequent conjugation of the pNuc-*cis* plasmid to naive recipients, but not for the pNuc-*trans* plasmid (Figure 2.2e). Furthermore, higher frequency conjugation of pNuc-*cis* was not due to higher copy number relative to pNuc-*trans* in the *E. coli* donor or *S. enterica* transconjugants (Figure 2.2f), or because pNuc-*cis* was significantly more stable than pNuc-*trans* (Figure 2.2g).

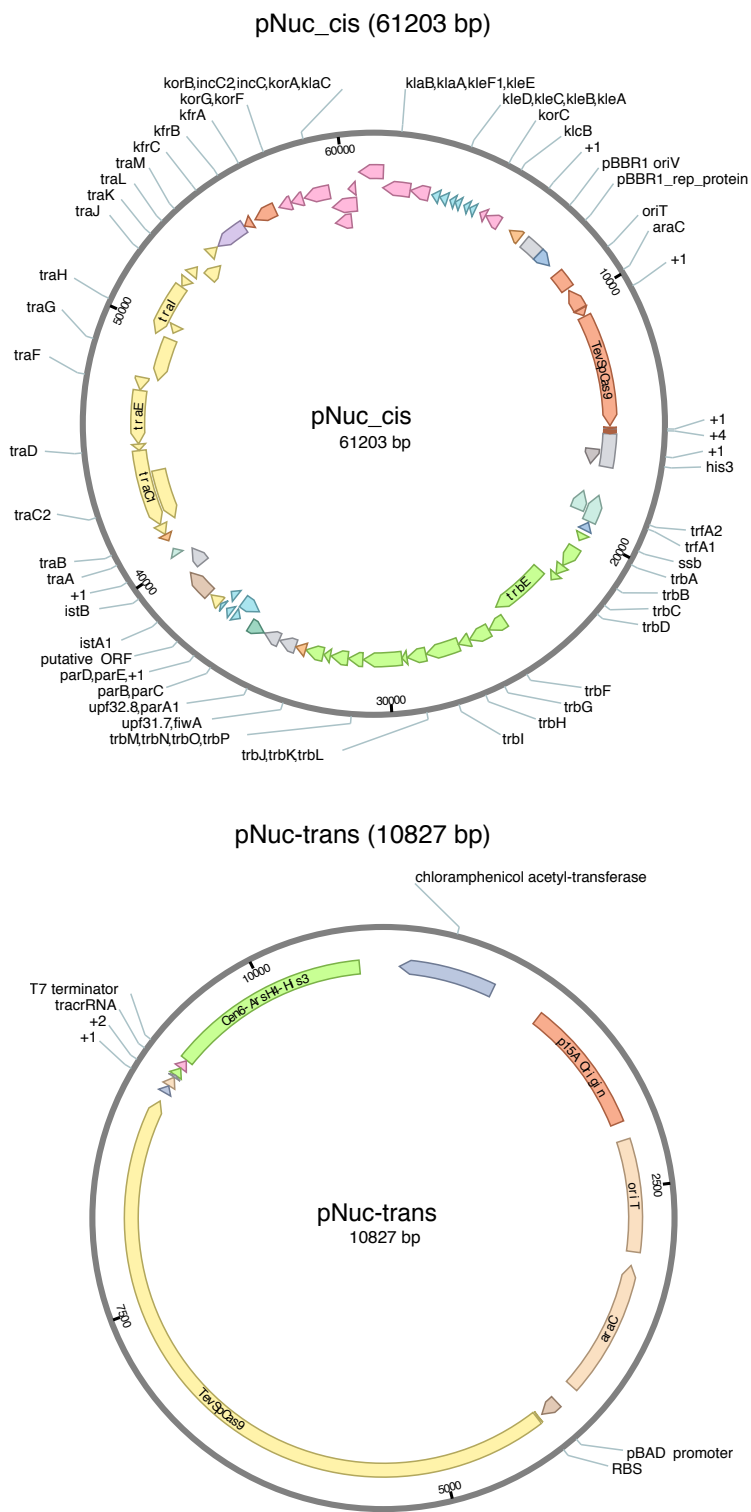


Figure 2.1: Plasmid maps of pNuc-cis and pNuc-trans.

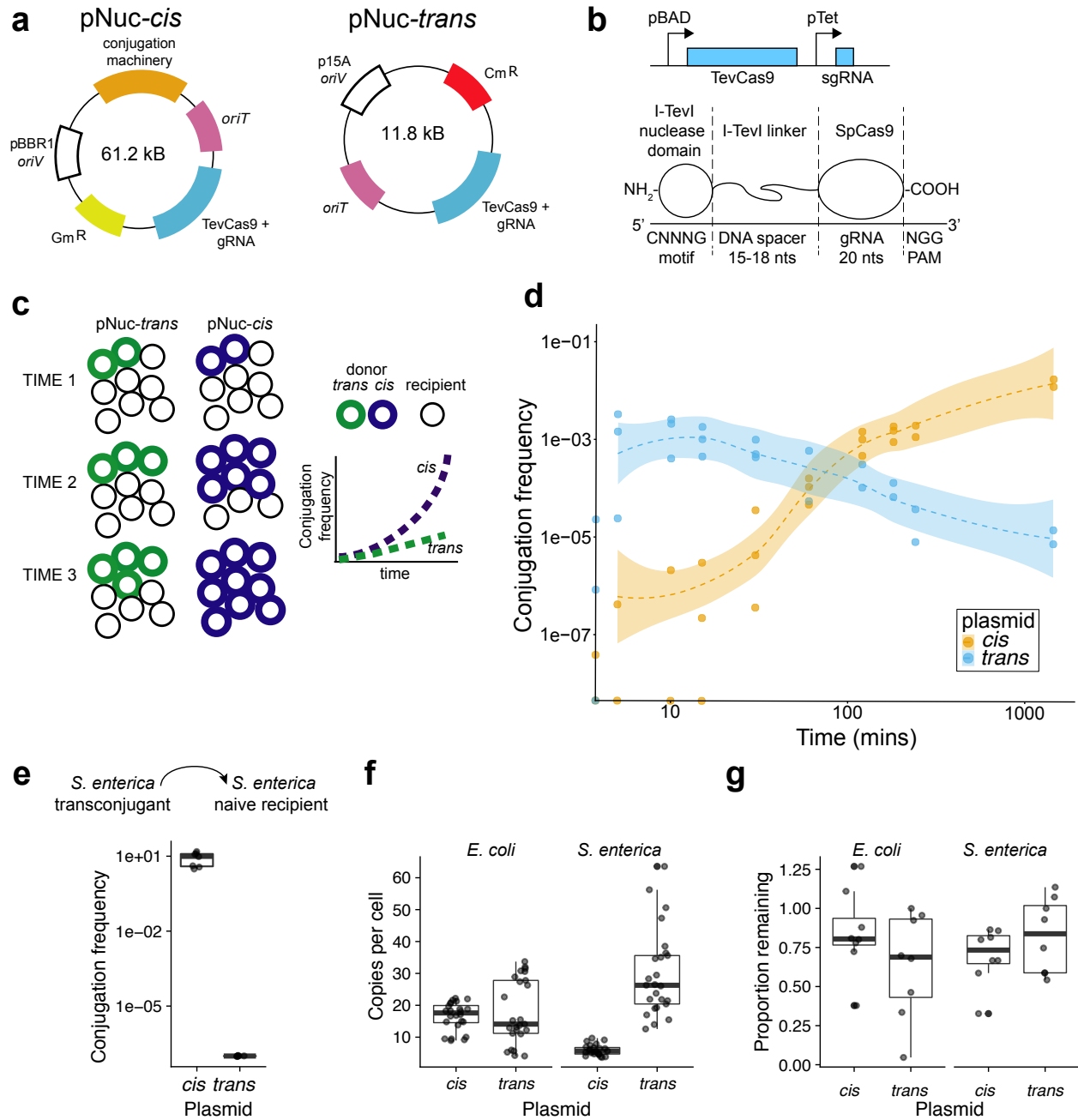


Figure 2.2: Impact of *cis* or *trans* localization of conjugative machinery on conjugation frequency. **a.** Schematic view of the pNuc-*cis* and pNuc-*trans* plasmids. *oriT*, conjugative origin of transfer; *oriV*, vegetative plasmid origin; Gm^R, gentamicin resistance gene; Cm^R, chloramphenicol resistance gene; TevSpCas9/sgRNA, coding region for TevSpCas9 nuclease gene and sgRNA; Conjugative machinery, genes required for conjugation derived from the IncP RK2 conjugative system. **b.**(Top) The TevSpCas9 and sgRNA cassette (not to scale) highlighting the arabinose regulated pBAD and constitutive pTet promoters. (Below) The modular TevSpCas9 protein and DNA-binding site. Interactions of the functional TevSpCas9 domains with the corresponding region of substrate are indicated. **c.** Model of pNuc spread after conjugation with the *cis* and *trans* setups. Cell growth overtime will account for increase of pNuc-*trans*. **d.** Filter mating assays performed over 24 hr demonstrate that pNuc-*cis* has a higher conjugation frequency than pNuc-*trans*. Points represent independent experimental replicates, and the 95% confidence intervals are indicated as the shaded areas. Conjugation frequency is reported as the number of transconjugants (Gm^R, Kan^R) per total recipient *S. enterica* cells (Kan^R). **e.** Conjugation frequency of *S. enterica* transconjugants harbouring either pNuc-*cis* or pNuc-*trans* to naive *S. enterica* recipients. Data are shown as boxplots with points representing individual replicate experiments **f.** pNuc-*cis* and pNuc-*trans* copy number determined by quantitative PCR in either *E. coli* or *S. enterica*. Data are shown as boxplots with solid lines indicating the median of the data, the rectangle the interquartile bounds, and the whiskers the range of the data. Points are individual experiments. **g.** pNuc-*cis* and pNuc-*trans* stability in *E. coli* or *S. enterica* determined as the ratio of cells harbouring the plasmid after 24 hrs growth without antibiotic selection over total cells.

To determine if longer incubation times resulted in higher conjugation frequency with the pNuc-*cis* system, we used a liquid conjugation assay consisting of low salt LB (LSLB) media into which varying ratios of donor *E. coli* and recipient *S. enterica* cells were added. After 72 hrs incubation at 37 °C with mild agitation at 60 RPM, we found that high donor to recipient ratios (1:1, 10:1 and 50:1) yielded more transconjugants per recipient than experiments with lower donor to recipient ratios (1:5 or 1:10) (Figure 2.3a). We also showed that decreasing the NaCl concentration of the media to 0.25% w/v resulted in an increased conjugation frequency at a 10:1 donor:recipient ratio (Figure 2.3b). Using the 10:1 donor:recipient ratio, and 0.25% NaCl LSLB media, we examined the effect of culture agitation on conjugation, finding that both 0 RPM and 60 RPM resulted in similar conjugation frequencies while a higher 120 RPM resulted in lower conjugation frequency (Figure 2.3c).

Collectively, these data show that pNuc-*cis* is ~1000-fold has a higher conjugation frequency than the pNuc-*trans* system at 24 hrs post-mixing because bacteria that receive pNuc-*cis* become donors for subsequent rounds of conjugation. This would lead to exponentially increasing numbers of conjugative donors in the population. Thus, our data differs significantly from previous studies that concluded that conjugation frequency with a *trans* system was a limiting factor for CRISPR delivery (10).

2.3.2 Cell-to-cell contact significantly increases conjugation

The previous experiments demonstrated that pNuc-*cis* was more efficient at conjugation in a filter mating assay on solid media. To test whether liquid culture conditions that enhanced cell-to-cell contact through biofilm formation resulted in increased conjugation with pNuc-*cis*, we included 0.5 mm glass beads in liquid cultures that would provide a solid surface for cell-to-cell contact (11, 28, 45) and observed conjugation frequencies as high as 100% with pNuc-*cis* (Figure 2.4a,b). This conjugation frequency represents a ~500-1000 fold enhancement compared to the solution or filter-based pNuc-*cis* assays. Increasing culture agitation to 60 RPM had no discernible effects on conjugation frequency with pNuc-*cis*. With the pNuc-*trans* plasmid, conjugation frequency ranged from 1×10^{-8} to 1×10^{-4} (Figure 2.4c), supporting the hypothesis that gains in conjugation frequency with the pNuc-*cis* system resulted from exponentially increasing number of cells that

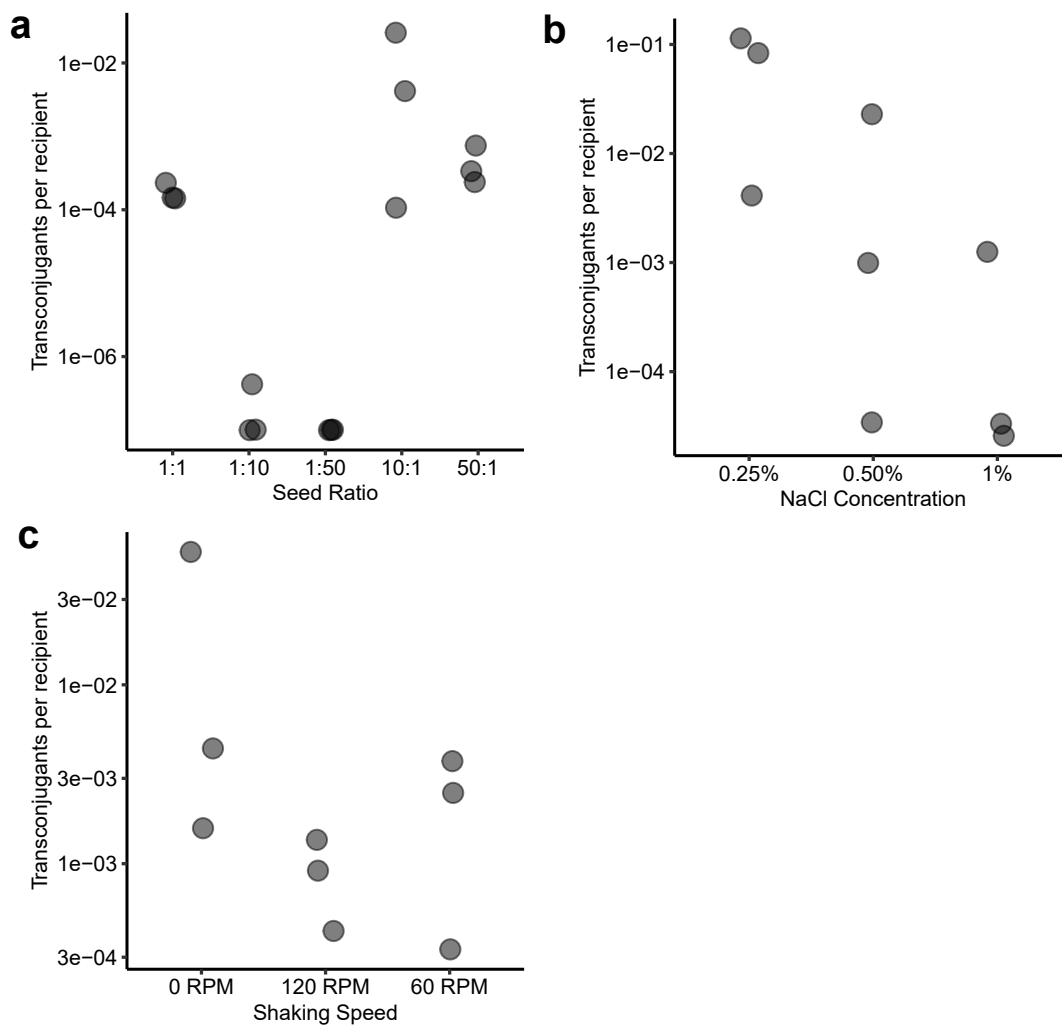


Figure 2.3: Optimizing liquid culture conditions for *E. coli* to *S. enterica* conjugation. **a.** Conjugation frequency for different sodium chloride (NaCl) media conditions. **b.** Conjugation frequency measured with different *E. coli* donor to *S. enterica* recipient ratios at the start of conjugation. **c.** Effect of culture agitation on conjugation frequency (RPM - revolutions per minute). For each plot, points indicate conjugation frequency for independent biological replicates.

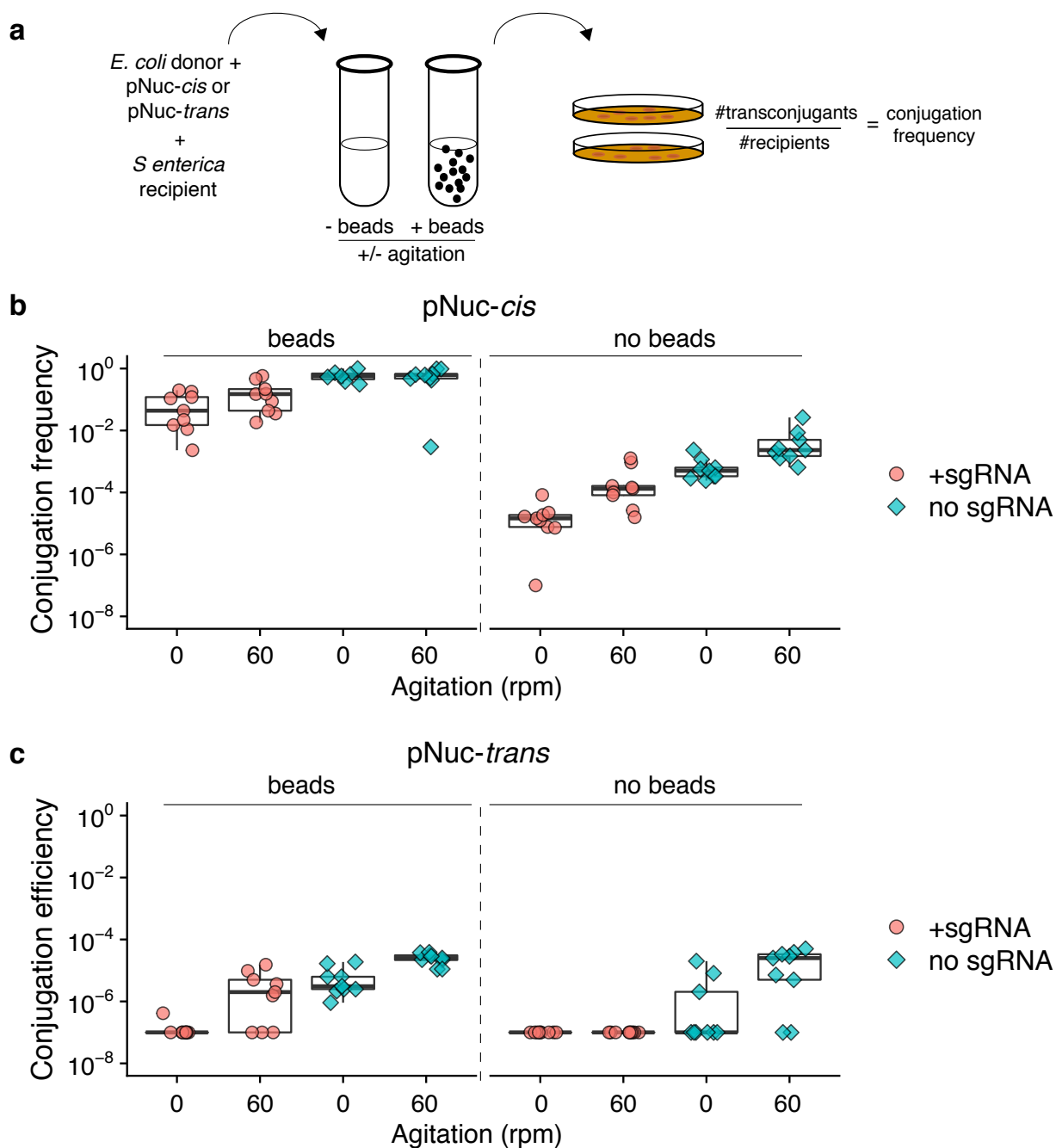


Figure 2.4: Influence of enhanced cell-to-cell contact on conjugation frequency. **a.** Schematic of experimental design. Liquid conjugation experiments in culture tubes with **b.** pNuc-*cis* and **c.** pNuc-*trans* were performed with 0.5 mm glass beads or without glass beads over 72 hrs at the indicated shaking speed (in revolutions per minute). Conjugations were performed with (filled circles) or without (filled diamonds) sgRNA targeting the STM1005 locus cloned into pNuc-*cis* and pNuc-*trans*. Both plasmids encoded the TevSpCas9 nuclease. Data are plotted on a log₁₀ as boxplots with data points from independent biological replicates. The solid line represents the median of data, the rectangle represents the interquartile range of the data, and the whiskers represent the maximum and minimum of the data.

become donors for subsequent rounds of conjugation after receiving the plasmid.

Interestingly, we observed a reduction in conjugation frequency when a *S. enterica* specific sgRNA was cloned onto pNuc-*cis* (the + guide condition) (Fig. 2.4b). We postulate that a proportion of *S. enterica* are killed immediately post-conjugation. We attribute this killing to leaky expression of the TevSpCas9 nuclease from the pBAD promoter under repressive culture conditions (+ 0.2% glucose).

2.3.3 *S. enterica* killing by conjugative delivery of Cas9 and sgRNAs

To demonstrate that the TevSpCas9 nuclease could be delivered by conjugation to eliminate specific bacterial species, we designed 65 total sgRNAs targeting 38 essential genes, 23 non-essential genes, and 4 genes with unresolved phenotypes (Figure 2.8a). The 65 sgRNA sites were arrayed around the *S. enterica* chromosome (Figure 2.8b), differed in their relative position within each gene, and what strand was being targeted. We assessed the efficacy of each sgRNA in killing *S. enterica* by comparing the ratio of *S. enterica* colony counts under conditions where TevSpCas9 expression from the pBAD promoter was induced with arabinose or repressed with glucose. Using *E. coli* as the conjugative donor, we found a range of *S. enterica* killing efficiencies between 1 and 100% (Figure 2.8a). To demonstrate that the I-TevI nuclease domain could function in the context of other Cas9 orthologs, we fused the I-TevI nuclease domain to SaCas9 from *Staphylococcus aureus* to create TevSaCas9. SaCas9 differs from SpCas9 in possessing a longer PAM requirement (39). With TevSaCas9 we observed high killing efficiency ($93 \pm 8\%$, mean \pm standard error) when TevSaCas9 was targeted to the *fepB* gene of *S. enterica* (Figure 2.5). sgRNAs expressed as pairs from separate promoters also yielded high killing efficiencies (Figure 2.6), demonstrating the potential for multiplexing guides to overcome mutational inactivation of individual guides. Sampling *S. enterica* colonies resistant to killing from experiments with different sgRNAs revealed three types of escape mutants: nucleotide polymorphisms in the chromosome target site that would weaken sgRNA-DNA interactions, transposable element insertions that inactivated sgRNA expression, and rearrangements of pNuc-*cis* that impacted TevSpCas9 function (Figure 2.7) (25).

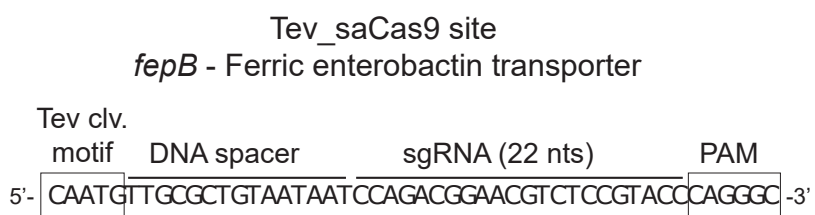
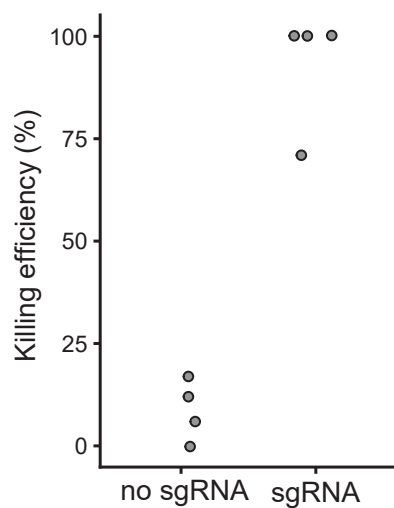
a**b**

Figure 2.5: Killing of *S. enterica* by conjugative delivery of TevSaCas9. **a.** Schematic of TevSaCas9 target site in the *fepB* gene of *S. enterica*, with the I-TevI cleavage motif, DNA spacer, sgRNA binding site and PAM motif indicated. **b.** Plot of *S. enterica* killing efficiency with no sgRNA cloned in pNuc, or the *fepB* sgRNA cloned in pNuc. Points are independent biological replicates.

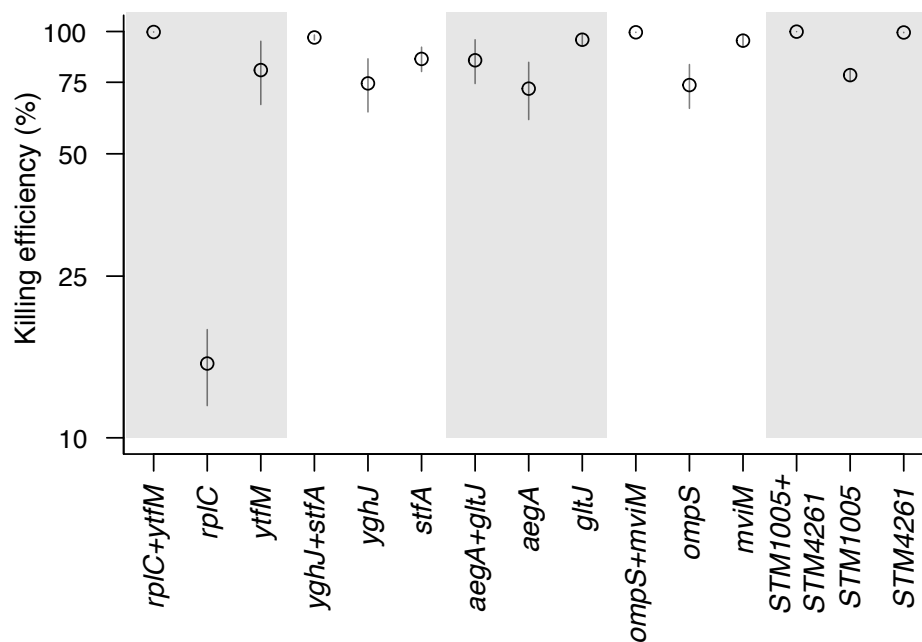


Figure 2.6: Killing efficiency of multiplexed pairs of sgRNAs, with single sgRNAs plotted for comparison. Data are plotted on log₁₀ scale as the mean of at least three independent biological replicates, with vertical lines representing the standard error of the mean. A Mann-Whitney Wilcox test comparing if multiplexed sgRNAs had a significantly higher killing efficiency as a group than their single sgRNA constituents yielded a p-value=0.003.

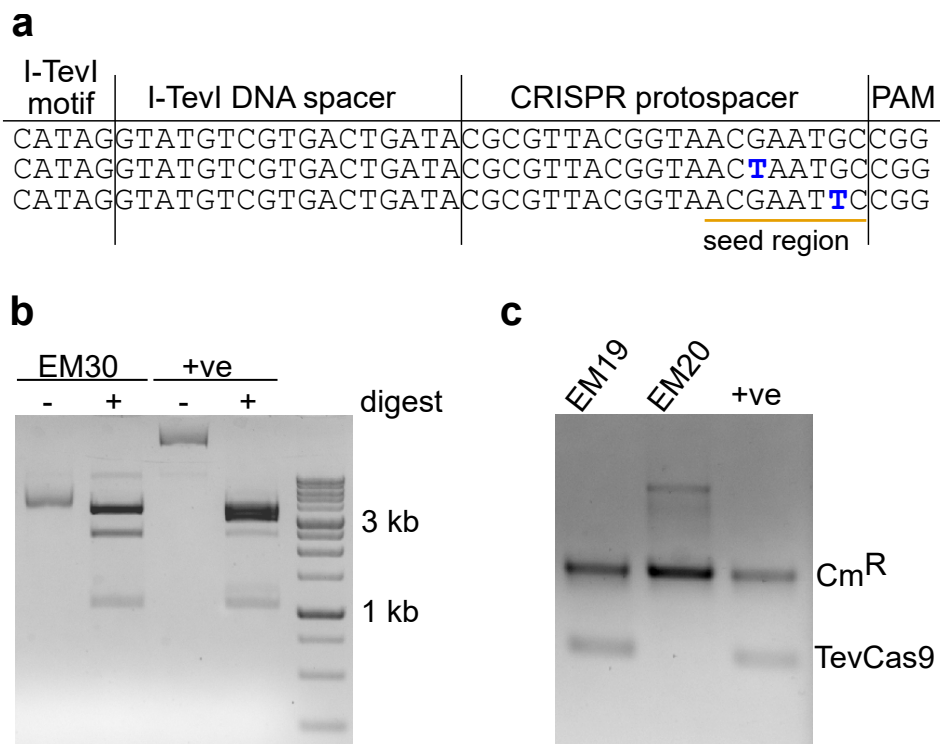


Figure 2.7: Examples of *S. enterica* escape mutants. **a.** Nucleotide sequence of the TevSpCas9 target site in the Gifsy prophage. Nucleotide substitutions in the seed region of the sgRNA are indicated and underlined. **b.** Example of an agarose gel of pNuc DNA isolated from EM30 or from wild-type pNuc (+ve) incubated with (+) or without (-) a mixture of FspI and MsiI restriction enzymes. Size standards in kilobase pairs (kb) are indicated to the right of the gel image. **c.** Example of multiplex PCR with pNuc DNA isolated from EM19, EM20 or wild-type pNuc (+ve) with primers specific for the Cm^R and TevSpCas9 coding regions.

We considered a number of variables that would influence sgRNA killing efficiency in *S. enterica* including predicted sgRNA activity according to an optimized prokaryotic model (19), targeting of the sense or anti-sense strands for transcription, the relative position of the sgRNA in the targeted gene, targeting of the leading or lagging replicative strands, and the essentiality of the targeted gene. Taken independently, no single variable was strongly correlated with sgRNA killing efficiency (Figure 2.11, Figure 2.9). A generalized linear model was used to assess the significance of each variable on sgRNA killing efficiency, revealing that sgRNA score positively correlated with predicted activity (p less than 0.02, t-test) while targeting essential genes was negatively correlated with killing efficiency (p less than 0.03, t-test) (Figure 2.9). The moderate statistical support from the linear model suggests that a robust understanding of parameters that influence sgRNA targeting and activity in prokaryotic genomes remains a work in progress, particularly in the context of conjugative plasmids.

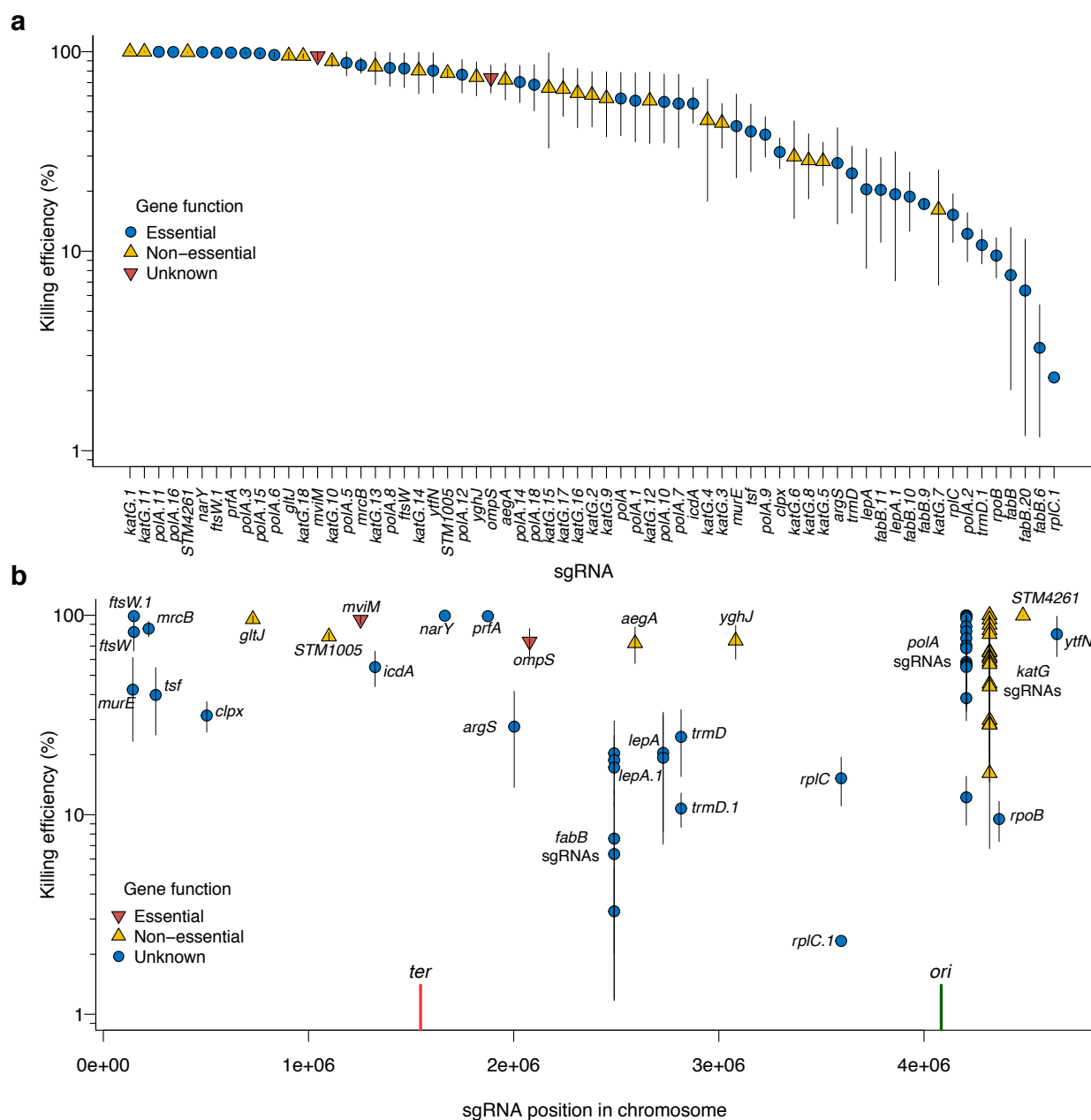


Figure 2.8: Killing efficiency of sgRNAs targeted to the *S. enterica* genome. **a.** Ranked killing efficiency of individual sgRNAs coded as to whether the target site is found in an essential gene (blue filled circles), non-essential gene (orange diamonds), or unknown if the gene is essential (inverted red triangles). Vertical lines represent the standard error of the data from at least 3 biological replicates. **b.** Killing efficiency of each sgRNA plotted relative to their position in the *S. enterica* genomes, color-coded as in panel **a**. The terminator region (*ter*) and origin of replication (*ori*) are indicated by vertical red and green lines, respectively.

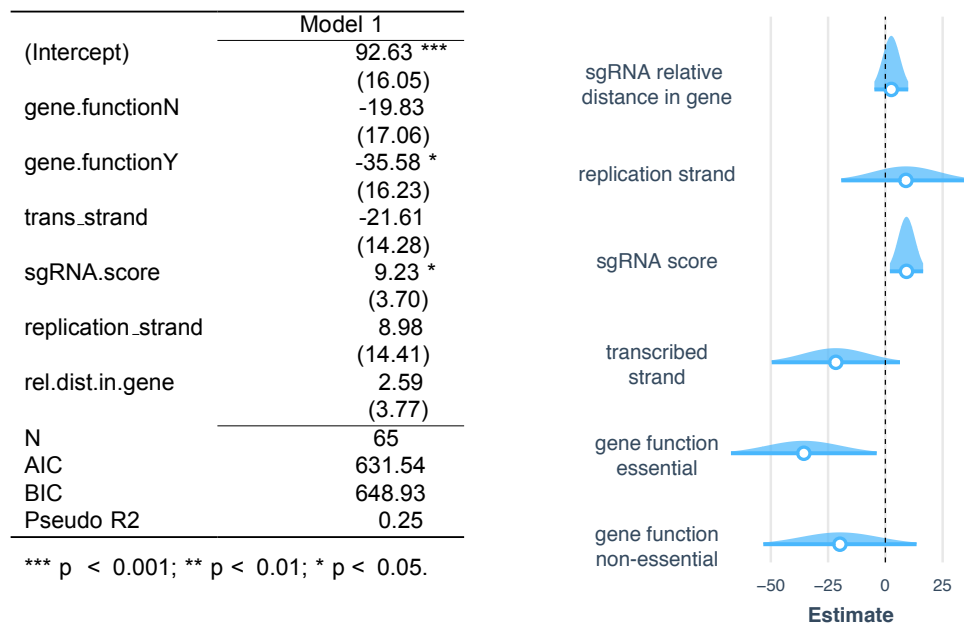


Figure 2.9: Summary of generalized linear model of sgRNA parameters that are indicative of killing efficiency with P-values indicated (left), and a graphical representation of the confidence intervals associated with each parameter. Note that parameters with confidence intervals that pass over the 0 line are not considered significant.

During the course of these experiments, we noted that some sgRNAs were recalcitrant to cloning (Figure 2.10). In particular, sgRNAs targeting essential genes in *S. enterica* were more likely to yield inactive clones than sgRNAs targeting non-essential genes. Whole plasmid sequencing revealed no insertions in 15 clones with sgRNAs targeting non-essential genes, whereas 7/13 sgRNA clones targeting essential genes had insertions. These findings suggest that leaky expression of the TevCas9 nuclease from the pBAD promoter is sufficient to cause cellular toxicity in *E. coli*, and selection for inactive plasmids. Thus, choosing sgRNAs with minimal identity and off-target sites in the *E. coli* genome will facilitate conjugative delivery of sgRNAs and CRISPR nucleases.

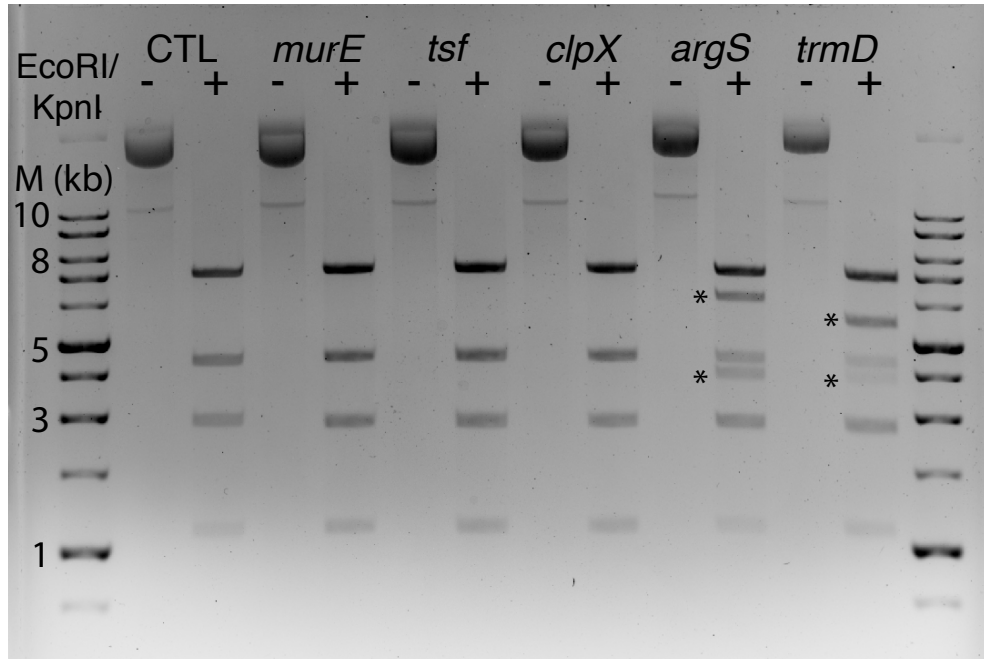


Figure 2.10: Example of agarose gel of diagnostic restriction digest of different guideRNAs cloned into pNuc-*trans*. Each plasmid was digested with EcoRI and KpnI and compared to the pNuc-*trans* backbone (CTL). Asterisks indicate unexpected digestion patterns. The size of the ladder is indicated in kilobase pairs (kb) to the left of the gel image.

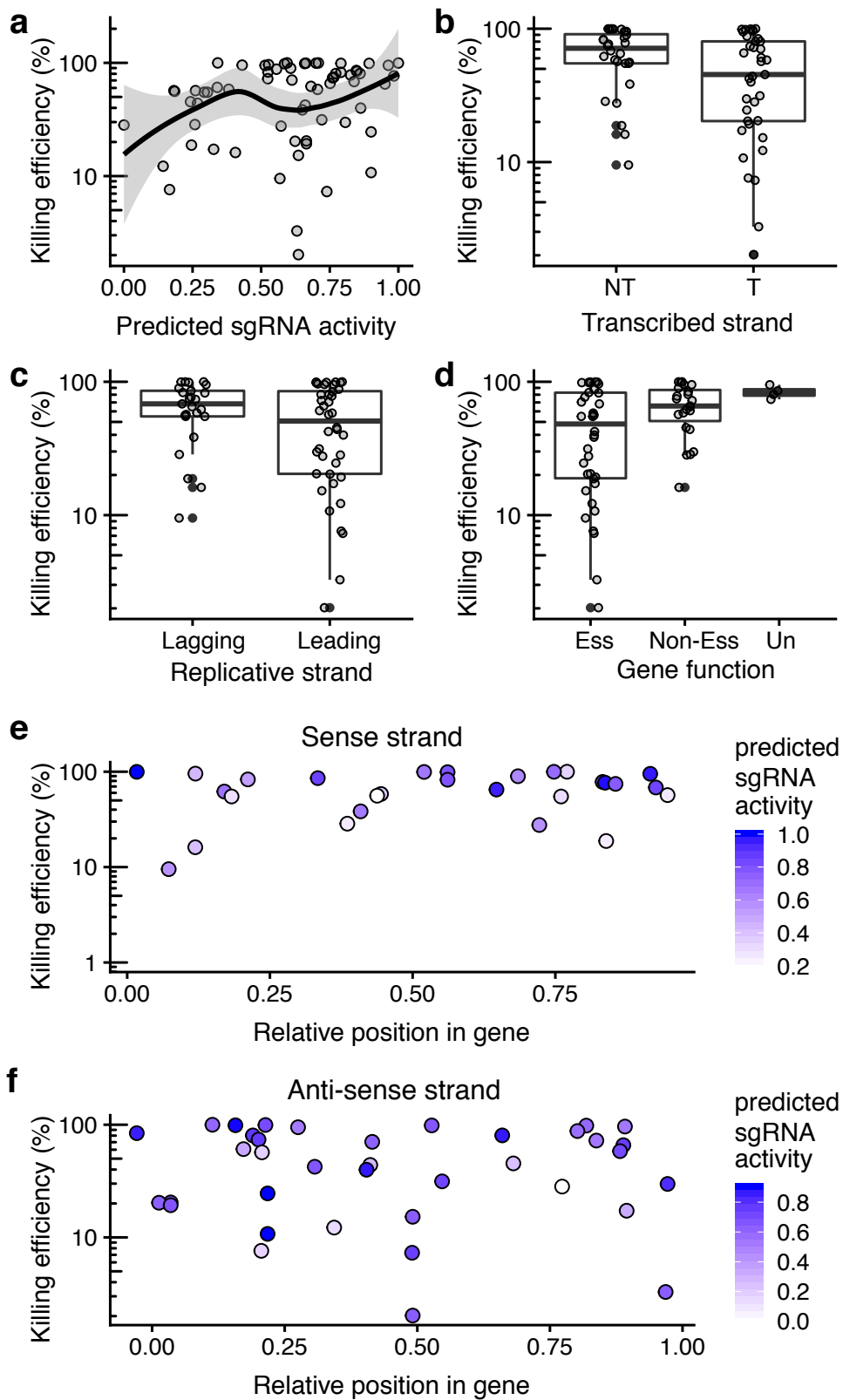


Figure 2.11: Effect of sgRNA targeting parameters on killing efficiency. **a.** Plot of predicted sgRNA activity versus *S. enterica* killing efficiency for all 65 sgRNAs. The shaded area is the 95% confidence interval of the line of best fit. Boxplots of sgRNAs targeting different strands for **b.** transcriptional (S, sense strand; AS, anti-sense strand) and **c.** replication, and **d.** sgRNAs targeting genes with essential (Ess), non-essential (NEss) or unresolved phenotypes (Un) versus killing efficiency. **e.** Plot of relative position of sgRNAs within genes versus average killing efficiency for the sense strand and **f.** anti-sense strand of targeted genes. For each plot, points are filled according to their predicted sgRNA activity. Killing efficiency is plotted on a log₁₀ scale.

2.4 Discussion

A central problem in microbiology and infectious disease control is the lack of tools to alter the composition of microbial communities or to control pathogenic species. One crucial concept in microbiome manipulation is that complete elimination of the target organism(s) is not required to restore the community because the constituent organisms of a bacterial population exhibit exponential growth (41). It is only necessary to reduce the relative abundance of the target organism below a threshold to achieve control. CRISPR-based nucleases can be easily re-purposed as sequence-specific anti-microbial agents, yet the development of a robust and broadly applicable delivery system remains a key milestone.

In this study, we adapted an IncP RK2 conjugative plasmid to deliver specific functional sequences to species of interest. Previous studies recognized the potential of conjugative delivery of CRISPR nucleases, emphasizing improvements in frequency as key to future applications (10). Our study differs from previous attempts in one key facet — we used a *cis* setup where the pNuc plasmid encoded the conjugative machinery as well as the TevSpCas9 nuclease. The pNuc-*cis* plasmid promotes increased occurrence of conjugation events because our data infers that transconjugants become donors for subsequent re-conjugation, leading to significant increases in conjugation frequency relative to the pNuc-*trans* plasmid. Previous studies employed strains with the conjugative machinery embedded in the chromosome of the donor bacteria (similar to the pNuc-*trans* setup), meaning that only a single round of conjugation could occur. In our two-species *E. coli*-*S. enterica* system, we observed conjugation frequencies approaching ~100% with pNuc-*cis* in culture conditions that promoted cell-to-cell contact and biofilm formation. Because the IncP RK2 system can be conjugated to a wide diversity of bacteria (27), and because conjugative systems are widespread in bacteria, our system in theory could be used to deliver the TevSpCas9 nuclease (or other CRISPR nuclease) in complex microbial communities.

It is possible that conjugation may not be the limiting factor in all systems. Indeed, improving regulation of TevSpCas9 to prevent cellular toxicity will improve conjugation efficiencies and counter negative selection on pNuc for inactivating mutations. Our data suggest that parameters that govern sgRNA activity in bacterial systems are poorly understood. Other factors, including compatibility with resident plasmids (6), expression of CRISPR and conjugation genes in diverse

bacteria, and targeting of conjugative plasmids by naturally occurring CRISPR systems (50), may also be relevant. Many of these issues have defined molecular solutions such as broad-host range plasmid origins, redundant sgRNAs, universal promoters and codon optimization for gene expression. Anti-CRISPR proteins (4, 34) that are specific for relevant CRISPR systems could also be included on pNuc-*cis* to prevent or reduce acquisition of CRISPR-mediated resistance. We also envision using multiple strains of donor bacteria harbouring versions of pNuc-*cis* based on different conjugative plasmid backbones (7), each encoding redundant programmable CRISPR nucleases or other microbial-modulating agents or sequences.

Microbial communities have complex bacterial compositions and they inhabit diverse environments. Many human microbial communities exist as biofilms (12), which presents a challenge for delivery of anti-microbial agents. Indeed, a number of disease conditions result from microbial imbalances in mucosal surfaces that are dominated by biofilms, for example *Clostridium difficile* infection (1). Rates of conjugation can be high in biofilms (21) and conjugative plasmids express factors that promote biofilm formation to enhance cell-to-cell contact necessary for formation of the conjugative pilus (16). By using a donor bacteria that is a native resident of the target biofilm the pNuc-*cis* plasmid could be introduced to microbial communities more readily than delivery vectors that have difficulty penetrating biofilms. Conversely, other delivery vectors, such as phage-based methods, are better suited to planktonic conditions where conjugation is less efficient. Depending on the nature of the microbiome and dysbiosis, a combination of conjugative- and phage-based CRISPR delivery systems may be appropriate.

2.5 References

- [1] Tanja apa, Rosanna Leuzzi, Yen K Ng, Soza T Baban, Roberto Adamo, Sarah A Kuehne, Maria Scarselli, Nigel P Minton, Davide Serruto, and Meera Unnikrishnan. Multiple factors modulate biofilm formation by the anaerobic pathogen *Clostridium difficile*. *Journal of Bacteriology*, 195(3):545–555, 2013.
- [2] Rodolphe Barrangou, Christophe Fremaux, H el ene Deveau, Melissa Richards, Patrick Boyaval, Sylvain Moineau, Dennis A Romero, and Philippe Horvath. CRISPR provides acquired resistance against viruses in prokaryotes. *Science*, 315(5819):1709–1712, 2007.
- [3] David Bikard, Chad W Euler, Wenyan Jiang, Philip M Nussenzweig, Gregory W Goldberg, Xavier Duportet, Vincent A Fischetti, and Luciano A Marraffini. Exploiting CRISPR-Cas nucleases to produce sequence-specific antimicrobials. *Nature Biotechnology*, 32(11):1146, 2014.
- [4] Joe Bondy-Denomy, April Pawluk, Karen L Maxwell, and Alan R Davidson. Bacteriophage genes that inactivate the CRISPR/Cas bacterial immune system. *Nature*, 493(7432):429, 2013.
- [5] Jennifer AN Brophy, Alexander J Triassi, Bryn L Adams, Rebecca L Renberg, Dimitra N Stratis-Cullum, Alan D Grossman, and Christopher A Voigt. Engineered integrative and conjugative elements for efficient and inducible DNA transfer to undomesticated bacteria. *Nature Microbiology*, 3(9):1043, 2018.
- [6] Michelle MC Buckner, Maria Laura Ciusa, and Laura JV Piddock. Strategies to combat antimicrobial resistance: anti-plasmid and plasmid curing. *FEMS Microbiology Reviews*, 42(6):781–804, 2018.
- [7] Elena Cabez on, Jorge Ripoll-Rozada, Alejandro Pe a, Fernando de la Cruz, and Ignacio Arechaga. Towards an integrated model of bacterial conjugation. *FEMS Microbiology Reviews*, 39(1):81–95, 2014.
- [8] Mai Huong Chatain-Ly. The factors affecting effectiveness of treatment in phages therapy. *Frontiers in Microbiology*, 5:51, 2014.
- [9] Ilseung Cho and Martin J Blaser. The human microbiome: at the interface of health and disease. *Nature Reviews Genetics*, 13(4):260, 2012.
- [10] Robert J Citorik, Mark Mimee, and Timothy K Lu. Sequence-specific antimicrobials using efficiently delivered RNA-guided nucleases. *Nature Biotechnology*, 32(11):1141, 2014.
- [11] Tom Coenye and Hans J Nelis. *In vitro* and *in vivo* model systems to study microbial biofilm formation. *Journal of Microbiological Methods*, 83(2):89–105, 2010.
- [12] Hans-Curt Flemming, Jost Wingender, Ulrich Szewzyk, Peter Steinberg, Scott A Rice, and Staffan Kjelleberg. Biofilms: an emergent form of bacterial life. *Nature Reviews Microbiology*, 14(9):563, 2016.

- [13] Josiane E Garneau, Marie-Ève Dupuis, Manuela Villion, Dennis A Romero, Rodolphe Barrangou, Patrick Boyaval, Christophe Fremaux, Philippe Horvath, Alfonso H Magadán, and Sylvain Moineau. The CRISPR/Cas bacterial immune system cleaves bacteriophage and plasmid DNA. *Nature*, 468(7320):67, 2010.
- [14] Giedrius Gasiunas, Rodolphe Barrangou, Philippe Horvath, and Virginijus Siksnys. Cas9-crRNA ribonucleoprotein complex mediates specific DNA cleavage for adaptive immunity in bacteria. *Proceedings of the National Academy of Sciences*, 109(39):E2579–E2586, 2012.
- [15] Philippe Gérard. Gut microbiota and obesity. *Cellular and molecular life sciences*, 73(1): 147–162, 2016.
- [16] Jean-Marc Ghigo. Natural conjugative plasmids induce bacterial biofilm development. *Nature*, 412(6845):442, 2001.
- [17] Daniel G Gibson. Synthesis of DNA fragments in yeast by one-step assembly of overlapping oligonucleotides. *Nucleic Acids Research*, 37(20):6984–6990, 2009.
- [18] Ahmed A Gomaa, Heidi E Klumpe, Michelle L Luo, Kurt Selle, Rodolphe Barrangou, and Chase L Beisel. Programmable removal of bacterial strains by use of genome-targeting CRISPR-Cas systems. *MBio*, 5(1):e00928–13, 2014.
- [19] Jiahui Guo, Tianmin Wang, Changge Guan, Bing Liu, Cheng Luo, Zhen Xie, Chong Zhang, and Xin-Hui Xing. Improved sgRNA design in bacteria via genome-wide activity profiling. *Nucleic Acids Research*, 46(14):7052–7069, 2018.
- [20] Luz-Maria Guzman, Dominique Belin, Michael J Carson, and JON Beckwith. Tight regulation, modulation, and high-level expression by vectors containing the arabinose PBAD promoter. *Journal of Bacteriology*, 177(14):4121–4130, 1995.
- [21] Martina Hausner and Stefan Wuerztz. High rates of conjugation in bacterial biofilms as determined by quantitative *in situ* analysis. *Applied and Environmental Microbiology*, 65(8): 3710–3713, 1999.
- [22] Aayushi Jain and Preeti Srivastava. Broad host range plasmids. *FEMS Microbiology Letters*, 348(2):87–96, 2013.
- [23] Ruud Jansen, Jan DA van Embden, Wim Gaastra, and Leo M Schouls. Identification of genes that are associated with DNA repeats in prokaryotes. *Molecular Microbiology*, 43(6): 1565–1575, 2002.
- [24] Martin Jinek, Krzysztof Chylinski, Ines Fonfara, Michael Hauer, Jennifer A Doudna, and Emmanuelle Charpentier. A programmable dual-RNA-guided DNA endonuclease in adaptive bacterial immunity. *Science*, page 1225829, 2012.
- [25] Bogumil J Karas, Rachel E Diner, Stephane C Lefebvre, Jeff McQuaid, Alex PR Phillips, Chari M Noddings, John K Brunson, Ruben E Valas, Thomas J Deerinck, Jelena Jablanovic, et al. Designer diatom episomes delivered by bacterial conjugation. *Nature Communications*, 6:6925, 2015.

- [26] Sahil Khanna, Yoshiki Vazquez-Baeza, Antonio González, Sophie Weiss, Bradley Schmidt, David A Muñoz-Pedrogo, John F Rainey, Patricia Kammer, Heidi Nelson, Michael Sadowsky, et al. Changes in microbial ecology after fecal microbiota transplantation for recurrent *C. difficile* infection affected by underlying inflammatory bowel disease. *Microbiome*, 5(1):55, 2017.
- [27] Uli Klümper, Leise Riber, Arnaud Dechesne, Analia Sannazzarro, Lars H Hansen, Søren J Sørensen, and Barth F Smets. Broad host range plasmids can invade an unexpectedly diverse fraction of a soil bacterial community. *The ISME Journal*, 9(4):934, 2015.
- [28] Katharina Konrat, Ingeborg Schwebke, Michael Laue, Christin Dittmann, Katja Levin, Ricarda Andrich, Mardjan Arvand, and Christoph Schaudinn. The bead assay for biofilms: a quick, easy and robust method for testing disinfectants. *PloS One*, 11(6):e0157663, 2016.
- [29] Rocío López-Igual, Joaquín Bernal-Bayard, Alfonso Rodríguez-Patón, Jean-Marc Ghigo, and Didier Mazel. Engineered toxin–intein antimicrobials can selectively target and kill antibiotic-resistant bacteria in mixed populations. *Nature Biotechnology*, page 1, 2019.
- [30] Sarah Lynn Martz, Mabel Guzman-Rodriguez, Shu-Mei He, Curtis Noordhof, David John Hurlbut, Gregory Brian Gloor, Christian Carlucci, Scott Weese, Emma Allen-Vercoe, Jun Sun, et al. A human gut ecosystem protects against *C. difficile* disease by targeting TcdA. *Journal of Gastroenterology*, 52(4):452–465, 2017.
- [31] Vladimir N Noskov, Bogumil J Karas, Lei Young, Ray-Yuan Chuang, Daniel G Gibson, Ying-Chi Lin, Jason Stam, Isaac T Yonemoto, Yo Suzuki, Cynthia Andrews-Pfannkoch, et al. Assembly of large, high G+C bacterial DNA fragments in yeast. *ACS Synthetic Biology*, 1(7):267–273, 2012.
- [32] Pedro H Oliveira, Marie Touchon, and Eduardo PC Rocha. The interplay of restriction-modification systems with mobile genetic elements and their prokaryotic hosts. *Nucleic Acids Research*, 42(16):10618–10631, 2014.
- [33] Paul W O’Toole and Ian B Jeffery. Gut microbiota and aging. *Science*, 350(6265):1214–1215, 2015.
- [34] April Pawluk, Nadia Amrani, Yan Zhang, Bianca Garcia, Yurima Hidalgo-Reyes, Jooyoung Lee, Alireza Edraki, Megha Shah, Erik J Sontheimer, Karen L Maxwell, et al. Naturally occurring off-switches for CRISPR-Cas9. *Cell*, 167(7):1829–1838, 2016.
- [35] Daniel Pérez-Mendoza and Fernando de la Cruz. *Escherichia coli* genes affecting recipient ability in plasmid conjugation: are there any? *BMC Genomics*, 10(1):71, 2009.
- [36] Jason M Peters, Byoung-Mo Koo, Ramiro Patino, Gary E Heussler, Cameron C Hearne, Jiuxin Qu, Yuki F Inclan, John S Hawkins, Candy HS Lu, Melanie R Silvis, et al. Enabling genetic analysis of diverse bacteria with Mobile-CRISPRi. *Nature Microbiology*, 4(2):244, 2019.

- [37] Elaine O Petrof, Gregory B Gloor, Stephen J Vanner, Scott J Weese, David Carter, Michelle C Daigneault, Eric M Brown, Kathleen Schroeter, and Emma Allen-Vercoe. Stool substitute transplant therapy for the eradication of *Clostridium difficile* infection: ‘RePOOPulating’ the gut. *Microbiome*, 1(1):3, 2013.
- [38] Kathryn J Pflughoeft and James Versalovic. Human microbiome in health and disease. *Annual Review of Pathology: Mechanisms of Disease*, 7:99–122, 2012.
- [39] F Ann Ran, Le Cong, Winston X Yan, David A Scott, Jonathan S Gootenberg, Andrea J Kriz, Bernd Zetsche, Ophir Shalem, Xuebing Wu, Kira S Makarova, et al. *In vivo* genome editing using *Staphylococcus aureus* Cas9. *Nature*, 520(7546):186, 2015.
- [40] Gregor Reid, Jessica A Younes, Henny C Van der Mei, Gregory B Gloor, Rob Knight, and Henk J Busscher. Microbiota restoration: natural and supplemented recovery of human microbial communities. *Nature Reviews Microbiology*, 9(1):27, 2011.
- [41] Dwayne R Roach, Chung Yin Leung, Marine Henry, Eric Morello, Devika Singh, James P Di Santo, Joshua S Weitz, and Laurent Debarbieux. Synergy between the host immune system and bacteriophage is essential for successful phage therapy against an acute respiratory pathogen. *Cell Host & Microbe*, 22(1):38–47, 2017.
- [42] Carlotta Ronda, Sway P Chen, Vitor Cabral, Stephanie J Yaung, and Harris H Wang. Metagenomic engineering of the mammalian gut microbiome *in situ*. *Nature Methods*, 16(2):167, 2019.
- [43] Samuel S Slattery, Andrew Diamond, Helen Wang, Jasmine A Therrien, Jeremy T Lant, Teah Jazey, Kyle Lee, Zachary Klassen, Isabel Desgagné-Penix, Bogumil J Karas, et al. An expanded plasmid-based genetic toolbox enables Cas9 genome editing and stable maintenance of synthetic pathways in *Phaeodactylum tricornutum*. *ACS Synthetic Biology*, 7(2):328–338, 2018.
- [44] Chris Smillie, M Pilar Garcillán-Barcia, M Victoria Francia, Eduardo PC Rocha, and Fernando de la Cruz. Mobility of plasmids. *Microbiology and Molecular Biology Reviews*, 74(3):434–452, 2010.
- [45] Hans P Steenackers, Ilse Parijs, Kevin R Foster, and Jozef Vanderleyden. Experimental evolution in biofilm populations. *FEMS Microbiology Reviews*, 40(3):373–397, 2016.
- [46] Trine Aakvik Strand, Rahmi Lale, Kristin Fløgstad Degnes, Malin Lando, and Svein Valla. A new and improved host-independent plasmid system for RK2-based conjugal transfer. *PLoS One*, 9(3):e90372, 2014.
- [47] Jun Sun and Ikuko Kato. Gut microbiota, inflammation and colorectal cancer. *Genes & Diseases*, 3(2):130–143, 2016.
- [48] U Theuretzbacher. Antibiotic innovation for future public health needs. *Clinical Microbiology and Infection*, 23(10):713–717, 2017.

- [49] Baohong Wang, Mingfei Yao, Longxian Lv, Zongxin Ling, and Lanjuan Li. The human microbiota in health and disease. *Engineering*, 3(1):71–82, 2017.
- [50] Edze R Westra, Raymond HJ Staals, Gerrit Gort, Søren Høgh, Sarah Neumann, Fernando de la Cruz, Peter C Fineran, and Stan JJ Brouns. CRISPR-Cas systems preferentially target the leading regions of MOBF conjugative plasmids. *RNA Biology*, 10(5):749–761, 2013.
- [51] Jason M Wolfs, Thomas A Hamilton, Jeremy T Lant, Marcon Laforet, Jenny Zhang, Louisa M Salemi, Gregory B Gloor, Caroline Schild-Poulter, and David R Edgell. Biasing genome-editing events toward precise length deletions with an RNA-guided TevCas9 dual nuclease. *Proceedings of the National Academy of Sciences*, 113(52):14988–14993, 2016.
- [52] Yang Yu, Jackson Champer, David Beynet, Jenny Kim, and Adam J Friedman. The role of the cutaneous microbiome in skin cancer: lessons learned from the gut. *Journal of Drugs in Dermatology*, 14(5):461–465, 2015.

Chapter 3

Functionalizing conjugative systems from metagenomic data for targeted delivery of a CRISPR nuclease

3.1 Introduction

Microbial ecosystems are an important factor in human health (10, 46, 47). The diversity of microbial species that comprise the human microbiome has gained renewed appreciation with the advent of large-scale sequencing studies. Metagenomic profiling has also highlighted the prevalence of antimicrobial resistance (AMR) genes and mobile genetic systems that can spread AMR genes (49). The development of multi-drug resistant bacteria has reduced the effectiveness of traditional antibiotics to treat microbial dysbioses that lead to acute disease or chronic conditions, necessitating alternative strategies to combat microbiome imbalances (36, 48). Recently, nucleases derived from the clustered regularly interspaced short palindromic repeat (CRISPR) system have been adapted to target specific bacteria for elimination based on the introduction of double-strand breaks in the chromosome that lead to cell death (3, 11, 20, 22, 35). A key unresolved issue in using CRISPR as an antimicrobial tool is delivery. In particular, delivery vectors used to date (phage, phagemids, conjugative plasmids) were primarily selected because they are characterized to some extent, replicate in *Escherichia coli* or other model bacteria, have known host ranges, and are amenable to genetic manipulation. This strategy, however, capitalizes on a fraction of the diversity of mobile genetic systems that could be re-purposed for CRISPR delivery, many of which are known only through metagenomic or other sequencing studies.

Bacterial conjugative systems are large, multi-component protein complexes that catalyze the unidirectional transfer of DNA from a donor to a recipient cell. Conjugative transfer is initiated by the relaxase protein that nicks DNA at a defined origin of transfer sequence (*oriT*). The subsequent protein-DNA complex, called the relaxosome, interacts with the type IV coupling protein, followed by interaction with the mating pair formation and type 4 secretion (T4SS) proteins to catalyze DNA transfer to the recipient (8, 30, 44). Conjugative systems can be encoded on plasmids as complete systems that are self transmissible, or as partial systems that are dependent on conjugative proteins encoded by other elements. Upon DNA transfer, some conjugative systems integrate into the chromosome as integrative conjugative elements (ICEs) (33, 39, 43).

Specificity of conjugation is partially due to proteins encoded by conjugative plasmids that are expressed on donor cell surfaces and that stabilize contact with recipients (31). Currently, the classification of conjugative systems is based on the identity of the relaxase protein and the *oriT* sequence (where identifiable) (16, 17). Conjugative plasmids are well suited as delivery vectors for CRISPR nucleases or other genetic tools. We, and others, have demonstrated that conjugative systems can deliver CRISPR nucleases with high efficiency *in vitro* and *in vivo*, with targeted elimination of bacteria in mouse models (22, 35, 50). The range of bacterial species that can be targeted by conjugative plasmids would be increased by expanding the current diversity of conjugative systems that are used for CRISPR delivery.

Here, we elaborate an approach to capitalize on the diversity of type IV conjugative systems from human metagenomic data for delivery of CRISPR nucleases or other genetic tools. We developed a bioinformatics pipeline and identified conjugative systems from 7 different bacterial phyla and belonging to 11 different MOB families. We selected a ~54 kb conjugative system identified on a *Citrobacter* spp. plasmid and synthesized it *de novo* to create a functional conjugative plasmid, p20298. Crucially, p20298 conjugates with a higher frequency to *Citrobacter* species than to other bacteria, is compatible with resident *Citrobacter* plasmids, and is stable over multiple generations. Programming p20298 with a TevCas9 dual nuclease and sgRNAs resulted in efficient killing of *Citrobacter rodentium*. This paper provides proof of principle that conjugative systems identified in genomic data can be synthesized *de novo* and functionalized for the targeted killing of bacteria.

3.2 Methods and Materials

3.2.1 Bacterial and yeast strains

All yeast assemblies were performed using *Saccharomyces cerevisiae* VL6-48 (*MATa*, *his3Δ200*, *trpΔ1*, *ura3-52*, *ade2-101*, *lys2*, *psi+cir^o*). *E. coli* EPI300 (F' λ *mcrA* Δ (*mrr-hsdRMS-mcrBC*) ϕ 80*dlacZΔM15* Δ (*lac*)X74 *recA1* *endA1* *araD139* Δ (*ara*, *leu*)7697 *galU* *galK* *rpsL* (Str^R) *nupG* *trfA* *dhfr*) (Epicentre) as well as a diaminopimelic acid (DAP) auxotroph of the strain (5) were used for cloning and as conjugative donors. *Citrobacter rodentium* DBS100, *Salmonella enterica* Typhimurium LT2, and *E. coli* (kan^R) were used as primary recipients. Seven additional *Citrobacter* spp. strains were used as recipients.

3.2.2 Identifying conjugative systems from gut metagenome data

The identification of conjugative systems from gut metagenome data, and construction of the conjugative systems database is described in detail in Benjamin Joris's PhD thesis (25). Briefly, two methods were used to assembly and identify conjugative systems from gut metagenome data. The first method started with short-read sequencing data which was deduplicated and trimmed using SRA toolkit version 2.9.2 (7) and Trimmomatic version 0.36 (4) respectively, followed by sample-by-sample assembly with SPAdes version 3.14.0 (38). The resulting assemblies were input into Anvi'o version 6.0 (14) where a Profile hidden Markov model (pHMM) was used to identify assembled contigs containing matches for relaxases, type 4 coupling proteins, and type 4 secretion pilus proteins. Identified contigs were annotated by alignment to the UniRef90 database (45) using Prodigal version 2.6.3 (24). The second method of identifying conjugative systems used protein alignments to identify conjugative systems. First, Prodigal version 2.6.3 (24) was used to predict ORFs in raw metagenomic data, which were then aligned to the UniRef90 database (45) using DIAMOND version 0.9.14 (6). Keyword searches were then used to identify contigs containing annotations for a relaxase and either a type IV secretion system protein, or type IV coupling protein.

3.2.3 Molecular cloning

The conjugative system identified from the conjugative contig “20298” was synthesized in 11 fragments from Twist Bioscience (San Francisco, USA) as clonal genes. One fragment of the sequence was additionally synthesized on a Telesis Bio (San Diego, USA) BioXP 3200. Fragments ordered from Twist Bioscience were released from their vectors using a PmeI digest, while the tile constructed using the BioXP 3200 was PCR amplified. Each tile contained 86-476 base pairs of homology with the adjacent fragment. The terminal DNA fragments contained homology with the backbone of plasmid pAGE1.0 (5), which was originally derived from p0521s (26). p20298-AGE was constructed with these fragments using a modified yeast assembly (18, 37), which is described in detail in chapter 2. Once it was identified that p20298-AGE contained mutations in the *traV* and *traY* genes, and that the pAGE replicon was non-functional in *C. rodentium*, the conjugative contig was re-cloned into the backbone derived from pNuc-*trans* (22). This contains a p15a origin, chloramphenicol-acetyltransferase and CEN6-ARS4-HIS3. The conjugative contig was re-amplified from p20298-AGE with PCR, using primers to fix the mutations in the *traV* and *traY* genes. The remainder of the plasmid was amplified in fragments ranging from 1209 base pairs to 6302 base pairs with homology. These fragments were then assembled in a yeast assembly as described above to generate p20298-15a.

3.2.4 sgRNA cloning

A gateway cloning entry vector was constructed into the pDONR221 backbone, containing an arabinose-inducible TevCas9 endonuclease and an sgRNA cloning cassette flanked by attL recombination sites to form pENTR-TC9. A corresponding gateway destination cassette containing a ccdB toxin and ampicillin resistance gene flanked by attR sites was cloned into p20298-15a, to generate p20298-15a-dest.

To select sgRNAs we utilized a generalizable model to identify sgRNAs that were predicted to have high killing efficiency (21). We cloned sgRNAs into pENTR-TC9 using golden gate assembly at the BsaI cassette. A gateway LR reaction was performed to insert the TevCas9 and sgRNA from pENTR-TC9 into p20298-15a-dest, forming p20298-TC9. The resulting plasmid was transformed into *E. coli* Epi300 (DAP-).

3.2.5 Bacterial conjugation assays

Donor and recipient strains were grown to saturation overnight in selective media. Saturated cultures were then diluted 1:50 into 5 mL non-selective LSLB (10 g/L tryptone, 5 g/L yeast extract, 5 g/L NaCl) supplemented with 60 $\mu\text{g}/\text{mL}$ diaminopimelic acid (DAP) and grown to an A600 of ~ 0.5 -1.0 and adjusted to an A600 of 0.5. Cultures were centrifuged at 4000 $\times g$ for 5 minutes and resuspended in 500 μL of 10% glycerol. Cells were aliquoted and frozen at $-80\text{ }^{\circ}\text{C}$.

During conjugations, cells were thawed on ice and 50 μL of donor strain were mixed with 50 μL recipient strain on LSLB plates supplemented with 60 $\mu\text{g}/\text{mL}$ DAP. Conjugations proceeded on plates at $37\text{ }^{\circ}\text{C}$ for 1 hour. Cells were scraped into 400 μL LSLB with a glass spreader. These cell suspensions were then serially diluted and plated on selection for donors, recipients, and transconjugants. Plates were incubated for 16-20 hours at $37\text{ }^{\circ}\text{C}$ and colonies were counted manually.

3.2.6 RNA-seq

Total RNA was prepared from three replicates each of p20298-15a electroporated into *E. coli* Epi300 (DAP-) and *C. rodentium*. A single colony from each transformation was grown overnight to saturation under selection. Saturated cultures were diluted 1:50 into non-selective LSLB, and LSLB supplemented with 60 $\mu\text{g}/\text{mL}$ DAP for *C. rodentium* and *E. coli* respectively. Cultures were grown for 2 hours at $37\text{ }^{\circ}\text{C}$ with 225 RPM shaking, reaching A600 between 0.4-0.6. 1.5 mL of culture was centrifuged at 16000 $\times g$ for 5 minutes at $4\text{ }^{\circ}\text{C}$. The supernatant was aspirated and the pellet was resuspended in 1 mL Trizol reagent (Invitrogen). Samples were incubated at $65\text{ }^{\circ}\text{C}$ for 10 minutes, and 0.2 mL of chloroform was added and mixed by inverting for 15 seconds. Samples were incubated at room temperature for 3 minutes before being centrifuged at 16000 $\times g$ for 5 minutes at $4\text{ }^{\circ}\text{C}$. The aqueous phase was transferred to a clean tube and 1 volume of ethanol was added to each. An NEB Monarch cleanup kit was used by adding samples to an RNA cleanup column and centrifuging at 11000 $\times g$ for 1 minute at room temperature. The column was washed twice by adding 500 μL of RNA cleanup wash buffer and centrifuging at 11000 $\times g$ for 1 minute. The column was spun for an additional 1 minute at 11000 $\times g$ to dry before eluted into 50 μL nuclease-free water by centrifuging at 11000 $\times g$ for 1 minute.

RNA libraries were prepared and sequenced using an Illumina NextSeq High Output 75 cycle

sequencing kit on an Illumina NextSeq. Resulting reads were trimmed with Trimmomatic version 0.36 (4) with options LEADING:10 TRAILING:10. Processed reads for *E. coli* Epi300 samples were mapped to the *E. coli* strain K-12 NEB 5-alpha genome (CP017100.1) and p20298-15a plasmid reference sequences using Hisat2 version 2.2.0 (27). Processed reads for *C. rodentium* samples were mapped to the *C. rodentium* strain DBS100 genome (CP038008.1) and p20298-15a plasmid reference sequences using the same workflow. Htseq-count version 0.13.5 (40) was used to count the number of reads mapping to each annotated feature within the genome and plasmid sequences. ALDEx2 (15) was used to determine differential gene expression. Positional read coverage was obtained using Samtools version 1.10 (13).

3.2.7 Plasmid stability assays

p20298-15a and pNuc-cis (22) were conjugated to *C. rodentium* as described in bacterial conjugation assays. Transconjugants were isolated and passaged on selective plates with overnight growth at 37 °C for 16-20 hours. Colonies were isolated from these plates and passaged once again on selective plates at 37 °C for 16-20 hours. Individual colonies were picked from these plates and grown overnight in selective liquid LSLB at 37 °C. Plasmids were extracted and diagnostic digests were performed with NotI-HF and NcoI-HF (New England Biolabs). Digests were analyzed on agarose gels for plasmid rearrangements.

3.2.8 *C. rodentium* killing assays

p20298-15-TC9 plasmids with *C. rodentium* targeted sgRNAs were conjugated from *E. coli* (DAP-) to *C. rodentium* on LSLB + DAP 60 µg/mL + 0.2 % glucose plates at a 4:1 donor:recipient ratio for 1 hour. Cells were scraped into 500 µL LSLB, and added to an additional 500 µL LSLB. 250 µL of the resulting cell suspension was diluted 1:2 into 2x selective and inducing LSLB (50 µg/mL chloramphenicol and 0.4 % arabinose) and selective and 2x repressing LSLB (50 µg/mL chloramphenicol and 0.4 % glucose). Cell suspensions are therefore at final concentrations of 25 µg/mL chloramphenicol and 0.2 % arabinose for induced, and 25 µg/mL chloramphenicol and 0.2 % glucose for repressed. Cells were then incubated at 37 °C with shaking for 2 hours to induce TevCas9 expression. After 2 hours of growth, the suspensions were centrifuged at 11000 xg for 1

minute and resuspended in LSLB supplemented with 25 $\mu\text{g}/\text{mL}$ chloramphenicol. Cell suspensions were then serially diluted and plated on LSLB supplemented with 25 $\mu\text{g}/\text{mL}$ chloramphenicol and 0.2 % glucose. Colonies were counted and killing efficiency was calculated.

3.3 Results

3.3.1 Identifying conjugative systems from metagenomic data

A non-redundant, near-complete collection of the human gut microbiome containing 2505 bacterial genomes (1) was used to identify the presence of conjugative systems in various cohorts. Using UniRef90 annotations for relaxases, type 4 secretion systems (T4SS) and type 4 coupling proteins (T4CP), we were able to identify 1598 contigs from 787 genomes that were potentially conjugative (Figure 3.1a). These systems represent the diverse conjugative systems that allow transfer of genetic material in the gut microbiome. Using MobScan (16) we were able to predict the MOB families of the relaxases that were present on the identified conjugative systems, and found a wide range of predicted relaxases. Interestingly, MOB_{P1}-type relaxases were found to be the majority conjugative system, with 865 represented systems, and all 9 of the relaxase MOB families were present. Furthermore, we used plasflow (28) to predict whether the conjugative systems were encoded on a chromosome or a plasmid and found that 57 were predicted to be plasmid-based, 1353 chromosomal, and the remaining 179 conjugative systems were unknown.

To begin the process of synthesizing a conjugative system from this data set, we first narrowed down to systems that were identified in the Proteobacteria clade. These systems were attractive as they represented good proof-of-principle systems for synthesis, as many were sequenced from reference isolates, and because it simplified and expedited the cloning and testing process. We identified a conjugative system “20298” that mapped to a reference isolate and was predicted to be a member of the *Citrobacter* genus. This was of interest to us because *Citrobacter* spp. have implications in human health (2, 41), and because *C. rodentium* is a well-studied mouse model for enterohemorrhagic *E. coli* (12, 34).

The conjugative system from contig “20298” (Figure 3.1b) has a predicted MOB_{P1} relaxase (16), and has similarity to conjugative systems from the IncI family (29). The conjugative system of

the contig was ~54 kb in size and was located on a larger contig of ~150 kb. BLAST results of the full length contig match primarily to plasmids identified in *Citrobacter* spp. isolates. Furthermore, we were able to identify the origin of transfer (*oriT*) located adjacent to the predicted relaxase using oritfinder (29).

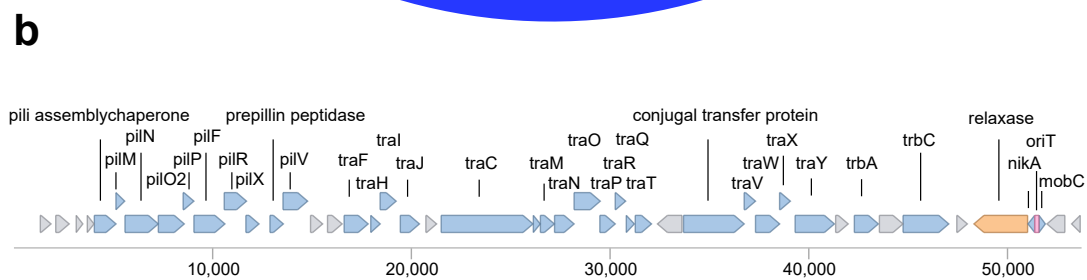
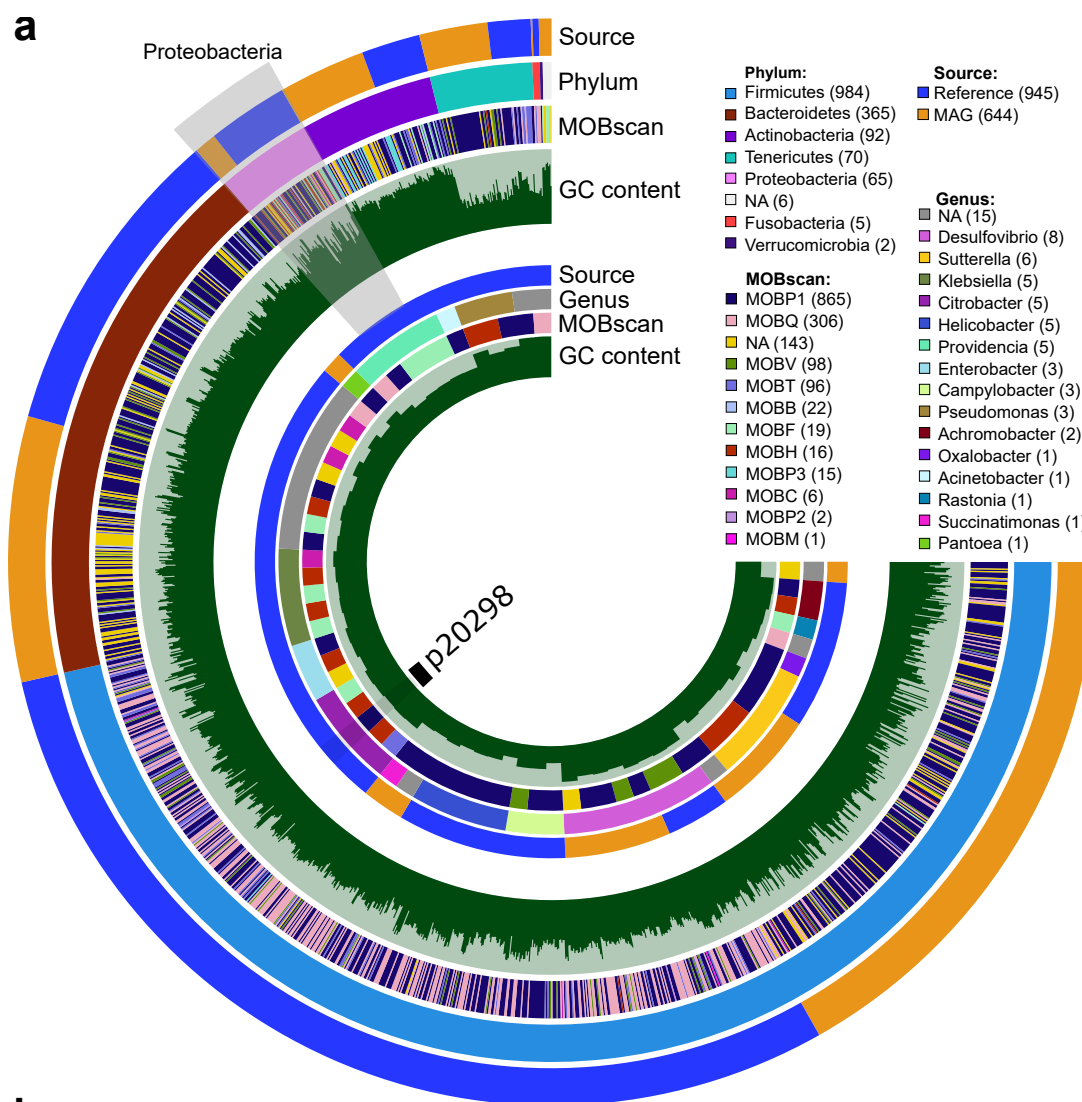


Figure 3.1: Identifying conjugative systems from gut metagenomic data. **a.** Conjugative systems were identified from a near-complete non-redundant gut database containing both reference genomes and metagenome-assembled genomes (MAGs). Relaxase families were predicted using MOBScan (16). The outer region represents all 1598 contigs containing putative conjugative systems. The inner region is a focused section of conjugative systems identified in the Proteobacteria clade. The highlighted system, 20298 is a conjugative system with a MOB1 relaxase that was chosen for synthesis. **b.** Predicted conjugative contig “20298” showing the trimmed part of the contig containing the predicted conjugative elements and which was then synthesized. The predicted relaxase is coloured orange, while the predicted *oriT* (29) is coloured pink.

3.3.2 Constructing a conjugative system *de novo*

We initially constructed a plasmid, p20298-AGE, which was designed to insert the approximately 54 kb conjugative system from the 20298 contig into the pAGE plasmid backbone (5) (Figure 3.2). To do this we first had to have the 20298 conjugative system sequence synthesized. For this to be done, we proceeded to split the sequence into 12 tiles of approximately 5 kb in length, each containing sequence homology at both ends to the adjacent fragments, with the terminal fragments containing homology to the pAGE backbone. We ordered these 12 tiles as clonal genes from Twist Bioscience that could easily be excised from their clonal vector by PmeI digest. During this process, one tile (tile 9) was unable to be successfully synthesized as a clonal gene. To address this, we synthesized it as four smaller DNA fragments using a Telesis Bio DNA BioXP 3200 (Figure 3.2a). A yeast assembly was used to clone the 4 BioXP fragments into a single 5 kb tile which was cloned into pAGE backbone for storage. The 11 synthesized fragments from TWIST were released from their backbones by PmeI digest, the BioXP tile 9 was PCR amplified, and all tiles were subsequently assembled in yeast before being moved to *E. coli* Epi300. Once moved to *E. coli* we screened 13 individual colonies by diagnostic digest, and found that 9 contained plasmids with the expected digest banding patterns (Figure 3.2c). We sequenced 5 clones using an Oxford nanopore Minion, and found mutations in each clone (Table 3.1). The clone with the highest fidelity relative to the 20298 contig sequence contained deletions in both the *traV* and *traY* genes. Moreover, attempts to conjugate this construct from *E. coli* to *E. coli* were unsuccessful (Figure 3.3b). We further attempted to transform p20298-AGE into *C. rodentium* via electroporation and were unable to successfully yield transformants, suggesting that the pAGE backbone could not replicate in *C. rodentium*. To verify this we attempted to transform pAGE1 (5) which also failed to yield transformants in *C. rodentium*. Using p20298-AGE as a template, we repaired the deletions in *traV* and *traY*, and replaced the pAGE backbone with the backbone from the pNuc-*trans* plasmid (22). The pNuc-*trans* backbone contains the p15a origin of replication and chloramphenicol acetyltransferase for replication and selection in *E. coli*. Importantly, it also contains a Cen-Ars-His yeast region to allow for DNA assembly and replication in *S. cerevisiae* yeast. We elected to use this backbone as we had previously found that it could replicate in *C. rodentium*, and because it contains the necessary elements for assembly and replication in yeast. Using p20298-AGE

as a template, we re-amplified the 20298 conjugative system using primers that simultaneously introduced corrections in the *traV* and *traY* genes. These new fragments were then assembled together in yeast to generate p20298-15a (Figure 3.3a). After confirming conjugative function of p20298-15a, we identified several mutations in the coding regions of the plasmid (Table 3.2) that were generated during construction. Additionally we constructed a version of the plasmid, p20298-15a-M, which changed the plasmid backbone but maintained the inactivating mutations in the *traV* and *traY* genes that were present in p20298-AGE.

Table 3.1: Identified mutations by full plasmid Nanopore sequencing in p20298-AGE clones isolated from *E. coli*.

p20298-AGE clone	Location of error	Error type
1-1	<i>traV</i>	1 bp deletion
	<i>traY</i>	1 bp deletion
	hypothetical orf	missense SNP
1-2	<i>traV</i>	1 bp deletion
	<i>traY</i>	1 bp deletion
	pili assembly chaperone	1 bp insertion
2-2	<i>traV</i>	1 bp deletion
	<i>traY</i>	1 bp deletion
	<i>traY</i>	missense SNP
2-3	<i>traV</i>	1 bp deletion
	<i>traY</i>	1 bp deletion
2-4	<i>traV</i>	1 bp deletion
	<i>traY</i>	1 bp deletion

Table 3.2: Identified mutations by full plasmid nanopore sequencing in p20298-15a.

Location of error	Error type	Impact
pili assembly chaperone	SNP	synonymous
<i>pilN</i>	SNP	missense; Met to Ile
<i>pilP</i>	SNP	nonsense; truncated orf
hypothetical orf	SNP	missense; Val to Ile
<i>traC</i>	SNP	missense; Asp to Asn
<i>traT</i>	SNP	missense; His to Tyr

3.3.3 Conjugation of p20298-15a

Using an *E. coli* Epi300 DAP- auxotrophic donor strain we attempted to conjugate p20298-15a to an *E. coli* recipient, *C. rodentium*, and *S. enterica* LT2 (Figure 3.3c). We observed successful

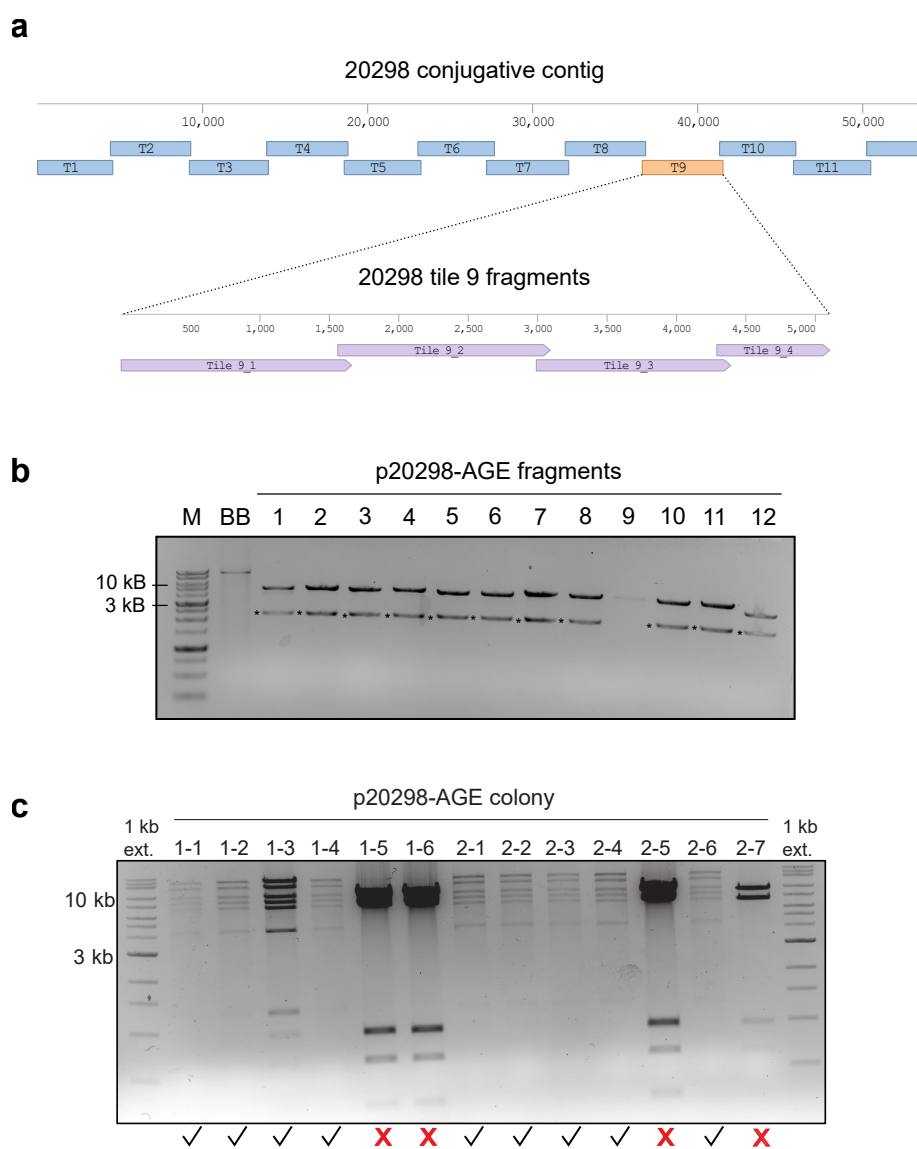


Figure 3.2: Synthesis and assembly of p20298-AGE. **a.** Schematic of assembly. 11 tiles were synthesized as clonal DNA fragments from TWIST Bioscience. Tile 9 could not be synthesized in this manner and was instead synthesized in 4 fragments by a Telesis Bio BioXP 3200. **b.** TAE-agarose gel showing fragments used for yeast assembly of p20298-AGE. Bands marked by asterisks represent the plasmid backbone the clonal fragments were excised from with PmeI. **c.** Diagnostic digest of yeast assembly clones that have been transformed into *E. coli*, isolated, and digested with NcoI-HF and NotI-HF. Checks indicate colonies with the correct expected banding pattern.

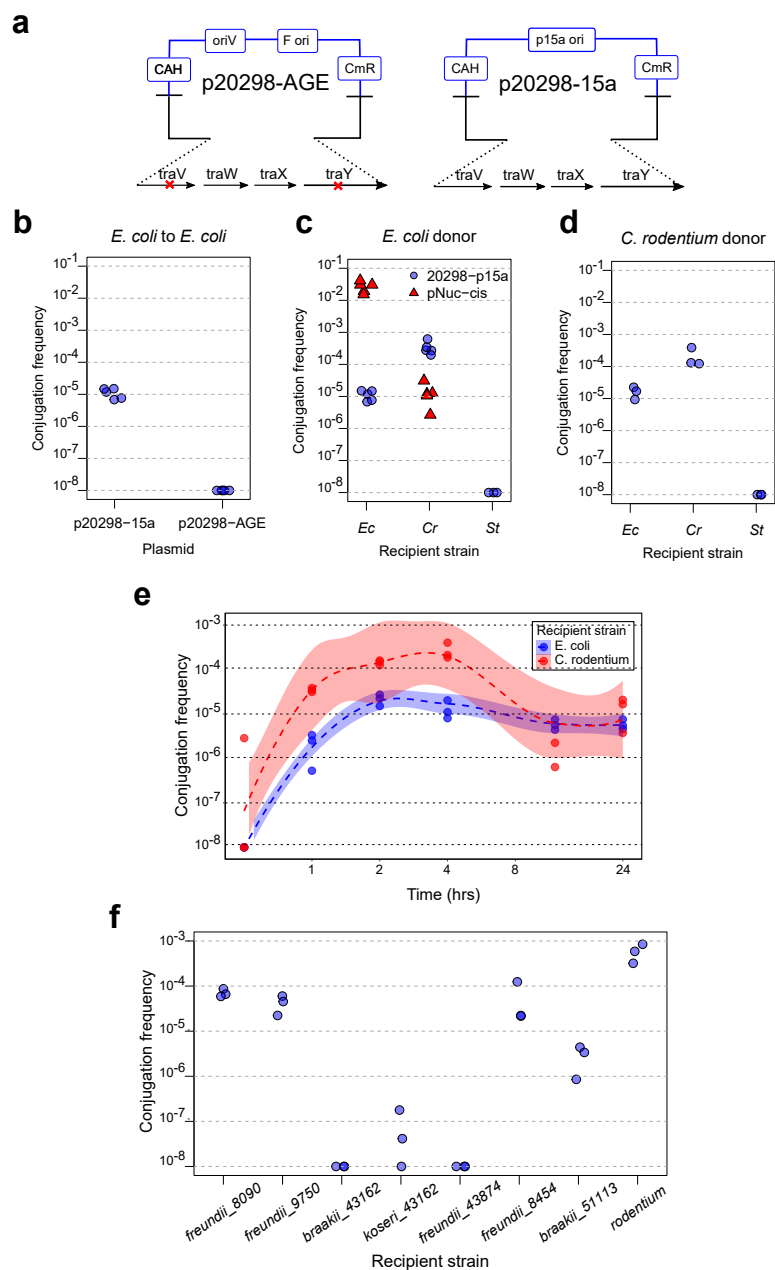


Figure 3.3: Conjugation of p20298. **a.** Diagram of conjugative plasmids p20298-AGE and p20298-15a showing the region of synthesis error and the difference in backbones. Deleterious mutations were present in both *traV* and *traY* in p20298-AGE that were repaired in 20298-15a. The plasmid backbone was simultaneously swapped from a pAGE backbone to a p15a backbone. **b.** Conjugation of p20298-15a, and p20298-AGE from an *E. coli* donor to an *E. coli* recipient. Five biological replicates were performed for each. **c.** Conjugation of p20298-15a from an *E. coli* donor (left) to *E. coli* (Ec), *C. rodentium* (Cr), and *Salmonella enterica* Typhimurium (St). Five biological replicates were performed for each. **d.** Conjugation from a *C. rodentium* donor (right) to *E. coli* (Ec), *C. rodentium* (Cr), and *Salmonella enterica* Typhimurium (St) (St). Three biological replicates were performed for each. **e.** Time-course conjugation from 30 minutes to 24 hours of p20298-15a from an *E. coli* Epi300 donor to an *E. coli* and a *C. rodentium* recipient. Three biological replicates were performed at each timepoint for each recipient strain. Shaded regions indicate the 95 % confidence interval. **f.** Conjugation of p20298-15a from *E. coli* to seven additional *Citrobacter* strains, with *C. rodentium* as a control. Three biological replicates were performed for each recipient strain.

conjugation to both *E. coli* and *C. rodentium*, however conjugation to *S. enterica* was unsuccessful. Interestingly, conjugation from the *E. coli* donor occurred at an approximately 30-fold higher frequency to *C. rodentium* than to an *E. coli* recipient after a 1 hour conjugation (p-value=0.005 by Welch's one-sided t-test). We proceeded to move p20298-15a into a *C. rodentium* donor strain, and performed conjugations to the same 3 recipients (Figure 3.3d). Conjugation from this strain resulted in a 13-fold higher conjugation frequency to *C. rodentium* than to *E. coli* (p-value=0.076 by Welch's one-sided t-test). Conjugation from *C. rodentium* to *S. enterica* was unsuccessful. The difference in conjugation from an *E. coli* or a *C. rodentium* donor was not significant (p-values of 0.32 and 0.32 to *E. coli* and *C. rodentium* recipients respectively by Welch's two-sided t-test). Taken together, both *E. coli* and *C. rodentium* were able to act as successful conjugative donors. Interestingly, no p20298-15a transconjugants were yielded in *S. enterica* from either donor strain. We proceeded to perform a time-course conjugation experiment using an *E. coli* Epi300 donor to both *E. coli* and *C. rodentium* recipients over 24 hours (Figure 3.3e). Conjugations were performed on LSLB agar plates, and cells were removed at the observed time-points. We generally observed a higher frequency of conjugation to *C. rodentium* than *E. coli* over the first 6 hours, as indicated by non-overlapping confidence intervals. Our observed conjugation frequencies plateaued at the 4 hour and 6 hour time-points for conjugation to *E. coli* and *C. rodentium* respectively. The 12 and 24 hour showed similar conjugation frequencies to both recipient strains.

Seven additional strains of *Citrobacter spp.* were obtained from Micronostyx to test as potential conjugative recipients (Figure 3.3f). Conjugations were performed for 1 hour on LSLB agar plates. Interestingly, the frequency of conjugation observed to these strains was widely variable. After a standard one hour conjugation from the *E. coli* donor, we observed moderate conjugation between 2.9×10^{-6} and 7×10^{-6} for four of the seven strains. The remaining 3 strains yielded minimal or no transconjugants. Conjugation was performed to *C. rodentium* in parallel and occurred at a higher frequency than any of the other *Citrobacter* species tested (5.9×10^{-4}). This indicates that the recipient range of p20298-15a is more specific than just the *Citrobacter* genus, as not all members of the genus are good recipients for the plasmid.

3.3.4 Conjugation in *trans* of a mobilizable plasmid containing the putative *oriT* from p20298

We identified the putative *oriT* for the p20298 conjugative system by analyzing the conjugative system with oriTfinder (29). We proceeded to clone a 1 kb fragment of DNA centered around the putative *oriT* into the plasmid backbone of the pProEX-Hta expression plasmid to form “p298-ori”. This backbone contains a compatible replicon with p20298-15a as well as an amp^R selection marker for compatible selection with p20298-15a. We transformed this plasmid into *E. coli* Epi300 alongside p20298-15a to generate a donor strain where p20298-15a was conjugative and p298-ori was mobilizable. We additionally transformed p298-ori with p20298-15a-M, which contains the identified mutations that eliminate conjugative ability in the *traV* and *traY* genes. With both these strains, we proceeded to conjugate to *C. rodentium* for 1 hour (Figure 3.4b) and selected for transconjugants of p298-oriT. We observed an average conjugation frequency of 3.2×10^{-4} for p298-oriT when mobilized by p20298-15a, and no conjugation when p298-oriT was harboured with p20298-15a-M. This experimentally validates the function of the putative *oriT*. Furthermore, it shows that the p20298-15a plasmid can be used mobilize a secondary mobilizable plasmid in *trans*.

3.3.5 p20298-15a stability in *C. rodentium* transconjugants

To evaluate the stability of p20298 in *C. rodentium* transconjugants, we isolated six p20298-15a transconjugants from a rifampin-sensitive *C. rodentium* strain to test as potential donors. We proceeded to perform conjugation assays from the rifampin-sensitive *C. rodentium* donors to rifampin-resistant *C. rodentium* recipients, and observed that each transconjugant was able to successfully conjugate the p20298-15a plasmid, suggesting the entirety of the plasmid is functional in transconjugants (Figure 3.4a).

To further evaluate the stability of the p20298-15a plasmid we performed diagnostic digests on plasmids extracted from *C. rodentium* transconjugants. First, 6 transconjugants were isolated and passaged on plates under chloramphenicol selection for the presence of the plasmid. Subsequently, 2 colonies from each initial passage were re-passaged on plates under chloramphenicol selection. After this passaging, 2 colonies from each were grown up overnight in liquid under chlorampheni-

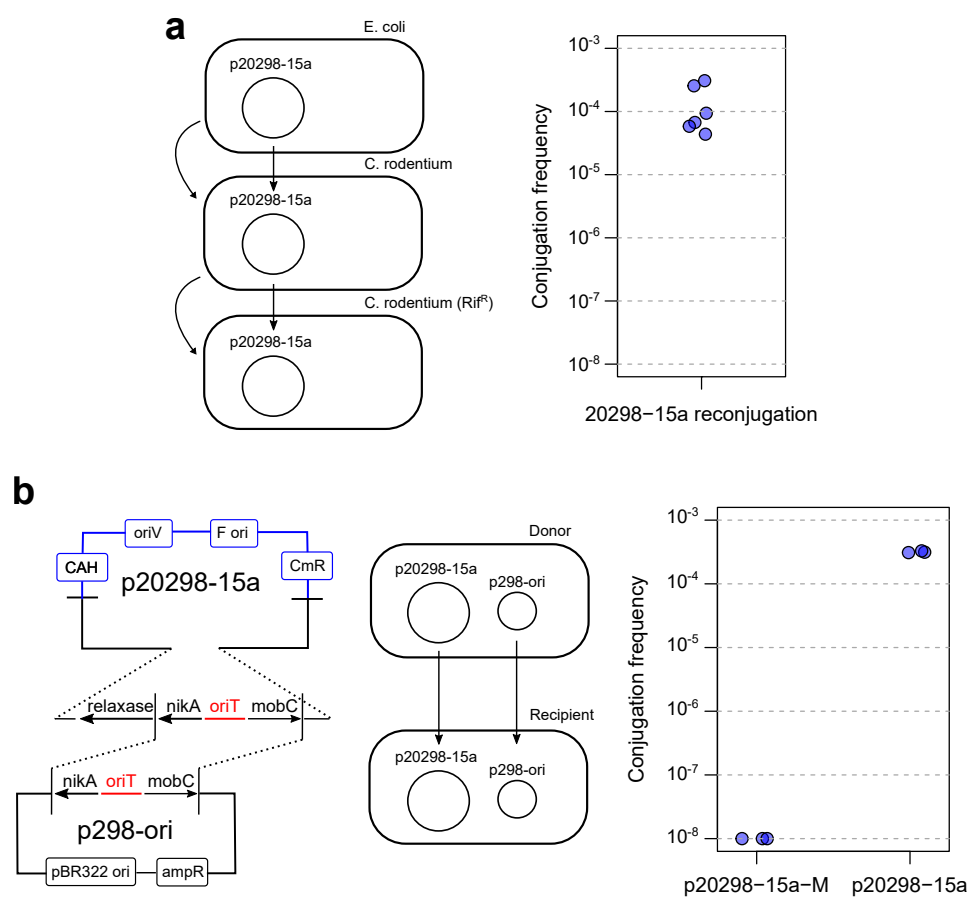


Figure 3.4: Evaluating p20298-15a function. **a.** Re-conjugation of *C. rodentium* transconjugants. Six *C. rodentium* transconjugants of p20298-15a were isolated and conjugated to a rifampin-resistant strain of *C. rodentium*. **b.** Conjugation of p298-oriT *in trans*. The p20298-15a oriT was predicted using oriTfinder (29), and cloned into a plasmid compatible with p20298-15a.

col selection, for a total of 24 colonies. We proceeded to extract plasmids from each and digested them with NotI-HF and NcoI-HF to assess the plasmids for gross rearrangements (Figure 3.6). In each case the diagnostic digest appeared normal, and no rearrangements were observed. Additional bands observed from the p20298 plasmids are expected from digests of native extracted *C. rodentium* plasmids (Figure 3.5). Overall, this indicates that the plasmid is generally stable under chloramphenicol selection after multiple passages.

3.3.6 RNA-seq of p20298-15a in *E. coli* Epi300 and *E. coli* to *C. rodentium*

To validate that genes on p20298-15a were being expressed in both *E. coli* and *C. rodentium*, we performed an RNA-seq experiment where the plasmid was being harboured in both strains. RNA was extracted at an A600 of ~0.4-0.6 for 3 replicates of both *E. coli* and *C. rodentium*. Analysis of the nucleotide coverage across the plasmid sequence in both *E. coli* (Figure 3.7a) and *C. rodentium* (Figure 3.7b) indicates that p20298-15a RNA is being transcribed from both strands. Interestingly, the difference in RNA coverage observed between the coding and non-coding strands is more distinguishable in *C. rodentium*, which may indicate that regulatory elements on the plasmid such as promoters and terminators are functioning more stringently in *C. rodentium* than in *E. coli*. Importantly, expression of all genes across the plasmid was observed in both strains.

We additionally compared the relative differential expression of plasmid genes when expressed in either *E. coli* Epi300 or *C. rodentium* using ALDeX2, a tool for analyzing differential abundance in RNA-seq data (15). From this RNA-seq analysis, we observed that many plasmid genes were significantly differentially expressed (greater than 2-fold differential expression and a p-value less than 0.01.) (Figure 3.8). Specifically, we found that 24 out of 49 genes had significant differential expression between the two strains. Interestingly, the relaxase gene *nikB* had significantly higher relative expression in *C. rodentium* than in *E. coli*. Additionally *traV* and *traY* also had higher relative expression in *C. rodentium*. Furthermore, genes encoding thin pilus proteins including *pilN* and *pilP* had lower relative expression in *C. rodentium* than in *E. coli*.

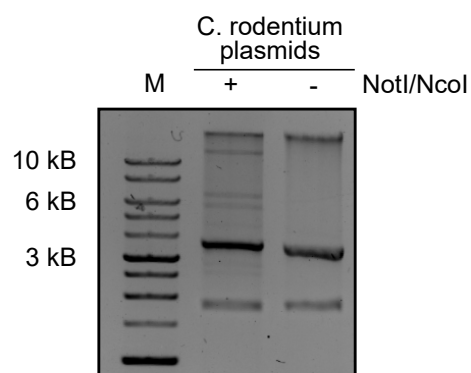


Figure 3.5: *C. rodentium* native plasmids. Plasmids were prepared and digested with NotI-HF and Nco-HF (NEB) and ran on a 0.8% TAE-agarose gel. Digested bands indicate expected background bands when digesting p20298-15a plasmids that were isolated from *C. rodentium*.

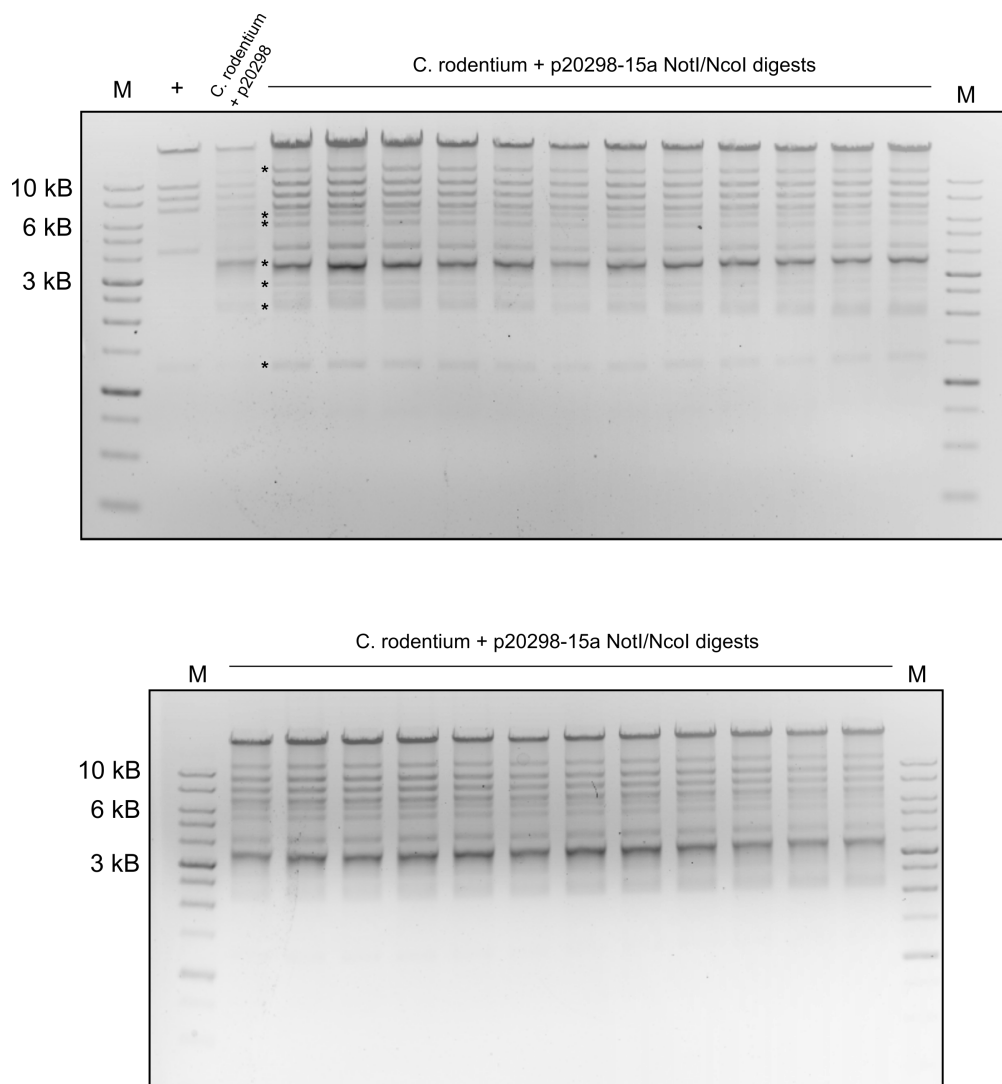


Figure 3.6: Diagnostic digests of p20298-15a isolated from *C. rodentium* after being passaged. Colonies were passaged twice on plates before being diluted and grown to saturation overnight for plasmid extraction. Extracted plasmids were digested with NotI-HF and NcoI-HF. This contains the complete digests that are partially shown in Figure 2. Asterisks indicate bands which result from digestion of native *C. rodentium* plasmids (see Figure 3.5).

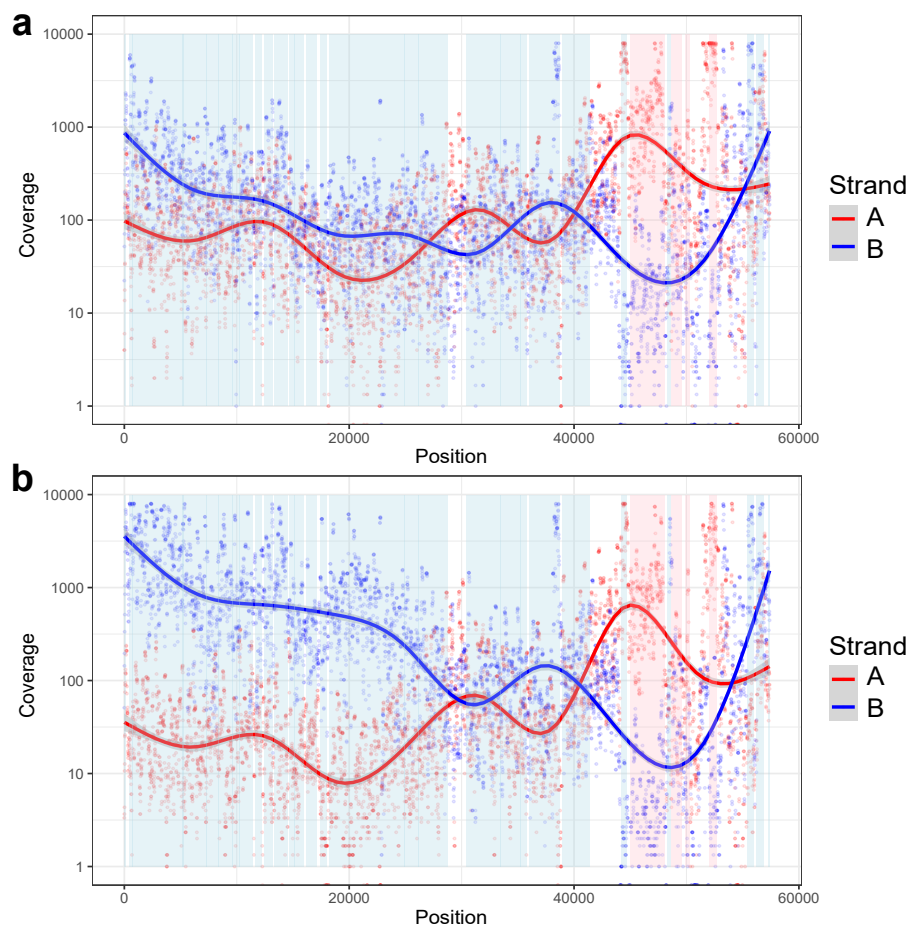


Figure 3.7: Nucleotide coverage from RNA-seq analysis of p20298-15a expression in **a.** *E. coli* Epi300 (DAP-) or **b.** *C. rodentium*. Coloured data represents nucleotide frequency on a given strand of the plasmid. Shaded regions indicate the orientation of reading frames on the plasmid.

p20298-15a differential gene expression
in *E. coli* vs. *C. rodentium*

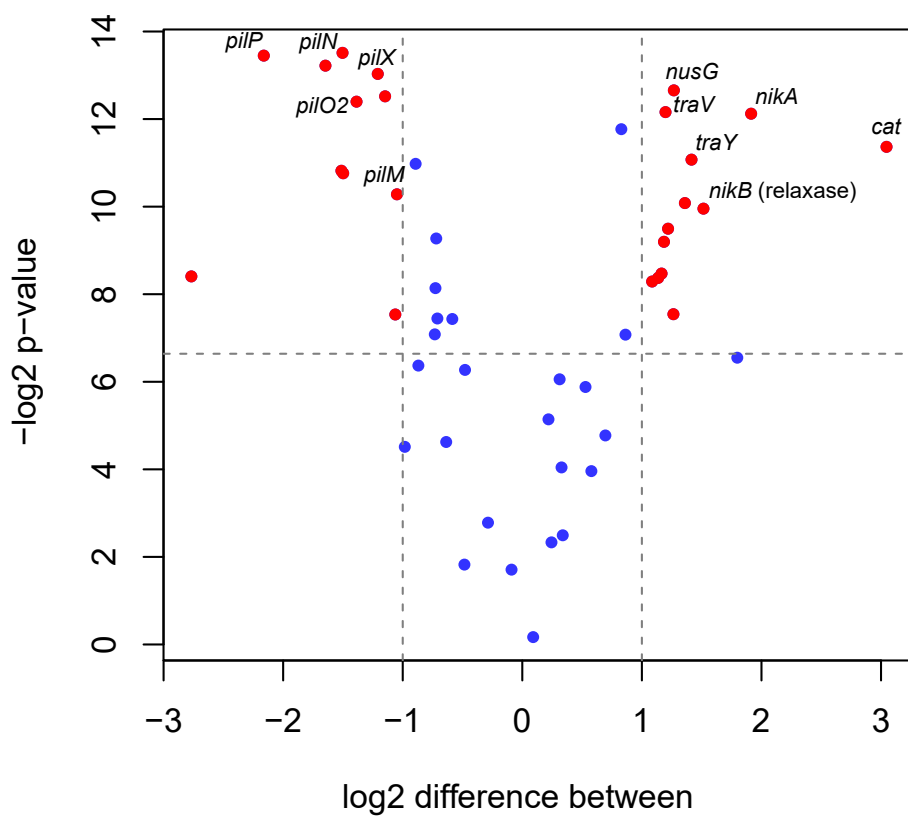


Figure 3.8: Volcano plot showing differential gene expression effect size of p20298 genes in *E. coli* compared to *C. rodentium*, with both axes on a log scale. Genes with 2-fold differential expression, and p-values less than 0.01 are located in the upper left and upper right quadrants and are coloured red. Genes in the upper right quadrant have higher relative expression in *C. rodentium*, genes in the upper left quadrant have higher relative expression in *E. coli*.

3.3.7 Functionalizing p20298 to kill *C. rodentium* with CRISPR-TevCas9

To facilitate cloning of cargo into p20298, we introduced a destination cassette for gateway recombination adjacent to the plasmid backbone in p20298-15a to generate p20298-dest. Gateway recombination utilizes the bacteriophage λ integrase system to recombine between a donor and recipient plasmid (23). As such, the destination cassette in p20298-dest contains a *ccdB* toxic gene that is constitutively expressed, and only removed upon successful recombination. This provided us a simple and rapid method to move cargo into the p20298 conjugative plasmid without the need to re-perform assemblies in yeast. To further our use of this system, we also generated pENTR-TC9. This plasmid contains the TevCas9 system under an arabinose-inducible promoter, and allows us to rapidly change sgRNAs by use of a golden gate cloning cassette. It is flanked by the required attL recombination sites to allow for recombination into the destination cassette of p20298-dest. Together, these plasmids allow us to rapidly change sgRNAs within the p20298 plasmid to target the *C. rodentium* genome (Figure 3.9a). We are able to screen for successful gateway recombination by a simple diagnostic restriction digest. This system is also desirable as it allows for the rapid insertion of other cargo through use of gateway recombination.

We proceeded to identify sgRNAs with high predicted activity for bacterial targeting using a generalizable machine learning trained prediction model (21). We individually cloned sgRNAs targeting the *C. rodentium* genome, and an sgRNA not targeting the *C. rodentium* genome, into p20298-dest using the aforementioned cloning method. We conjugated p20298-TC9 plasmids from *E. coli* Epi300 (DAP-) to *C. rodentium* under glucose repression on plates and subsequently split the suspension and selected for transconjugants in inducing (with arabinose) and repressing (with glucose) conditions. After 2 hours of induction at 37 °C we plated the outgrowths on repressive plates, and counted colonies the following day. We determined the killing efficiency by comparing colony counts between the 2 conditions (Figure 3.9b) and observed that all sgRNAs targeting the *C. rodentium* genome were able to kill, with the lowest efficiency being 82 % (Figure 3.9c). Some sgRNAs performed better and more consistently than others. In particular, the sgRNA targeting *glpG* had an average killing efficiency of 99.9 % and was consistent across replicates. Taken together, this data shows that the p20298 conjugative plasmid can be used to successfully deliver a TevCas9 nuclease for targeted bacterial killing of *C. rodentium*.

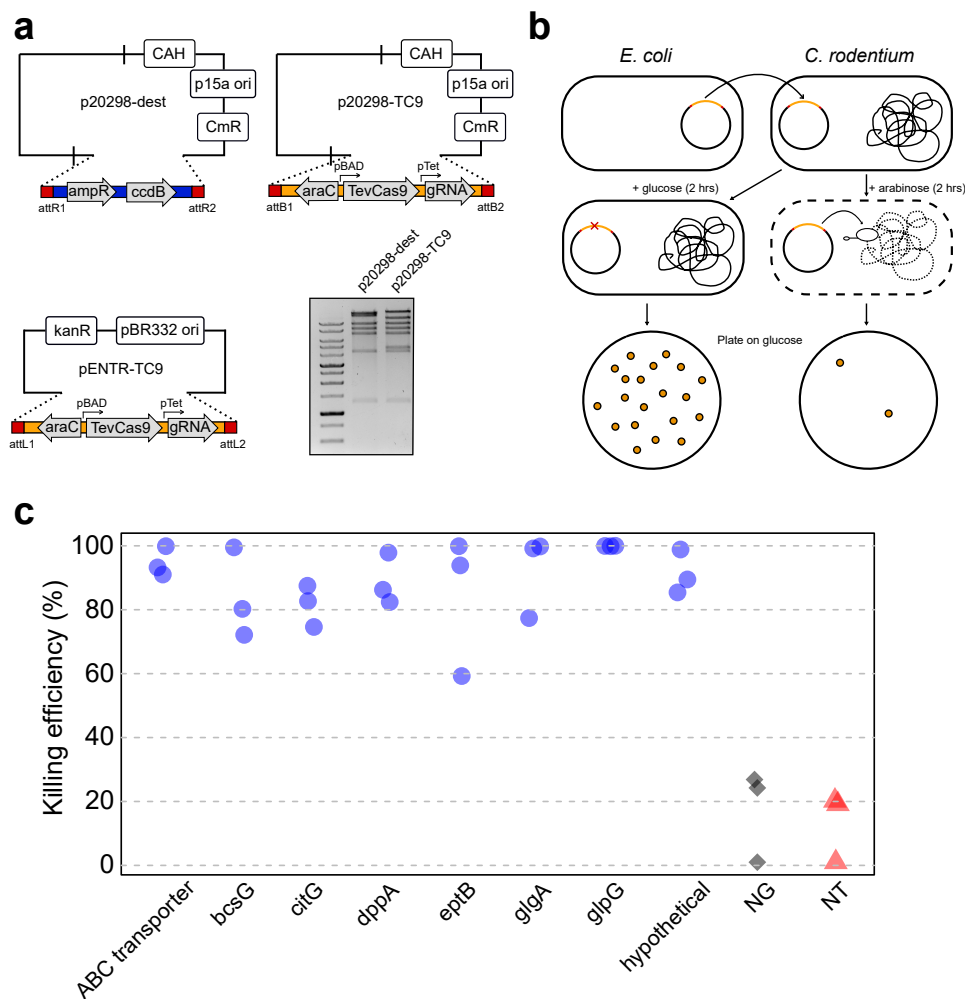


Figure 3.9: Functionalizing p20298 to kill *C. rodentium*. **a.** p20298 was modified to include a gateway destination cassette for cargo insertion to create p20298-dest. pENTR-TC9 was constructed to facilitate the recombination of CRISPR-TevCas9 with various sgRNAs into the p20298-dest plasmid. **b.** Schematic of chromosomal targeting by a conjugated p20298-TC9 plasmid. p20298-TC9 is conjugated from *E. coli* to *C. rodentium*. CRISPR-TevCas9 targeting the *C. rodentium* genome is either induced with arabinose, or repressed with glucose and allowed to outgrow for 2 hours to kill. The remaining transconjugants are grown overnight on plates, and killing efficiency is calculated by comparing these conditions. **c.** Killing efficiency of *C. rodentium* with p20298-TC9. 8 sgRNAs targeting the *C. rodentium* genome (blue circle), a non-targeted sgRNA (red triangle), and an empty sgRNA cassette control (black diamond) were tested in three biological replicates each. Killing efficiencies were calculated as described above and expressed as a percent.

3.4 Discussion

As methods for the assembly of large DNA fragments improve, and the cost of *de novo* DNA synthesis becomes more affordable, constructing functional multi-gene systems becomes more accessible. Here we showed that we can take advantage of these changes to synthesize an entire conjugative system identified in a metagenomic database *de novo*. Evolving DNA sequencing technology has resulted in a constantly increasing number of high-throughput sequencing experiments, many of which store their raw data in readily-accessible databases online. As these databases continue to grow, access to more novel sequences will only increase. This includes data sets that can be associated with both health-related microbiome, or environmental microbiome samples. A shortcoming of metagenomic data is the inherent depletion of plasmids during the binning of metagenomic sequencing data (32). This results in an under-representation of conjugative plasmids within metagenomic data. When we investigate the full ~150 kb contig from which we identified the 20298 conjugative system, we find genes for antitoxins and *repA* which are indicative of a plasmid origin. Together, this suggests that the origin of the 20298 sequence is conjugative plasmid-based in nature, however, recent research suggests that the divide between conjugative plasmids and ICEs is perhaps smaller than we thought (9).

The identification of inactivating mutations in the *traV* and *traY* genes of p20298-AGE indicates some selective disadvantage of these two genes may have prevented successful synthesis. Both these genes were present in the DNA tile that could not be synthesized and sequence-verified by Twist Biosciences, and resulted in a secondary synthesis technique being required where the mutations occurred. In the IncI1 plasmid R64 both gene products are involved in conjugal transfer, with the *traY* product being a predicted integral membrane protein (42). Although neither gene is anticipated to have independent toxic effects, it is possible that toxicity may be driving these mutations in the absence of the entire conjugative apparatus, resulting in the issues obtaining sequence-verified DNA products. Consideration on the impact of segmented gene systems is critical moving forward with future construction of large conjugative systems, particularly when toxic genes or toxin-antitoxin systems might be included.

Interestingly, we observed a higher frequency of conjugation to a *C. rodentium* recipient than an *E. coli* recipient after a standard, one hour conjugation. This is interesting as the conjugative system

originates from the *Citrobacter* genus. While we do not know the precise molecular reason for this preference, we can speculate based on previous findings. It has been shown that efficient DNA transfer relies on precise interactions between plasmid-expressed outer-membrane proteins and recipient outer-membrane proteins to stabilize mating pair formation (31). This specificity highlights the importance of identifying conjugative systems that have evolved to have high potential for successful conjugation to target species of interest. Furthermore, plasmid origin incompatibility with domestic plasmids in desired recipient strains means that careful consideration needs to be made when determining a suitable backbone for a conjugative delivery plasmid. Using conjugative plasmids for biotechnology applications in complex microbial systems, such as the gut, is reliant on the ability to robustly conjugate to, and replicate in species of interest. The variable conjugation frequency we observed to different *Citrobacter* strains demonstrates the complexity of interactions between engineered conjugative plasmids and their recipients. It is therefore imperative that a broad range of replicative origins and conjugative systems are available for targeting of future recipients. Our work here demonstrates that metagenomic data sets are a reservoir for sequences of these systems that can be constructed for this purpose.

Importantly, we also identified several errors in coding regions within p20298-15a. While the full impact of these mutations was not explored, it is possible that resolving these errors may impact conjugation frequency. In particular, fixing errors in the thin pilus genes might improve conjugation, particularly if the system proceeds into a mouse model, where the presence of a functional thin pilus has been found to greatly improve conjugation frequency (35).

Critically, we were able to demonstrate the ability to functionalize p20298-15a to deliver a TevCas9 nuclease for targeted killing of *C. rodentium*. Sequence-specific antimicrobials are an important step forward in combating antimicrobial resistance in bacteria. Conjugative systems could be further used to deliver genes and systems of importance within microbial ecosystems, such as metabolic pathways, and gene regulatory systems (i.e. CRISPRi). Beyond this, functionalizing the conjugative plasmid for delivery shows how systems identified in metagenomic or genomic data can be further engineered for synthetic biology applications. This shows how advancements in both DNA sequencing and DNA synthesis can evolve the way we approach functional metagenomics. To conclude, we were able to construct a large synthetic genetic system *de novo* that contains at least 47 genes, and show conjugative function of the system. While the construction of large

synthetic systems is not new, considering the construction of a “synthetic cell” (19), this work emphasizes the ability to identify and construct functionally important biological systems from the largely untapped reservoir of metagenomic data. While conjugative systems represent a useful tool for applications in microbial systems, this principle is translatable to identifying other systems of functional interest such as natural metabolic and biosynthetic pathways. As the cost of synthetic DNA synthesis decreases, and the tools for assembly of these systems improve, this process will only become more simpler and more affordable.

3.5 References

- [1] Alexandre Almeida, Alex L Mitchell, Miguel Boland, Samuel C Forster, Gregory B Gloor, Aleksandra Tarkowska, Trevor D Lawley, and Robert D Finn. A new genomic blueprint of the human gut microbiota. *Nature*, 568(7753):499–504, 2019.
- [2] Li Bai, Shengli Xia, Ruiting Lan, Liyun Liu, Changyun Ye, Yiting Wang, Dong Jin, Zhigang Cui, Huaiqi Jing, Yanwen Xiong, et al. Isolation and characterization of cytotoxic, aggregative *Citrobacter freundii*. *PLoS One*, 7(3):e33054, 2012.
- [3] David Bikard, Chad W Euler, Wenyan Jiang, Philip M Nussenzweig, Gregory W Goldberg, Xavier Duportet, Vincent A Fischetti, and Luciano A Marraffini. Exploiting CRISPR-Cas nucleases to produce sequence-specific antimicrobials. *Nature Biotechnology*, 32(11):1146, 2014.
- [4] Anthony M Bolger, Marc Lohse, and Bjoern Usadel. Trimmomatic: a flexible trimmer for Illumina sequence data. *Bioinformatics*, 30(15):2114–2120, 2014.
- [5] Stephanie L Brumwell, Michael R MacLeod, Tony Huang, Ryan R Cochrane, Rebecca S Meaney, Maryam Zamani, Ola Matysiakiewicz, Kaitlyn N Dan, Preetam Janakirama, David R Edgell, et al. Designer *Sinorhizobium meliloti* strains and multi-functional vectors enable direct inter-kingdom DNA transfer. *PLoS One*, 14(6):e0206781, 2019.
- [6] Benjamin Buchfink, Chao Xie, and Daniel H Huson. Fast and sensitive protein alignment using DIAMOND. *Nature Methods*, 12(1):59–60, 2015.
- [7] Brian Bushnell, Jonathan Rood, and Esther Singer. BBMerge—accurate paired shotgun read merging via overlap. *PloS One*, 12(10):e0185056, 2017.
- [8] Elena Cabezón, Jorge Ripoll-Rozada, Alejandro Peña, Fernando De La Cruz, and Ignacio Arechaga. Towards an integrated model of bacterial conjugation. *FEMS Microbiology Reviews*, 39(1):81–95, 2015.
- [9] Nicolas Carraro, Dominique Poulin, and Vincent Burrus. Replication and active partition of integrative and conjugative elements (ICEs) of the SXT/R391 family: the line between ICEs and conjugative plasmids is getting thinner. *PLoS Genetics*, 11(6):e1005298, 2015.
- [10] Indranil Chattopadhyay, Ruby Dhar, Karthikeyan Pethusamy, Ashikh Seethy, Tryambak Srivastava, Ramkishor Sah, Jyoti Sharma, and Subhradip Karmakar. Exploring the role of gut microbiome in colon cancer. *Applied Biochemistry and Biotechnology*, 193(6):1780–1799, 2021.
- [11] Robert J Citorik, Mark Mimee, and Timothy K Lu. Sequence-specific antimicrobials using efficiently delivered RNA-guided nucleases. *Nature Biotechnology*, 32(11):1141, 2014.
- [12] James W Collins, Kristie M Keeney, Valerie F Crepin, Vijay AK Rathinam, Katherine A Fitzgerald, B Brett Finlay, and Gad Frankel. *Citrobacter rodentium*: infection, inflammation and the microbiota. *Nature Reviews Microbiology*, 12(9):612–623, 2014.

- [13] Petr Danecek, James K Bonfield, Jennifer Liddle, John Marshall, Valeriu Ohan, Martin O Pollard, Andrew Whitwham, Thomas Keane, Shane A McCarthy, Robert M Davies, et al. Twelve years of samtools and bcftools. *Gigascience*, 10(2):giab008, 2021.
- [14] A Murat Eren, Özcan C Esen, Christopher Quince, Joseph H Vineis, Hilary G Morrison, Mitchell L Sogin, and Tom O Delmont. Anvi'o: an advanced analysis and visualization platform for 'omics data. *PeerJ*, 3:e1319, 2015.
- [15] Andrew D Fernandes, Jean M Macklaim, Thomas G Linn, Gregor Reid, and Gregory B Gloor. ANOVA-like differential expression (ALDEx) analysis for mixed population RNA-Seq. *PLoS One*, 8(7):e67019, 2013.
- [16] M Pilar Garcillán-Barcia, Santiago Redondo-Salvo, Luis Vielva, and Fernando de la Cruz. MOBscan: automated annotation of MOB relaxases. *Horizontal Gene transfer: Methods and Protocols*, pages 295–308, 2020.
- [17] María Pilar Garcillán-Barcia, María Victoria Francia, and Fernando de La Cruz. The diversity of conjugative relaxases and its application in plasmid classification. *FEMS Microbiology Reviews*, 33(3):657–687, 2009.
- [18] Daniel G Gibson. Synthesis of DNA fragments in yeast by one-step assembly of overlapping oligonucleotides. *Nucleic Acids Research*, 37(20):6984–6990, 2009.
- [19] Daniel G Gibson, John I Glass, Carole Lartigue, Vladimir N Noskov, Ray-Yuan Chuang, Mikkel A Algire, Gwynedd A Benders, Michael G Montague, Li Ma, Monzia M Moodie, et al. Creation of a bacterial cell controlled by a chemically synthesized genome. *Science*, 329(5987):52–56, 2010.
- [20] Ahmed A Goma, Heidi E Klumpe, Michelle L Luo, Kurt Selle, Rodolphe Barrangou, and Chase L Beisel. Programmable removal of bacterial strains by use of genome-targeting CRISPR-Cas systems. *MBio*, 5(1):e00928–13, 2014.
- [21] Dalton T Ham, Tyler S Browne, Pooja N Bangalorewala, Tyler Wilson, Richard Michael, Gregory B Gloor, and David R Edgell. A generalizable Cas9/sgRNA prediction model using machine transfer learning with small high-quality datasets. *BioRxiv*, pages 2023–02, 2023.
- [22] Thomas A Hamilton, Gregory M Pellegrino, Jasmine A Therrien, Dalton T Ham, Peter C Bartlett, Bogumil J Karas, Gregory B Gloor, and David R Edgell. Efficient inter-species conjugative transfer of a CRISPR nuclease for targeted bacterial killing. *Nature Communications*, 10(1):1–9, 2019.
- [23] James L Hartley, Gary F Temple, and Michael A Brasch. DNA cloning using in vitro site-specific recombination. *Genome Research*, 10(11):1788–1795, 2000.
- [24] Doug Hyatt, Gwo-Liang Chen, Philip F LoCascio, Miriam L Land, Frank W Larimer, and Loren J Hauser. Prodigal: prokaryotic gene recognition and translation initiation site identification. *BMC Bioinformatics*, 11(1):1–11, 2010.

- [25] Benjamin R Joris. *Towards more complete metagenomic analyses through circularized genomes and conjugative elements*. PhD thesis, The University of Western Ontario, 2022.
- [26] Bogumil J Karas, Rachel E Diner, Stephane C Lefebvre, Jeff McQuaid, Alex PR Phillips, Chari M Noddings, John K Brunson, Ruben E Valas, Thomas J Deerinck, Jelena Jablanovic, et al. Designer diatom episomes delivered by bacterial conjugation. *Nature Communications*, 6:6925, 2015.
- [27] Daehwan Kim, Ben Langmead, and Steven L Salzberg. HISAT: a fast spliced aligner with low memory requirements. *Nature Methods*, 12(4):357–360, 2015.
- [28] Pawel S Krawczyk, Leszek Lipinski, and Andrzej Dziembowski. PlasFlow: predicting plasmid sequences in metagenomic data using genome signatures. *Nucleic Acids Research*, 46(6):e35–e35, 2018.
- [29] Xiaobin Li, Yingzhou Xie, Meng Liu, Cui Tai, Jingyong Sun, Zixin Deng, and Hong-Yu Ou. oriTfinder: a web-based tool for the identification of origin of transfers in DNA sequences of bacterial mobile genetic elements. *Nucleic Acids Research*, 46(W1):W229–W234, 2018.
- [30] Matxalen Llosa, F Xavier Gomis-Rüth, Miquel Coll, and Fernando de la Cruz. Bacterial conjugation: a two-step mechanism for DNA transport. *Molecular Microbiology*, 45(1):1–8, 2002.
- [31] Wen Wen Low, Joshua LC Wong, Leticia C Beltran, Chloe Seddon, Sophia David, Hok-Sau Kwong, Tatiana Bizeau, Fengbin Wang, Alejandro Peña, Tiago RD Costa, et al. Mating pair stabilization mediates bacterial conjugation species specificity. *Nature Microbiology*, 7(7):1016–1027, 2022.
- [32] Finlay Maguire, Baofeng Jia, Kristen L Gray, Wing Yin Venus Lau, Robert G Beiko, and Fiona SL Brinkman. Metagenome-assembled genome binning methods with short reads disproportionately fail for plasmids and genomic islands. *Microbial Genomics*, 6(10), 2020.
- [33] Ross S McInnes, Gregory E McCallum, Lisa E Lamberte, and Willem van Schaik. Horizontal transfer of antibiotic resistance genes in the human gut microbiome. *Current Opinion in Microbiology*, 53:35–43, 2020.
- [34] Rosanna Mundy, Thomas T MacDonald, Gordon Dougan, Gad Frankel, and Siouxsie Wiles. *Citrobacter rodentium* of mice and man. *Cellular Microbiology*, 7(12):1697–1706, 2005.
- [35] Kevin Neil, Nancy Allard, Patricia Roy, Frédéric Grenier, Alfredo Menendez, Vincent Burrus, and Sébastien Rodrigue. High-efficiency delivery of CRISPR-Cas9 by engineered probiotics enables precise microbiome editing. *Molecular Systems Biology*, 17(10):e10335, 2021.
- [36] Harold C Neu. The crisis in antibiotic resistance. *Science*, 257(5073):1064–1073, 1992.
- [37] Vladimir N Noskov, Bogumil J Karas, Lei Young, Ray-Yuan Chuang, Daniel G Gibson, Ying-Chi Lin, Jason Stam, Isaac T Yonemoto, Yo Suzuki, Cynthia Andrews-Pfannkoch, et al. Assembly of large, high G+C bacterial DNA fragments in yeast. *ACS Synthetic Biology*, 1(7):267–273, 2012.

- [38] Sergey Nurk, Dmitry Meleshko, Anton Korobeynikov, and Pavel A Pevzner. metaSPAdes: a new versatile metagenomic assembler. *Genome Research*, 27(5):824–834, 2017.
- [39] Asmus K Olesen, Rafael Pinilla-Redondo, Mads F Hansen, Jakob Russel, Arnaud Dechesne, Barth F Smets, Jonas S Madsen, Joseph Nesme, and Søren J Sørensen. IncHI1A plasmids potentially facilitate horizontal flow of antibiotic resistance genes to pathogens in microbial communities of urban residential sewage. *Molecular Ecology*, 31(5):1595–1608, 2022.
- [40] Givanna H Putri, Simon Anders, Paul Theodor Pyl, John E Pimanda, and Fabio Zanini. Analysing high-throughput sequencing data in Python with HTSeq 2.0. *Bioinformatics*, 38(10):2943–2945, 2022.
- [41] KP Ranjan and Neelima Ranjan. *Citrobacter*: An emerging health care associated urinary pathogen. *Urology Annals*, 5(4):313, 2013.
- [42] Gen-ichi Sampei, Nobuhisa Furuya, Keiko Tachibana, Yasuhiro Saitou, Takuji Suzuki, Kiyoshi Mizobuchi, and Teruya Komano. Complete genome sequence of the incompatibility group I1 plasmid R64. *Plasmid*, 64(2):92–103, 2010.
- [43] Alvaro San Millan. Evolution of plasmid-mediated antibiotic resistance in the clinical context. *Trends in Microbiology*, 26(12):978–985, 2018.
- [44] Chris Smillie, M Pilar Garcillán-Barcia, M Victoria Francia, Eduardo PC Rocha, and Fernando de la Cruz. Mobility of plasmids. *Microbiology and Molecular Biology Reviews*, 74(3):434–452, 2010.
- [45] Baris E Suzek, Yuqi Wang, Hongzhan Huang, Peter B McGarvey, Cathy H Wu, and UniProt Consortium. UniRef clusters: a comprehensive and scalable alternative for improving sequence similarity searches. *Bioinformatics*, 31(6):926–932, 2015.
- [46] Ching-Hung Tseng and Chun-Ying Wu. The gut microbiome in obesity. *Journal of the Formosan Medical Association*, 118:S3–S9, 2019.
- [47] Mireia Valles-Colomer, Gwen Falony, Youssef Darzi, Ettje F Tigchelaar, Jun Wang, Raul Y Tito, Carmen Schiweck, Alexander Kurilshikov, Marie Joossens, Cisca Wijmenga, et al. The neuroactive potential of the human gut microbiota in quality of life and depression. *Nature Microbiology*, 4(4):623–632, 2019.
- [48] C Lee Ventola. The antibiotic resistance crisis: part 1: causes and threats. *Pharmacy and Therapeutics*, 40(4):277, 2015.
- [49] Zhu Wang, Xu-Xiang Zhang, Kailong Huang, Yu Miao, Peng Shi, Bo Liu, Chao Long, and Aimin Li. Metagenomic profiling of antibiotic resistance genes and mobile genetic elements in a tannery wastewater treatment plant. *PloS One*, 8(10):e76079, 2013.
- [50] Ying Zhou, Yang Yang, Xiaobin Li, Dongxing Tian, Wenxiu Ai, Weiwen Wang, Bingjie Wang, Barry N Kreiswirth, Fangyou Yu, Liang Chen, et al. Exploiting a conjugative endogenous CRISPR-Cas3 system to tackle multidrug-resistant *Klebsiella pneumoniae*. *EBioMedicine*, 88:104445, 2023.

Chapter 4

Discussion

4.1 Manipulating bacteria with CRISPR nucleases

The continued development of novel CRISPR-based tools has revolutionized methodological approaches in biotechnology over the past decade. In both Chapters 2 and 3, the use of TevCas9 as a tool for targeted bacterial killing was demonstrated, killing both *Salmonella enterica*, and *Citrobacter rodentium*. While the focus of this thesis was primarily on the delivery of CRISPR tools for killing, it also addresses the question of sgRNA dependence for bacterial elimination. Indeed, 65 different TevSpCas9 sgRNAs were delivered to *S. enterica* yielding diverse killing efficiencies. We were unable to identify any strong correlations between our observed sgRNA activity and numerous parameters, including predictions from an optimized prokaryotic model (8), which shows that current understanding of sgRNA function in bacteria is limited and needs to be improved. This problem has recently been addressed by generating a machine transfer learning architecture that is aimed at making generalizable SpCas9 sgRNA activity predictions (9). This model was used to predict high activity sgRNAs for targeting *C. rodentium* in Chapter 3.

Another consideration for highly efficient killing is through the multiplexing of sgRNAs, which can serve two key purposes in targeting bacteria. The first purpose is to target multiple sites on the genome of a target bacterium which was demonstrated to yield high killing efficiencies in Chapter 2. This is critical because it may allow for good sgRNAs to compensate for worse sgRNAs as a means of redundancy. The second purpose of multiplexing is to provide sgRNAs targeting multiple genomes to attempt simultaneous killing of different strains. Recently, systems to enable the construction of long sgRNA arrays have been engineered to facilitate construction and use of

multiple guides simultaneously (28), which has the potential to greatly improve sequence-specific bacterial genome targeting.

While using TevCas9 or Cas9 as sequence targeted antimicrobials is an innovative use of CRISPR technology, demonstrated both in this thesis and in other works (1, 4, 7, 24), the development of other CRISPR-based tools presents interesting possibilities for manipulating microbes. For instance, CRISPRi can be used for targeted gene repression in bacteria, which has been demonstrated in a number of instances including for virulence attenuation, and for modulating GUS activity (26, 27). Additionally, CRISPRa fusion proteins such as dCas9-AsiA can be utilized in bacteria to further modulate gene expression at diverse promoters (11). Efficient delivery of these systems is imperative for the therapeutic usage of these tools in complex communities just as it is when using CRISPR nucleases as antimicrobial agents.

4.2 On the future of conjugative delivery to bacteria

Conjugative systems are widespread throughout microbes in diverse communities, making them versatile for delivering genetic cargo to bacteria. In both Chapters 2 and 3, CRISPR nucleases were successfully delivered to *S. enterica* and *C. rodentium* using two different conjugative systems. Importantly, with pNuc-*cis* we found that the conditions under which conjugation occurs greatly impact the frequency of conjugation to *S. enterica*, and that mobilization in *cis* was critical. With p20298-15a we found that conjugation frequency was highly variable depending on the recipient strain. Taken together this emphasizes that no conjugative plasmid is a "master key" for delivery, as the conditions under which mobilization will occur, and the desired target, will both greatly affect the efficiency of cargo delivery. This perhaps explains why previous attempts to deliver CRISPR nucleases for bacterial killing using conjugation were unsuccessful, as the system was used in *trans*, and no real optimization of conjugation was performed (4). This illustrates the need to have a robust library of conjugative systems available for use as delivery tools to different bacteria in variable environments. This thesis further addresses this problem by introducing a pipeline for constructing conjugative systems to facilitate delivery of genetic cargo to diverse bacteria, including those that are difficult to culture and under-studied.

The primary focus of this thesis was placed on conjugation to Proteobacteria, as many exam-

ple species are often pathogenic, and because they are relatively easy to manipulate in laboratory settings. These bacteria, including *S. enterica*, and *Citrobacter* spp. represent clinically significant pathogens, which are key targets for antimicrobial therapeutics. While conjugation to this clade was demonstrated, conjugative systems were also present in other clinically relevant phyla of bacteria including Firmicutes and Bacteroidetes, as shown in Chapter 3. These two clades of bacteria have drawn a substantial amount of research interest, with the potential link to obesity (19, 32), beyond which both phyla are abundant in the healthy gut microbiome (31, 34). Furthermore, non-Proteobacter pathogens, including *Staphylococcus aureus* (5), and *Streptococcus agalactiae* (2), are known to harbour conjugative plasmids. These species represent potential therapeutic targets where conjugative systems are naturally present and could be adapted and engineered to deliver either a CRISPR-based killing device, or other genetic cargo. The range of targets with significant human health implications is large, and adapting natural conjugative systems for delivery is a logical step in tool development for these organisms.

A further consideration for the advancement of bacterial conjugation in synthetic biology is through the inclusion of additional genetic systems to help enable successful delivery. For example, a recent study showing the importance of plasmid expressed proteins for mating pair stabilization with specific recipients indicates the potential to use these types of cell surface proteins to enhance conjugation to targets of interest (21). Naturally occurring conjugative plasmids have also been shown to encode anti-CRISPR proteins which help evade host CRISPR systems (22). Inclusion of anti-CRISPR elements on engineered conjugative plasmids when targeting bacterial communities with characterized CRISPR systems could prove beneficial for increasing overall efficiency of delivery. These examples highlight how plasmids have naturally evolved to efficiently conjugate to new hosts, and represent additional systems that can be searched for in microbiome data sets.

A reasonable concern surrounding conjugative delivery technology is with bio-containment of engineered plasmids in complex microbial ecosystems. It is desirable that there be a mechanism to eliminate plasmid and donor strain persistence in populations after effective use of the construct has been completed. Targeted kill-switch circuits have been engineered for such purposes including CRISPR-based kill-switches (29) and the “deadman” and “passcode” system (3). Furthermore, future use of a thermo-sensitive endonuclease to act as a sequence-specific targeted kill-switch may be used to activate elimination when the plasmid is excreted from the gastrointestinal tract (18).

Ultimately the inclusion of these types of devices are a necessity moving forward with conjugative delivery to microbial communities.

4.3 Functionalizing metagenomic sequencing data

Functional metagenomics has traditionally enabled the study of genes and systems that exhibit unique activities in microbial ecosystems through library screening of community-isolated DNA (17). It is a valuable method for identifying and characterizing the activity of enzymes and pathways in both culturable and non-culturable bacteria, and importantly can identify genetic systems with potential uses in biotechnology. Examples of identified systems with relevant applications have been found in environmental samples with thermostable polymerases (23), and genes for naphthalene degradation (33). Further genetic elements have been found in human microbiome samples including bile salt hydrolase genes (14). It is evident that microbial ecosystems in both environmental and human samples contain interesting and utilizable genetic systems that can serve a variety of functions.

As DNA sequencing and synthesis technologies continue to advance, data mining approaches for synthetic biology applications have begun to offer an alternative approach to the traditional library-based screening for genetic elements. For example, mining of sequencing data has been performed to build libraries of prokaryotic regulatory elements (13, 30) that can be used for constructing synthetic circuits. This represents the synthesis of relatively small elements identified in metagenomic data. Additionally, genes encoding enzymes with desirable activity can be identified in sequencing data, allowing for PCR-based amplification from the isolated DNA (35). This is also a viable approach for constructing genetic systems, but is limited by the requirement to have access to the community-isolated DNA.

This thesis presents evidence showing the cloning of a large, functional conjugative system of ~54 kb containing over 40 genes and native regulatory elements. The conjugative system was constructed synthetically and did not require access to isolated DNA. While synthesis from sequence has been performed prior to this for smaller genes and regulatory elements, this demonstrates the capability to scale construction of elements identified in metagenomic data up to the system level. This same approach could be readily applied to metabolic pathways and other more complex sys-

tems identified in environmental and human data sets.

An important consideration in synthesizing systems from data is the reliance on accurate DNA sequencing, as errors in reference sequences may fail to produce functional genetic systems once constructed. Critically, the tools that are used to analyze metagenomic data are variable in their accuracy (20), meaning that the way in which the data is handled may greatly impact the potential for success when constructing systems identified within it. As improved methods for analysis continue to be developed, the reliability of sequencing data will hopefully continue to improve to further increase trustworthiness, and ultimately the likelihood of constructing functional systems.

A further limitation to this approach is that it presupposes sufficient knowledge of the desired systems to enable identification in large data sets. As conjugative systems are well-characterized, we were able to generate methods to identify them. For genetic systems that are less understood this may be more difficult, however, as our understanding of gene and pathway activity in bacteria grows, this process should become more versatile. In fact, new technologies such as AlphaFold (15) have begun to bridge the gap between sequence and protein structure. With the engineering and construction of a synthetic bacterial genome (6) it has become evident that DNA synthesis has great potential moving forward, and perhaps it will eventually be possible to construct a synthetic bacterium identified in metagenomic data.

4.4 Techniques and challenges for the synthesis and construction of large plasmids

Advancements in the *de novo* synthesis of DNA have been critical in allowing commercial access to synthetic genetic elements at large-scale and reasonable cost (16). Synthesis of DNA begins at the oligonucleotide level which can then be assembled into gene-sized products. These products are essential for synthesizing larger genetic constructs, including conjugative systems, directly from a DNA sequence. Some genetic constructs can be more difficult to synthesize as a result of secondary-structure and repetitive sequence (12). Beyond these issues, errors in synthesis can still occur despite correction techniques which improve the overall correctness of the generated DNA (12, 16). Due to the inherent risk of incorrect sequence production, screening of produced

genetic material is required to ensure accuracy prior to downstream construction of plasmids or other elements. Fortunately, with increased commercialization it is possible to obtain sequence-verified DNA products to expedite the assembly of large plasmids. In this thesis, synthetic DNA was initially ordered as sequence-verified clones from TWIST Biosciences, however, one ~5 kb tile could not be successfully cloned and was instead constructed using a BioXP 3200.

An important consideration in DNA synthesis at scale is the cost to produce desired products. Synthesis of the 11 DNA fragments in clonal genes used to construct p20298 was ~\$8,000, including the cost of sequence-verification by the supplier. Synthesis of the BioXP tile was an additional \$800, meaning total synthesis of the ~54 kb plasmid was less than \$9,000. This highlights the approximate cost of synthesizing systems at scale. The ability to order sequence-verified clones of products from companies like TWIST Biosciences is crucial, because it improves the likelihood of assembling correct sequences downstream. Where a sequence-verified clone of tile 9 could not be synthesized by TWIST, it could be successfully assembled using the BioXP 3200. Importantly, mutations in the *traV* and *traY* genes were identified within the tile 9 sequence after construction of p20298-AGE. These errors may have occurred as a direct result of being difficult to synthesize sequences, or perhaps toxicity of the genes outside their native context lead to selection for the mutations. In either case, this illustrates that there are trade-offs when synthesizing genetic material by different methods, as the BioXP allowed us to obtain DNA that TWIST could not produce, although the sequence was not perfect. This also highlights the need to screen for errors in synthesis to ensure fidelity when constructing genetic elements.

While synthesis of DNA is now commercially achievable at scale, assembly of these products into large plasmids is still challenging, and traditional cloning is generally not suitable. Homology-based cloning in yeast is beneficial as it can be used to assemble large fragments of bacterial DNA, even with high GC content (25). This thesis utilized homology-based DNA assembly for construction of pNuc and p20298 variants, which was critical for building these plasmids from smaller DNA fragments. This approach is becoming more common, and was also used for upper level assemblies of the chemically synthesized *Mycoplasma mycoides* genome (6). While this assembly procedure is effective, it requires the addition of yeast replication elements and selection markers for construction which may not be desirable to include in all applications. Furthermore, preparation of fragments for subsequent assemblies of plasmid variants typically require PCR amplification,

which is inherently mutagenic. To limit the amount of required amplification steps in new p20298 constructs, I integrated a destination cassette to allow for *in vitro* Gateway recombination (10). Having this type of landing pad for insertion of elements allows for integration of new genetic cargo while limiting the requirement for potentially mutagenic amplification.

Ultimately, when synthesizing genetic constructs using sequences identified in metagenomic data, errors can occur in sequencing, synthesis, and assembly. It is therefore imperative that focus be put on limiting these errors at all stages to ensure the highest likelihood of producing functional systems.

4.5 Conclusions

This thesis explores the use of conjugative plasmids as tools for the delivery of a TevCas9 nuclease for inducible and targeted bacterial killing. Importantly, I found that the frequency of conjugation is heavily dependent on environmental conditions and critically demonstrated that *cis*-conjugative plasmids conjugate at a higher frequency than mobilizable plasmids, particularly over longer time periods. This is crucial as other efforts to use conjugation for the delivery of CRISPR nucleases were ineffective, but did not use a *cis*-conjugative plasmid or optimize delivery conditions. I also show that conjugation frequency of plasmids is highly variable depending on the recipient bacterium. Together, these data demonstrate the need to have a diverse collection of conjugative systems ready to be used as delivery vehicles in synthetic biology. Using metagenomic data mining, thousands of conjugative systems were identified, providing a reservoir of potential new delivery vehicles. Critically, I demonstrate a method for the *de novo* synthesis and construction of a conjugative system identified in a gut microbiome data set. Construction of large DNA elements is challenging, but utilization of molecular biology techniques make it reliable to assemble synthetic DNA into large plasmids, and to further functionalize them for the insertion of other genetic elements. Importantly, this thesis provides key evidence that conjugative plasmids can be used as efficient delivery tools for CRISPR nucleases, and shows that large, functional genetic systems can be identified in sequencing data and constructed synthetically.

4.6 References

- [1] David Bikard, Chad W Euler, Wenyan Jiang, Philip M Nussenzweig, Gregory W Goldberg, Xavier Duportet, Vincent A Fischetti, and Luciano A Marraffini. Exploiting CRISPR-Cas nucleases to produce sequence-specific antimicrobials. *Nature Biotechnology*, 32(11):1146, 2014.
- [2] Sabine Brantl, Detlev Behnke, and Juan C Alonso. Molecular analysis of the replication region of the conjugative *Streptococcus agalactiae* plasmid pIP501 in *Bacillus subtilis*. comparison with plasmids pAM β 1 and pSM 19035. *Nucleic Acids Research*, 18(16):4783–4790, 1990.
- [3] Clement TY Chan, Jeong Wook Lee, D Ewen Cameron, Caleb J Bashor, and James J Collins. 'Deadman' and 'Passcode' microbial kill switches for bacterial containment. *Nature chemical biology*, 12(2):82–86, 2016.
- [4] Robert J Citorik, Mark Mimee, and Timothy K Lu. Sequence-specific antimicrobials using efficiently delivered RNA-guided nucleases. *Nature Biotechnology*, 32(11):1141, 2014.
- [5] Jane Evans and KGH Dyke. Characterization of the conjugation system associated with the *Staphylococcus aureus* plasmid pJE1. *Microbiology*, 134(1):1–8, 1988.
- [6] Daniel G Gibson, John I Glass, Carole Lartigue, Vladimir N Noskov, Ray-Yuan Chuang, Mikkel A Algire, Gwynedd A Benders, Michael G Montague, Li Ma, Monzia M Moodie, et al. Creation of a bacterial cell controlled by a chemically synthesized genome. *Science*, 329(5987):52–56, 2010.
- [7] Ahmed A Goma, Heidi E Klumpe, Michelle L Luo, Kurt Selle, Rodolphe Barrangou, and Chase L Beisel. Programmable removal of bacterial strains by use of genome-targeting CRISPR-Cas systems. *MBio*, 5(1):e00928–13, 2014.
- [8] Jiahui Guo, Tianmin Wang, Changge Guan, Bing Liu, Cheng Luo, Zhen Xie, Chong Zhang, and Xin-Hui Xing. Improved sgRNA design in bacteria via genome-wide activity profiling. *Nucleic Acids Research*, 46(14):7052–7069, 2018.
- [9] Dalton T Ham, Tyler S Browne, Pooja N Bangalorewala, Tyler Wilson, Richard Michael, Gregory B Gloor, and David R Edgell. A generalizable Cas9/sgRNA prediction model using machine transfer learning with small high-quality datasets. *BioRxiv*, pages 2023–02, 2023.
- [10] James L Hartley, Gary F Temple, and Michael A Brasch. DNA cloning using in vitro site-specific recombination. *Genome Research*, 10(11):1788–1795, 2000.
- [11] Hsing-I Ho, Jennifer R Fang, Jacky Cheung, and Harris H Wang. Programmable CRISPR-Cas transcriptional activation in bacteria. *Molecular Systems Biology*, 16(7):e9427, 2020.
- [12] Randall A Hughes and Andrew D Ellington. Synthetic DNA synthesis and assembly: putting the synthetic in synthetic biology. *Cold Spring Harbor Perspectives in Biology*, 9(1):a023812, 2017.

- [13] Nathan I Johns, Antonio LC Gomes, Sung Sun Yim, Anthony Yang, Tomasz Blazejewski, Christopher S Smillie, Mark B Smith, Eric J Alm, Sriram Kosuri, and Harris H Wang. Metagenomic mining of regulatory elements enables programmable species-selective gene expression. *Nature Methods*, 15(5):323–329, 2018.
- [14] Brian V Jones, Máire Begley, Colin Hill, Cormac GM Gahan, and Julian R Marchesi. Functional and comparative metagenomic analysis of bile salt hydrolase activity in the human gut microbiome. *Proceedings of the National Academy of Sciences*, 105(36):13580–13585, 2008.
- [15] John Jumper, Richard Evans, Alexander Pritzel, Tim Green, Michael Figurnov, Olaf Ronneberger, Kathryn Tunyasuvunakool, Russ Bates, Augustin Židek, Anna Potapenko, et al. Highly accurate protein structure prediction with AlphaFold. *Nature*, 596(7873):583–589, 2021.
- [16] Sriram Kosuri and George M Church. Large-scale *de novo* DNA synthesis: technologies and applications. *Nature Methods*, 11(5):499–507, 2014.
- [17] Kathy N Lam, JiuJun Cheng, Katja Engel, Josh D Neufeld, and Trevor C Charles. Current and future resources for functional metagenomics. *Frontiers in Microbiology*, 6:1196, 2015.
- [18] Christopher D Leichthammer. *Development of a Thermosensitive Endonuclease to Act as a Plasmid Kill-Switch*. PhD thesis, The University of Western Ontario, 2020.
- [19] Ruth E Ley, Fredrik Bäckhed, Peter Turnbaugh, Catherine A Lozupone, Robin D Knight, and Jeffrey I Gordon. Obesity alters gut microbial ecology. *Proceedings of the National Academy of Sciences*, 102(31):11070–11075, 2005.
- [20] Stinus Lindgreen, Karen L Adair, and Paul P Gardner. An evaluation of the accuracy and speed of metagenome analysis tools. *Scientific Reports*, 6(1):19233, 2016.
- [21] Wen Wen Low, Joshua LC Wong, Leticia C Beltran, Chloe Seddon, Sophia David, Hok-Sau Kwong, Tatiana Bizeau, Fengbin Wang, Alejandro Peña, Tiago RD Costa, et al. Mating pair stabilization mediates bacterial conjugation species specificity. *Nature Microbiology*, 7(7):1016–1027, 2022.
- [22] Caroline Mahendra, Kathleen A Christie, Beatriz A Osuna, Rafael Pinilla-Redondo, Benjamin P Kleinstiver, and Joseph Bondy-Denomy. Broad-spectrum anti-crispr proteins facilitate horizontal gene transfer. *Nature Microbiology*, 5(4):620–629, 2020.
- [23] Michael J Moser, Robert A DiFrancesco, Krishne Gowda, Audrey J Klingele, Darby R Sugar, Stacy Stocki, David A Mead, and Thomas W Schoenfeld. Thermostable DNA polymerase from a viral metagenome is a potent RT-PCR enzyme. *PLoS One*, 7(6):e38371, 2012.
- [24] Kevin Neil, Nancy Allard, Patricia Roy, Frédéric Grenier, Alfredo Menendez, Vincent Burrus, and Sébastien Rodrigue. High-efficiency delivery of CRISPR-Cas9 by engineered probiotics enables precise microbiome editing. *Molecular Systems Biology*, 17(10):e10335, 2021.

- [25] Vladimir N Noskov, Bogumil J Karas, Lei Young, Ray-Yuan Chuang, Daniel G Gibson, Ying-Chi Lin, Jason Stam, Isaac T Yonemoto, Yo Suzuki, Cynthia Andrews-Pfannkoch, et al. Assembly of large, high G+C bacterial DNA fragments in yeast. *ACS Synthetic Biology*, 1(7):267–273, 2012.
- [26] Gregory M Pellegrino, Tyler S Browne, Keerthana Sharath, Khaleda A Bari, Sarah J Van-curen, Emma Allen-Vercoe, Gregory B Gloor, and David R Edgell. Metabolically-targeted dCas9 expression in bacteria. *Nucleic Acids Research*, 2023.
- [27] Jiuxin Qu, Neha K Prasad, Michelle A Yu, Shuyan Chen, Amy Lyden, Nadia Herrera, Melanie R Silvis, Emily Crawford, Mark R Looney, Jason M Peters, et al. Modulating pathogenesis with mobile-CRISPRi. *Journal of Bacteriology*, 201(22):e00304–19, 2019.
- [28] Alexander C Reis, Sean M Halper, Grace E Vezeau, Daniel P Cetnar, Ayaan Hossain, Phillip R Clauer, and Howard M Salis. Simultaneous repression of multiple bacterial genes using nonrepetitive extra-long sgRNA arrays. *Nature Biotechnology*, 37(11):1294–1301, 2019.
- [29] Austin G Rottinghaus, Aura Ferreiro, Skye RS Fishbein, Gautam Dantas, and Tae Seok Moon. Genetically stable CRISPR-based kill switches for engineered microbes. *Nature Communications*, 13(1):672, 2022.
- [30] Brynne C Stanton, Alec AK Nielsen, Alvin Tamsir, Kevin Clancy, Todd Peterson, and Christopher A Voigt. Genomic mining of prokaryotic repressors for orthogonal logic gates. *Nature Chemical Biology*, 10(2):99–105, 2014.
- [31] Yonggan Sun, Shanshan Zhang, Qixing Nie, Huijun He, Huizi Tan, Fang Geng, Haihua Ji, Jielun Hu, and Shaoping Nie. Gut *firmicutes*: Relationship with dietary fiber and role in host homeostasis. *Critical Reviews in Food Science and Nutrition*, pages 1–16, 2022.
- [32] Peter J Turnbaugh, Ruth E Ley, Michael A Mahowald, Vincent Magrini, Elaine R Mardis, and Jeffrey I Gordon. An obesity-associated gut microbiome with increased capacity for energy harvest. *Nature*, 444(7122):1027–1031, 2006.
- [33] Yun Wang, Yin Chen, Qian Zhou, Shi Huang, Kang Ning, Jian Xu, Robert M Kalin, Stephen Rolfe, and Wei E Huang. A culture-independent approach to unravel uncultured bacteria and functional genes in a complex microbial community. *PLoS One*, 7(10):e47530, 2012.
- [34] Hassan Zafar and Milton H Saier Jr. Gut *Bacteroides* species in health and disease. *Gut Microbes*, 13(1):1848158, 2021.
- [35] Dimitra Zarafeta, Danai Moschidi, Efthymios Ladoukakis, Sergey Gavrillov, Evangelia D Chrysina, Aristotelis Chatziioannou, Ilya Kublanov, Georgios Skretas, and Fragiskos N Koli-sis. Metagenomic mining for thermostable esterolytic enzymes uncovers a new family of bacterial esterases. *Scientific Reports*, 6(1):1–16, 2016.

Appendix A

Supplemental Material for Chapter 2

Table A.1: Table of primers used in chapter 2.

Name	Sequence (5'-3')	Notes
DE-2031	gggcggttggaatccagaaacc	Forward primer to amplify TevCas9 fragment from within the I-TevI domain
DE-3116	ttacgccccgcctgccaact	Reverse primer to amplify chloramphenicol resistance gene fragment
DE-3302	GGCATCGGTCGAGATCCCGGTGCCT AATGAGTGAGCTAACTTACATTAAT TGCGTTGCGCGATCGTCTTGCCCTTG CTCGT	Forward primer to amplify OriT fragment with overlap to pACYC backbone fragment to clone pNuc-trans
DE-3303	GTAGCATAGGGTTTGCAGAATCCCTGCT TCGTCCATTTGACAGGCACATTATG- CATCGATATCTTCCGCTGCATAACCCT	Reverse primer to amplify OriT fragment with overlap to AraC/pBad fragment to clone pNuc-trans
DE-3304	GATGGATATACCGAAAAAATCGCTA TAATGACCCCGAAGCAGGGTTATGC AGCGGAAGATATCGATGCATAATGT GCCTG	Forward primer to amplify AraC/pBAD fragment with overlap to OriT fragment to clone pNuc-trans

DE-3305	CCATGGTATATCTCCTTATTAAAGT TAAACAAAATTATTTCTACAGGGCT AGCCCAAAAAACGGG	Reverse primer to amplify AraC/pBAD fragment with overlap to TevCas9 fragment to clone pNuc-trans
DE-3306	GACGCTTTTTATCGCAACTCTCTAC TGTTTCTCCATACCCGTTTTTTTGGGC- TAGCCCTGTAGAAATAATTTGTTAAC	Forward primer to amplify TevCas9 with overlap to AraC/pBad fragment to clone pNuc-trans
DE-3307	TCTCCCgtgctcagtatctctatcactgatagggatg tcaatctctatcactgatagggaATTTTCGATTATGCG- GCCGTG	Reverse primer to amplify TevCas9 with overlap to the gRNA cassette to clone pNuc-trans
DE-3308	CGAAATtcctatcagtgatagagattgacatcccta tcagtgatagagatactgagcacGGGAGACCCATGC- CATAGCG	Forward primer to amplify gRNA cassette with overlap to TevCas9 fragment to clone pNuc-trans
DE-3309	GCTCCATCAAGAAGAGGCACTTCGA GCTGTAAGTACATCACCGACGAGCAAG- GCAAGACGATCGCGCAACGCAATTAATG	Reverse primer to amplify pACYC backbone with overlap to OriT fragment to clone pNuc-trans
DE-3315	TTTATATATTTATATTAATAAAATTTAAAT TATAATTATTTTATAGCACGTGATGctcgc- CAAAAACCCCTCAAGACCC	Reverse primer to amplify gRNA cassette with overlap to CEN-ARS-HIS fragment to clone pNuc-trans
DE-3316	GCTCCGCTGAGCAATAACTAGCATA ACCCCTTGGGGCCTC- TAAACGGGTCTTGAGGGGTTTTTTG- gcgagCATCACGTGC	Forward primer to amplify CEN-ARS-HIS with overlap to gRNA cassette to clone pNuc-trans

DE-3351	tattgactaccggaagcagtgtgaccgtgtgcttctcaaatgcc tgaggttcagTCAAGTCCAGACTCCTGTG- TAAAAC	Reverse primer to amplify CEN-ARS-HIS with overlap to pACYC backbone (p15A origin and CAT gene) to clone pNuc-trans
DE-3352	ACGATGTTCCCTCCACCAAAGGTGTTC TTATGTAGTTTTACACAGGAGTCTG- GACTTGActgaaacctcaggcatttgag	Forward primer to amplify pACYC backbone with overlap to CEN-ARS-HIS fragment to clone pNuc-trans
DE-3365	CACGCGCGTTACGGTAACGAATGCG	Top strand oligo to clone sgRNA 9 targeting STM1005
DE-3366	AAAACGCATTCGTTACCGTAACGCG	Bottom strand oligo to clone sgRNA 9 targeting STM1005
DE-3367	CACGCCAGGGAATACGTGGGCGGAG	Top strand oligo to clone sgRNA 10 targeting STM4261
DE-3368	AAAACTCCGCCACGTATTCCCTGG	Bottom strand oligo to clone sgRNA 10 targeting STM4261
DE-3424	GAATTTCTGCCATTCATCCGCTTATTAT CACTTATTCAGGCGTAGCACCAGGCGTT- TAACGATCGTCTTGCTTGCTCGT	Forward primer to amplify pNuc-trans with overlap to pTA-mob AvrII site to clone pNuc-cis
DE-3425	GCGTCCTGCTCGTGATCGGGAGTAT CTGGCTGGGCCAACGTTCCAACCG- CACTCCTAGTCAAGTCCAGACTCCTGTG- TAA	Reverse primer to amplify pNuc-trans with overlap to pTA-mob AvrII site to clone pNuc-cis

DE-3537	GAGGGCACCGATAAGATTCTT	Reverse primer to amplify TevCas9 gene fragment from within Cas9 domain
DE-3748	CCTGGTTGAGCAGAGAAACCT	Forward primer to amplify STM1005 target site from Salmonella genomic DNA
DE-3749	GTTGCGGGAATATGGACAAT	Reverse primer to amplify STM1005 target site from Salmonella genomic DNA
DE-3750	CTGCTTTCTAAGGATGATACGG	Forward primer to amplify STM4261 target site from Salmonella genomic DNA
DE-3751	TTATCGCCTTTCACGCC	Reverse primer to amplify STM4261 target site from Salmonella genomic DNA
DE-3752	GTCCGAATAGCGCTAATAGCATATCAT ACGgcgagCATCACGTGCTATAA	Forward primer to amplify backbone and initial sgRNA (overhang A) for multiplexing sgRNAs
DE-3753	CGTATGATATGCTATTAGCGCTATTCG GACCAAAAAACCCCTCAAGACCC	Reverse primer to amplify second sgRNA to 5' end of backbone (overhang A) for multiplexing sgRNAs
DE-3754	accgtagcatcgatctacacattaggacaGTATTGTAC ACGGCCGCATA	Forward primer to amplify second sgRNA cassette (overhang B) for multiplexing sgRNAs

DE-3755	tgtcctaattgttagatcgatgctaacggt CAAAAAACC-CCTCAAGACCC	Reverse primer to amplify backbone with overhang to second sgRNA cassette (overhang B) for multiplexing sgRNAs
DE-3777	atggagaaaaaatcactggatatac	Forward primer to amplify chloramphenicol resistance gene fragment
DE-4018	CACGGTTAAAAAAGTTGACGTAACG	Top strand oligo to clone sgRNA 1 targeting rplC gene
DE-4019	AAAACGTTACGTCAACTTTTTTAAC	Bottom strand oligo to clone sgRNA 1 targeting rplC gene
DE-4020	CACGCTGAATATCGAGTCATTTCCGG	Top strand oligo to clone sgRNA 2 targeting ytfM gene
DE-4021	AAAACCGAAATGACTCGATATTCAG	Bottom strand oligo to clone sgRNA 2 targeting ytfM gene
DE-4022	CACGGTTGATCGGTTTCATAAAACGG	Top strand oligo to clone sgRNA 3 targeting yhgJ gene
DE-4023	AAAACCGTTTTATGAACCGATCAAC	Bottom strand oligo to clone sgRNA 3 targeting yhgJ gene
DE-4024	CACGACGCCAGTATGATCTTTCCGG	Top strand oligo to clone sgRNA 4 targeting stfA gene
DE-4025	AAAACGCGAAAGATCATACTGGCGT	Bottom strand oligo to clone sgRNA 4 targeting stfA gene
DE-4026	CACGACGCGGCTTGGCGAACCGGAG	Top strand oligo to clone sgRNA 5 targeting aegA gene
DE-4027	AAAACCTCCGGTTCGCCAAGCCGCGT	Bottom strand oligo to clone sgRNA 5 targeting aegA gene

DE-4028	CACGCCATAGCCAGCCGAGATAGGG	Top strand oligo to clone sgRNA 6 targeting gltJ gene
DE-4029	AAAACCCTATCTCGGCTGGCTATGG	Bottom strand oligo to clone sgRNA 6 targeting gltJ gene
DE-4030	CACGATTAAGGTAAACACCACCGAG	Top strand oligo to clone sgRNA 7 targeting ompS gene
DE-4031	AAAACTCGGTGGTGTTTACCTTAAT	Bottom strand oligo to clone sgRNA 7 targeting ompS gene
DE-4032	CACGTGCCGGCGTCCATGTCTGCGG	Top strand oligo to clone sgRNA 8 targeting mviM gene
DE-4033	AAAACCGCAGACATGGACGCCGGCA	Bottom strand oligo to clone sgRNA 8 targeting mviM gene
DE-4186	GTAGTAAATGCAGAAATGGTGGTTC TGGTGGTACCGGAGGTAGCGGTATC- CACGGAGTCC	top strand oligo for SaCas9 guide targetting FepB
DE-4187	GTGTACAATAGGTACGCGTGCGGCC GCTTAATTAAGTTAGGATCC- CTTTTTCTTTTTTGC	bottom strand oligo for SaCas9 guide targetting FepB
DE-4188	AATGCCGTGTTTATCTCGTCAACTT GTTGGCGAGATTTTTTCCGCTGAG- CAATAACTAGC	Forward primer to amplify saCas9 with homololgy to I-TevI linker in pNuc construct
DE-4189	CCAGGATGTAGTTCCGCTTGGCTGC TGGGACTCCGTGGATACCGCTACCTCCG- GTACCAC	Reverse primer to amplify saCas9 with homology to gRNA cassette in pNuc construct

DE-4255	CACGCCAGACGGAACGTCTCCGTACC	Forward primer to amplify pNuc backbone with homology to the RNA cassette
DE-4256	AAACGGTACGGAGACGTTCCGTCTGG	Reverse primer to amplify pNuc with Tev backbone with homology to saCas9
DE-4259	CACGAGGCAGTGGCCGACGCCGGTCG	Top strand oligo to clone sgRNA 11 targeting FabB gene
DE-4260	AAAACGACCGGCGTCGGCCACTGCCT	Bottom strand oligo to clone sgRNA 11 targeting FabB gene
DE-4261	CACGGATCCCGACGGAGAACACAACG	Top strand oligo to clone sgRNA 12 targeting MurE gene
DE-4262	AAAACGTTGTGTTCTCCGTCGGGATC	Bottom strand oligo to clone sgRNA 12 targeting MurE gene
DE-4263	CACGTCGAAGAAGAGCGCGTTGCTCG	Top strand oligo to clone sgRNA 13 targeting Tsf gene
DE-4264	AAAACGAGCAACGCGCTCTTCTTCGA	Bottom strand oligo to clone sgRNA 13 targeting Tsf gene
DE-4359	CACGCGAGATGCCCATCCCGATAAG	Top strand oligo to clone sgRNA 14 targeting FtsW gene
DE-4360	AAAACCTTATCGGGATGGGCATCTCG	Bottom strand oligo to clone sgRNA 14 targeting FtsW gene

DE-4361	CACGGCGAGAATTCGTACTGGCGCG	Top strand oligo to clone sgRNA 15 targeting GlnS gene
DE-4362	AAAACGCGCCAGTACGAATTCTCGC	Bottom strand oligo to clone sgRNA 15 targeting GlnS gene
DE-4363	CACGTACGCGCAGCGGTGCGGAATG	Top strand oligo to clone sgRNA 16 targeting RpoB gene
DE-4364	AAAACATTCCGCACCGCTGCGCGTA	Bottom strand oligo to clone sgRNA 16 targeting RpoB gene
DE-4365	CACGAGGGGCGCCGCCTTTACCTGCG	Top strand oligo to clone sgRNA 17 targeting PolA gene
DE-4366	AAAACGCAGGTAAAGGCGGCGCCCCT	Bottom strand oligo to clone sgRNA 17 targeting PolA gene
DE-4367	CACGATCTGAGTAACGTTGATCTGCG	Top strand oligo to clone sgRNA 18 targeting DnaC gene
DE-4368	AAAACGCAGATCAACGTTACTCAGAT	Bottom strand oligo to clone sgRNA 18 targeting DnaC gene
DE-4439	CACGAACCTGAGCCGCCAGGGCATG	Top strand oligo to clone sgRNA 19 targeting IcdA gene

DE-4440	AAAACATGCCCTGGCGGCTCAGGTT	Bottom strand oligo to clone sgRNA 19 targeting IcdA gene
DE-4441	CACGATAACGAATGCGCCCGACGCG	Top strand oligo to clone sgRNA 20 targeting NarY gene
DE-4442	AAAACGCGTCGGGCGCATTCGTTAT	Bottom strand oligo to clone sgRNA 20 targeting NarY gene
DE-4443	CACGATCCGCAGCAGGAGTTCTTACG	Top strand oligo to clone sgRNA 21 targeting ClpX gene
DE-4444	AAAACGTAAGAACTCCTGCTGCGGAT	Bottom strand oligo to clone sgRNA 21 targeting ClpX gene
DE-4445	CACGGCTCGTCAGCCGGCATATCCG	Top strand oligo to clone sgRNA 22 targeting ArgS gene
DE-4446	AAAACGGATATGCCGGCTGACGAGC	Bottom strand oligo to clone sgRNA 22 targeting ArgS gene
DE-4447	CACGACATCGAGCCTTTGGACTCGG	Top strand oligo to clone sgRNA 23 targeting ValS gene
DE-4448	AAAACCGAGTCCAAAGGCTCGATGT	Bottom strand oligo to clone sgRNA 23 targeting ValS gene

DE-4449	CACGGGCGGACCGGGGATGTTAATGAG	Top strand oligo to clone sgRNA 24 targeting TrmD gene
DE-4450	AAAACTCATTAACATCCCCGGTCCGCC	Bottom strand oligo to clone sgRNA 24 targeting TrmD gene
DE-4451	CACGAGGTTTCAGGACGATATCGAGAG	Top strand oligo to clone sgRNA 25 targeting PrfA gene
DE-4452	AAAACCTCTCGATATCGTCCTGAACCT	Bottom strand oligo to clone sgRNA 25 targeting PrfA gene
DE-4453	CACGTGACCGTATTATCCAAATCTGG	Top strand oligo to clone sgRNA 26 targeting LepA gene
DE-4454	AAAACCAGATTTGGATAATACGGTCA	Bottom strand oligo to clone sgRNA 26 targeting LepA gene
DE-4455	CACGTATTCCGGGCGTACCAGGCGG	Top strand oligo for Sp-Cas9 guide targeting coding pos580 PolA +prediction
DE-4456	AAAACCGCCTGGTACGCCCGGAATA	Bottom strand oligo for Sp-Cas9 guide targeting coding pos580 PolA +prediction
DE-4457	CACGATCGCCCAGCGAACCGGCAGG	Top strand oligo for Sp-Cas9 guide targeting coding pos961 PolA +prediction

DE-4458	AAAACCTGCCGGTTCGCTGGGCGAT	Bottom strand oligo for Sp-Cas9 guide targeting coding pos961 PolA +prediction
DE-4459	CACGAGATCGCACTGGAGGAAGCGG	Top strand oligo for Sp-Cas9 guide targeting coding pos1476 PolA +prediction
DE-4460	AAAACCGCTTCCTCCAGTGCGATCT	Bottom strand oligo for Sp-Cas9 guide targeting coding pos1476 PolA +prediction
DE-4461	CACGGGTGCTGGAAGAGCTGGCGCG	Top strand oligo for Sp-Cas9 guide targeting coding pos1849 PolA +prediction
DE-4462	AAAACGCGCCAGCTCTTCCAGCACCC	Bottom strand oligo for Sp-Cas9 guide targeting coding pos1849 PolA +prediction
DE-4463	CACGGCCGCTGGATAGCGTGACCGG	Top strand oligo for Sp-Cas9 guide targeting coding pos2245 PolA +prediction
DE-4464	AAAACCGGTCACGCTATCCAGCGGC	Bottom strand oligo for Sp-Cas9 guide targeting coding pos2245 PolA +prediction
DE-4465	CACGTAAATCCAGCAACGCGGCGG	Top strand oligo for Sp-Cas9 guide targeting coding pos2496 PolA +prediction
DE-4466	AAAACCGCCGCGTTGCTGGATTTAA	Bottom strand oligo for Sp-Cas9 guide targeting coding pos2496 PolA +prediction

DE-4467	CACGTAACGACTTCATCCGGGCCGG	Top strand oligo for Sp-Cas9 guide targeting template pos490 PolA +prediction
DE-4468	AAAACCGGCCCGGATGAAGTCGTTA	Bottom strand oligo for Sp-Cas9 guide targeting template pos490 PolA +prediction
DE-4469	CACGTACGCCCGGAATATTATCCGG	Top strand oligo for Sp-Cas9 guide targeting template pos570 PolA +prediction
DE-4470	AAAACCGGATAATATTCCGGGCGTA	Bottom strand oligo for Sp-Cas9 guide targeting template pos570 PolA +prediction
DE-4471	CACGCAGGTTTCGATGGCAAACGAGG	Top strand oligo for Sp-Cas9 guide targeting template pos1123 PolA +prediction
DE-4472	AAAACCTCGTTTGCCATCGAACCTG	Bottom strand oligo for Sp-Cas9 guide targeting template pos1123 PolA +prediction
DE-4473	CACGGCAGTTCCAGAGCACGCTGGG	Top strand oligo for Sp-Cas9 guide targeting template pos1204 PolA +prediction
DE-4474	AAAACCCAGCGTGCTCTGGAAGTGC	Bottom strand oligo for Sp-Cas9 guide targeting template pos1204 PolA +prediction
DE-4475	CACGTAAATGCCTGACGAATGCGGG	Top strand oligo for Sp-Cas9 guide targeting template pos2071 PolA +prediction

DE-4476	AAAACCCGCATTCGTCAGGCATTTA	Bottom strand oligo for Sp-Cas9 guide targeting template pos2071 PolA +prediction
DE-4477	CACGAAGCTGGCGAGAAAGACCGAG	Top strand oligo for Sp-Cas9 guide targeting template pos2322 PolA +prediction
DE-4478	AAAACCTCGGTCTTTCTCGCCAGCTT	Bottom strand oligo for Sp-Cas9 guide targeting template pos2322 PolA +prediction
DE-4479	CACGAACCCACTTATTCTCGTAGAG	Top strand oligo for SpCas9 guide targeting coding pos32 PolA -prediction
DE-4480	AAAACCTCTACGAGAATAAGTGGGTT	Bottom strand oligo for Sp-Cas9 guide targeting coding pos32 PolA -prediction
DE-4481	CACGACCTGTGCGCATGATTATCG	Top strand oligo for Sp-Cas9 guide targeting coding pos1162 PolA -prediction
DE-4482	AAAACGATAATCATGCGCGACAGGT	Bottom strand oligo for Sp-Cas9 guide targeting coding pos1162 PolA -prediction
DE-4483	CACGTAACTTTGGCCTGATTTACG	Top strand oligo for Sp-Cas9 guide targeting coding pos2292 PolA -prediction
DE-4484	AAAACGTAAATCAGGCCAAAGTTAA	Bottom strand oligo for Sp-Cas9 guide targeting coding pos2292 PolA -prediction

DE-4485	CACGCGAGAATAAGTGGGTTTTCTG	Top strand oligo for Sp-Cas9 guide targeting template pos25 PolA -prediction
DE-4486	AAAACAGAAAACCCACTTATTCTCG	Bottom strand oligo for Sp-Cas9 guide targeting template pos25 PolA -prediction
DE-4487	CACGTTTCTTCCGAATGTTTGTGCG	Top strand oligo for Sp-Cas9 guide targeting template pos1666 PolA -prediction
DE-4488	AAAACGCACAAACATTCGGAAGAAA	Bottom strand oligo for Sp-Cas9 guide targeting template pos1666 PolA -prediction
DE-4489	CACGCATGGCGCGCTTGATGATATG	Top strand oligo for Sp-Cas9 guide targeting template pos2571 PolA -prediction
DE-4490	AAAACATATCATCAAGCGCGCCATG	Bottom strand oligo for Sp-Cas9 guide targeting template pos2571 PolA -prediction
DE-4491	CACGGTGGCCGAACCAGCTTCGCGG	Top strand oligo for Sp-Cas9 guide targeting coding pos266 KatG +prediction
DE-4492	AAAACCGCGAAGCTGGTTCGGCCAC	Bottom strand oligo for Sp-Cas9 guide targeting coding pos266 KatG +prediction
DE-4493	CACGTGACCGATTCACAACCGTGGG	Top strand oligo for Sp-Cas9 guide targeting coding pos403 KatG +prediction

DE-4494	AAAACCCACGGTTGTGAATCGGTCA	Bottom strand oligo for Sp-Cas9 guide targeting coding pos403 KatG +prediction
DE-4495	CACGCCTCGGTAAAACCCACGGCGG	Top strand oligo for Sp-Cas9 guide targeting coding pos962 KatG +prediction
DE-4496	AAAACCGCCGTGGGTTTTACCGAGG	Bottom strand oligo for Sp-Cas9 guide targeting coding pos962 KatG +prediction
DE-4497	CACGCGCGGCGGCGATAAGCGTGGG	Top strand oligo for Sp-Cas9 guide targeting coding pos1593 KatG +prediction
DE-4498	AAAACCCACGCTTATCGCCGCCGCG	Bottom strand oligo for Sp-Cas9 guide targeting coding pos1593 KatG +prediction
DE-4499	CACGACCTTTTGCGCCGGGCCGGGG	Top strand oligo for Sp-Cas9 guide targeting coding pos1808 KatG +prediction
DE-4500	AAAACCCCGGCCCGGCGCAAAAGGT	Bottom strand oligo for Sp-Cas9 guide targeting coding pos1808 KatG +prediction
DE-4501	CACGGTTTGTGAAGGACTTCGTCGG	Top strand oligo for Sp-Cas9 guide targeting coding pos2273 KatG +prediction
DE-4502	AAAACCGACGAAGTCCTTCACAAAC	Bottom strand oligo for Sp-Cas9 guide targeting coding pos2273 KatG +prediction

DE-4503	CACGGCTGGTTCGGCCACCAGTCGG	Top strand oligo for Sp-Cas9 guide targeting template pos257 KatG +prediction
DE-4504	AAAACCGACTGGTGGCCGAACCAGC	Bottom strand oligo for Sp-Cas9 guide targeting template pos257 KatG +prediction
DE-4505	CACGGGTAGCGCGAATAGCGGCGGG	Top strand oligo for Sp-Cas9 guide targeting template pos880 KatG +prediction
DE-4506	AAAACCCGCCGCTATTCGCGCTACC	Bottom strand oligo for Sp-Cas9 guide targeting template pos880 KatG +prediction
DE-4507	CACGGCCCTGCGCTTCAATCGGCGG	Top strand oligo for Sp-Cas9 guide targeting template pos1018 KatG +prediction
DE-4508	AAAACCGCCGATTGAAGCGCAGGGC	Bottom strand oligo for Sp-Cas9 guide targeting template pos1018 KatG +prediction
DE-4509	CACGGCCGCCGCGGAAAGTAGACGG	Top strand oligo for Sp-Cas9 guide targeting template pos1579 KatG +prediction
DE-4510	AAAACCGTCTACTTTCCGCGGCGGC	Bottom strand oligo for Sp-Cas9 guide targeting template pos1579 KatG +prediction
DE-4511	CACGGATGCTGACACCCGCAGCAGG	Top strand oligo for Sp-Cas9 guide targeting template pos1780 KatG +prediction

DE-4512	AAAACCTGCTGCGGGTGTTCAGCATC	Bottom strand oligo for Sp-Cas9 guide targeting template pos1780 KatG +prediction
DE-4513	CACGAACCAAACACCAGATCGGCGG	Top strand oligo for Sp-Cas9 guide targeting template pos2192 KatG +prediction
DE-4514	AAAACCGCCGATCTGGTGTTTGGTT	Bottom strand oligo for Sp-Cas9 guide targeting template pos2192 KatG +prediction
DE-4515	CACGCAACTATATCTATTTGCTCCG	Top strand oligo for SpCas9 guide targeting coding pos96 KatG -prediction
DE-4516	AAAACGGAGCAAATAGATATAGTTG	Bottom strand oligo for Sp-Cas9 guide targeting coding pos96 KatG -prediction
DE-4517	CACGTTCTATTAGCGAGATGGTTTG	Top strand oligo for Sp-Cas9 guide targeting coding pos1544 KatG -prediction
DE-4518	AAAACAAACCATCTCGCTAATAGAA	Bottom strand oligo for Sp-Cas9 guide targeting coding pos1544 KatG -prediction
DE-4519	CACGTGACTTCTTCGCTAATCTGCG	Top strand oligo for Sp-Cas9 guide targeting coding pos2078 KatG -prediction
DE-4520	AAAACGCAGATTAGCGAAGAAGTCA	Bottom strand oligo for Sp-Cas9 guide targeting coding pos2078 KatG -prediction

DE-4521	CACGCGCCTTGAGATCCCCTTTCAG	Top strand oligo for Sp-Cas9 guide targeting template pos376 KatG -prediction
DE-4522	AAAACCTGAAAGGGGATCTCAAGGCG	Bottom strand oligo for Sp-Cas9 guide targeting template pos376 KatG -prediction
DE-4523	CACGTTGATAATGTCTTCCTGCGTG	Top strand oligo for Sp-Cas9 guide targeting template pos1491 KatG -prediction
DE-4524	AAAACACGCAGGAAGACATTATCAA	Bottom strand oligo for Sp-Cas9 guide targeting template pos1491 KatG -prediction
DE-4525	CACGAGCTCATTAGCGTCGTCGGTG	Top strand oligo for Sp-Cas9 guide targeting template pos2121 KatG -prediction
DE-4526	AAAACACCGACGACGCTAATGAGCT	Bottom strand oligo for Sp-Cas9 guide targeting template pos2121 KatG -prediction
DE-4635	CGGCCAGTTAAGCCATTC	Forward primer to amplify region of plasmids for pNuc copy number qPCR
DE-4636	GCCAGGAGAGATTCATCAC	Reverse primer to amplify region of plasmids for pNuc copy number qPCR
DE-4745	CACGACGCATCACAGCGTGGCGTG	"Good gRNA" targeting <i>S. enterica</i> LT2 fabB gene - guide 1 top strand

DE-4746	AAAACACGCCACGCTGGTGATGCGT	"Good gRNA" targeting <i>S. enterica</i> LT2 fabB gene - guide 1 bottom strand
DE-4747	CACGCTGCTGGTTATTACCGATGCG	"Good gRNA" targeting <i>S. enterica</i> LT2 fabB gene - guide 2 top strand
DE-4748	AAAACGCATCGGTAATAACCAGCAG	"Good gRNA" targeting <i>S. enterica</i> LT2 fabB gene - guide 2 bottom strand
DE-4749	CACGGACATCGTTTTTGCTGGCGGG	"Good gRNA" targeting <i>S. enterica</i> LT2 fabB gene - guide 3 top strand
DE-4750	AAAACCCGCCAGCAAAAACGATGTC	"Good gRNA" targeting <i>S. enterica</i> LT2 fabB gene - guide 3 bottom strand
DE-4751	CACGGAGCTGGATGAGCAGGCTGCG	"Good gRNA" targeting <i>S. enterica</i> LT2 fabB gene - guide 4 top strand
DE-4752	AAAACGCAGCCTGCTCAGCCAGCTC	"Good gRNA" targeting <i>S. enterica</i> LT2 fabB gene - guide 4 bottom strand
DE-4753	CACGCATCGCGGGCGGTGGCGGTAG	"Good gRNA" targeting <i>S. enterica</i> LT2 fabB gene - guide 5 top strand
DE-4754	AAAACACTACCGCCACCGCCCGCGATG	"Good gRNA" targeting <i>S. enterica</i> LT2 fabB gene - guide 5 bottom strand

DE-4755	CACGTGGCGGCACCAACGCCACGCG	"Good gRNA" targeting <i>S. enterica</i> LT2 fabB gene - guide 6 top strand
DE-4756	AAAACGCGTGGCGTTGGTGCCGCCA	"Good gRNA" targeting <i>S. enterica</i> LT2 fabB gene - guide 6 bottom strand
DE-4757	CACGCATCGAAGAGCTGGATGAGCG	"Good gRNA" targeting <i>S. enterica</i> LT2 fabB gene - guide 7 top strand
DE-4758	AAAACGCTCATCCAGCTCTTCGATG	"Good gRNA" targeting <i>S. enterica</i> LT2 fabB gene - guide 7 bottom strand
DE-4759	CACGAGTGTTTGGCGATAACAGCCG	"Good gRNA" targeting <i>S. enterica</i> LT2 fabB gene - guide 8 top strand
DE-4760	AAAACGGCTGTTATCGCCAAACACT	"Good gRNA" targeting <i>S. enterica</i> LT2 fabB gene - guide 8 bottom strand
DE-4761	CACGAGAGCTGGATGAGCAGGCTGG	"Good gRNA" targeting <i>S. enterica</i> LT2 fabB gene - guide 9 top strand
DE-4762	AAAACCAGCCTGCTCATCCAGCTCT	"Good gRNA" targeting <i>S. enterica</i> LT2 fabB gene - guide 9 bottom strand
DE-4763	CACGCGCCAGCCGCGCCAGCGAGG	"Good gRNA" targeting <i>S. enterica</i> LT2 fabB gene - guide 10 top strand

DE-4764	AAAACCTCGCTGGGCGCGGCTGGCG	"Good gRNA" targeting S. enterica LT2 fabB gene - guide 10 bottom strand
DE-4765	CACGCGTGCAGTGATTACTGGCCTG	"Bad gRNA" targeting S. enterica LT2 fabB gene - guide 11 top strand
DE-4766	AAAACAGGCCAGTAATCACTGCACG	"Bad gRNA" targeting S. enterica LT2 fabB gene - guide 11 bottom strand
DE-4767	CACGAACGTAAACTGGATAACCACG	"Bad gRNA" targeting S. enterica LT2 fabB gene - guide 12 top strand
DE-4768	AAAACGTGGTATCCAGTTTTACGTT	"Bad gRNA" targeting S. enterica LT2 fabB gene - guide 12 bottom strand
DE-4769	CACGGCGACCTCCGCACACTGTATG	"Bad gRNA" targeting S. enterica LT2 fabB gene - guide 13 top strand
DE-4770	AAAACATACAGTGTGCGGAGGTCGC	"Bad gRNA" targeting S. enterica LT2 fabB gene - guide 13 bottom strand
DE-4771	CACGACAGATCCAACTGGGCAAACG	"Bad gRNA" targeting S. enterica LT2 fabB gene - guide 14 top strand
DE-4772	AAAACGTTTGCCCAGTTGGATCTGT	"Bad gRNA" targeting S. enterica LT2 fabB gene - guide 14 bottom strand

DE-4773	CACGTAGGTACGGGACGCTTTTTTCG	"Bad gRNA" targeting S. enterica LT2 fabB gene - guide 15 top strand
DE-4774	AAAACGAAAAAGCGTCCCGTACCTA	"Bad gRNA" targeting S. enterica LT2 fabB gene - guide 15 bottom strand
DE-4775	CACGCGCAGTACGTTGCATGCAGAG	"Bad gRNA" targeting S. enterica LT2 fabB gene - guide 16 top strand
DE-4776	AAAACTCTGCATGCAACGTA CTGCG	"Bad gRNA" targeting S. enterica LT2 fabB gene - guide 16 bottom strand
DE-4777	CACGCATCTACTCTCTGCTAATGCG	"Bad gRNA" targeting S. enterica LT2 fabB gene - guide 17 top strand
DE-4778	AAAACGCATTAGCAGAGAGTAGATG	"Bad gRNA" targeting S. enterica LT2 fabB gene - guide 17 bottom strand
DE-4779	CACGACGTGCAGTGATTACTGGCCG	"Bad gRNA" targeting S. enterica LT2 fabB gene - guide 18 top strand
DE-4780	AAAACGGCCAGTAATCACTGCACGT	"Bad gRNA" targeting S. enterica LT2 fabB gene - guide 18 bottom strand
DE-4781	CACGACCGTAATGTCTAACAGCTTG	"Bad gRNA" targeting S. enterica LT2 fabB gene - guide 19 top strand

DE-4782	AAAACAAGCTGTTAGACATTACGGT	"Bad gRNA" targeting S. enterica LT2 fabB gene - guide 19 bottom strand
DE-4783	CACGGGCCTGTGAGTTCGATGCGAG	"Bad gRNA" targeting S. enterica LT2 fabB gene - guide 20 top strand
DE-4784	AAAACTCGCATCGAACTCACAGGCC	"Bad gRNA" targeting S. enterica LT2 fabB gene - guide 20 bottom strand

Appendix B

Supplemental Material for Chapter 3

Table B.1: Table of primers used in chapter 3.

Primer	Sequence (5'-3')	Notes
298-ACYC-T12R	GATCGTAAGAAGAACGCCACAGGCT TCTTGTGGAGCCCGACGATCAGTAGCG- TATACAGC	reverse primer to reamplify fragment 12 of p20298-AGE to construct p20298-15a and fix traV error
298-ACYC-T2R	TTTGATTATCGGCAGCAGTTCC	reverse primer to reamplify fragment 2 of p20298-AGE to construct p20298-15a
298-ACYC-T4F	GCAGACGCATCATATGTTTGG	forward primer to reamplify fragment 4 of p20298-AGE to construct p20298-15a
298-ACYC-T7R	ATGACTGTACGGGGTTCAGC	reverse primer to reamplify fragment 7 of p20298-AGE to construct p20298-15a
298-ACYC-T8R	TTCTCGCCGTTCACCTTCTTT	reverse primer to reamplify fragment 8 of p20298-AGE to construct p20298-15a

298-ACYC-T6F	GACTGGGTTGAAGGCTCTCAAGGGC ATCGGTCGAGATCCTAACCATTAACCAT- GCGCCTG	forward primer to amplify fragment 6 of p20298-AGE with homology to the pNuc- trans backbone
298-ACYC-T1R	GTATTGGCAGCATCCCGACCACCAA GGAAGGAAATGACG- TAGTCAGGTAAATAGGCCTGC	reverse primer to reamplify fragment 1 of p20298-AGE to construct p20298-15a and fix traY error
298-ACYC- T5(bb)R	TTTAGAGTCTCAGGATTCTCAGGCGC ATGGTTAATGGTTAGGATCTCGACCGAT- GCCCTT	reverse primer to amplify pNuc-trans backbone with homology to 20298 conjuga- tive system
298-ACYC-T3R	CACTATGGCCCGTTTAGCAT	reverse primer to reamplify fragment 3 of p20298-AGE to construct p20298-15a
298-ACYC-T4R	ATTTAAATTATAATTATTTTTATAG CACGTGATGCTCGCCGCCATTTACCT- GAACGGTGA	reverse primer to amplify fragment 4 of p20298-AGE with homology to the pNuc- trans backbone
298-ACYC- T5(bb)F	AAGGTCACAGCACGCAATAAATTCAC CGTTCAGGTAAATGGCGGCGAGCAT- CACGTGCTA	forward primer to amplify pNuc-trans backbone with homology to 20298 conjuga- tive system
298-ACYC-T10F	AGAAGGCGGTCTTGTCTTCA	forward primer to reamplify fragment 10 of p20298-AGE to construct p20298-15a
298-ACYC-T8F	GCTTTTGCTTCTGGTCCTTG	forward primer to reamplify fragment 8 of p20298-AGE to construct p20298-15a

298-ACYC-T9R	CGCCTAAAACAGACGTGTCA	reverse primer to reamplify fragment 9 of p20298-AGE to construct p20298-15a
298-ACYC-T6R	CAGGTAAAACACGATGGTGCC	reverse primer to reamplify fragment 6 of p20298-AGE to construct p20298-15a
298-ACYC-T7F	CACCAACAACCACTGACCTG	forward primer to reamplify fragment 7 of p20298-AGE to construct p20298-15a
298-ACYC-T7R	GCTGAACCCCGTACAGTCAT	reverse primer to reamplify fragment 7 of p20298-AGE to construct p20298-15a
298-ACYC-T9F	TTGCTGTTGTCGTGAAGTCC	forward primer to reamplify fragment 9 of p20298-AGE to construct p20298-15a
298-ACYC-T10R	GTATGACCGCAACCACCTCT	reverse primer to reamplify fragment 10 of p20298-AGE to construct p20298-15a
298-ACYC-T12F	CAGGTACGCTTCATGATGATGAC	forward primer to reamplify fragment 12 of p20298-AGE to construct p20298-15a
298-ACYC-T11R	GCGTAAAAGCGTCGTAAAGC	reverse primer to reamplify fragment 11 of p20298-AGE to construct p20298-15a
298-ACYC-T11F	ACAGTCGGGAAAATCGTCAC	forward primer to reamplify fragment 11 of p20298-AGE to construct p20298-15a

298-ACYC-T1F	ACTCTCGGGCTGTATACGCTACTGA TCGTCGGGCTCCACAAGAAGCCTGTG- GCGTTCTTC	forward primer to reamplify fragment 1 of p20298-AGE to construct p20298-15a and fix traV error
298-ACYC-T2F	CTGACTACGTCATTCCTTCCTTGG TGGTCGGGATGCTGCCAATACCCTTG- GAAGTATGG	forward primer to reamplify fragment 2 of p20298-AGE to construct p20298-15a and fix traY error
298-ACYC- T12R-nofix	TCCTGTTGTAGTACCAGTCCC	reverse primer to amplify fragment 12 of p20298 in as- sembly of p20298-15a-M to maintain traV and traY errors
298-ACYC-T2F- nofix	TTCAGCGCGTTAATGAGTACC	forward primer to amplify fragment 2 of p20298 in as- sembly of p20298-15a-M to maintain traV and traY errors
298-ACYC-T3F	CGCTGGAGATAATCAGCACA	forward primer to reamplify fragment 3 of p20298-AGE to construct p20298-15a
298_mpx_1F	CTCCGTCCTGTAACATAACCC	forward primer for multiplex PCR screening target 1 of p20298-15a assembly
298_mpx_1R	TGGTAATGAGCCACTCATCTG	reverse primer for multiplex PCR screening target 1 of p20298-15a assembly
298_mpx_2F	GACAGAGCCATCCAGATCG	forward primer for multiplex PCR screening target 2 of p20298-15a assembly

298_mpx_2R	TTTCCGGAACCTGTTTCGC	reverse primer for multiplex PCR screening target 2 of p20298-15a assembly
298_mpx_3F	GGCATATTGTCTGGTACCACC	forward primer for multiplex PCR screening target 3 of p20298-15a assembly
298_mpx_3R	AAATCAGGGCTGCCGTCAG	reverse primer for multiplex PCR screening target 3 of p20298-15a assembly
298_mpx_4F	TTATCGGTATCGAAGGCGTG	forward primer for multiplex PCR screening target 4 of p20298-15a assembly
298_mpx_4R	ATCTTAACCGTCTCGCTTACAG	reverse primer for multiplex PCR screening target 4 of p20298-15a assembly
298-ACYC-T2F	TTTGCATTGCAGGCCTATTTACCTG ACTACGTCATTTCTTCCTTGGTG- GTCGGGATGCT	forward primer to reamplify fragment 2 of p20298-AGE to construct p20298-15a
pProEx-298-oriT-rev	ACGGAGATAAGAAGAACATCATTTTGCC GATTTCCGGCC	reverse primer to amplify pProEx backbone with homology to 20298 oriT fragment
298-oriT-pProEx-fwd	GGCCGAAATCGGCAAATGATGTTC TTCTTATCTCCGTTC	forward primer to amplify 20298 oriT fragment with homology to pProEx backbone
pProEx-298-oriT-fwd	TCTGCACCATTTTATCCCGGCATCAAAT TAAGCAGAAGGCC	forward primer to amplify pProEx backbone with homology to 20298 oriT fragment

298-oriT-pproex-rev	GCCTTCTGCTTAATTTGATGCCGGG ATAAAATGGTGCAGA	reverse primer to amplify 20298 oriT fragment with homology to pProEx backbone
298-ACYC-T6F-v2	TTCTGGATTAGCTTTAAGCTCAG	replacement primer for 298-ACYC-T6F to allow for insertion of gateway destination cassette via yeast assembly
20298-p15a-dest-5R	ACTAGTAACATCGACTGATGGC	replacement primer for 298-ACYC-T5R to allow for insertion of gateway destination cassette via yeast assembly
pNuc-attB1-fwd	GGGGACAAGTTTGTACAAAAAAGCA GGCTCCTAATGTGCCTGTCAAATGGACG	forward primer to amplify arabinose inducible TevCas9 system with sgRNA cassette to build pENTR-TC9
pNuc-attB2-rev	GGGGACCACTTTGTACAAGAAAGCT GGGTCCAAAAAACCCTCAAGACCCG	reverse primer to amplify arabinose inducible TevCas9 system with sgRNA cassette to build pENTR-TC9
cr-sgrna-citg-top	CACGGTTTCCGCACATCTTGCAGCG	forward primer to clone Sp-Cas9 sgRNA targeting <i>C. rodentium</i> citG into pENTR-TC9 golden gate cassette
cr-sgrna-citg-bot	AAAACGCTGCAAGATGTGCGGAAAC	reverse primer to clone Sp-Cas9 sgRNA targeting <i>C. rodentium</i> citG into pENTR-TC9 golden gate cassette

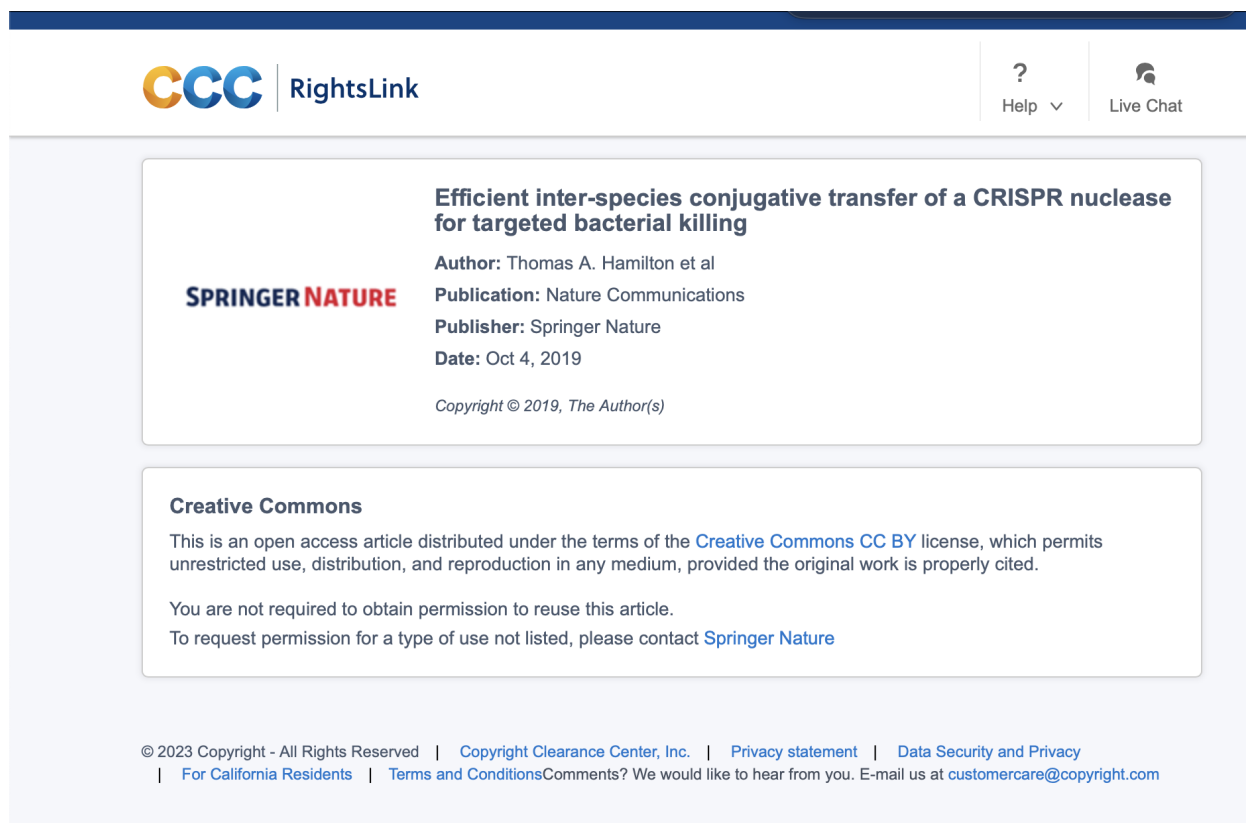
cr-sgrna-dppa-top	CACGTCCACCAGGCGGTTATAGATG	forward primer to clone Sp-Cas9 sgRNA targeting <i>C. rodentium</i> dppA into pENTR-TC9 golden gate cassette
cr-sgrna-dppa-bot	AAAACATCTATAACCGCCTGGTGGA	reverse primer to clone Sp-Cas9 sgRNA targeting <i>C. rodentium</i> dppA into pENTR-TC9 golden gate cassette
cr-sgrna-19070-top	CACGAAGCCCGGCAATATTGCAGCG	forward primer to clone Sp-Cas9 sgRNA targeting <i>C. rodentium</i> E2R62_19070 into pENTR-TC9 golden gate cassette
cr-sgrna-19070-bot	AAAACGCTGCAATATTGCCGGGCTT	reverse primer to clone Sp-Cas9 sgRNA targeting <i>C. rodentium</i> E2R62_19070 into pENTR-TC9 golden gate cassette
cr-sgrna-glga-top	CACGTTCGGTAATCTCCCGCGCATG	forward primer to clone Sp-Cas9 sgRNA targeting <i>C. rodentium</i> glgA into pENTR-TC9 golden gate cassette
cr-sgrna-glga-bot	AAAACATGCGCGGGAGATTACCGAA	reverse primer to clone Sp-Cas9 sgRNA targeting <i>C. rodentium</i> glgA into pENTR-TC9 golden gate cassette

cr-sgrna-eptb-top	CACGATTTTCATGCAAGCAAGCTCTG	forward primer to clone Sp-Cas9 sgRNA targeting <i>C. rodentium</i> eptB into pENTR-TC9 golden gate cassette
cr-sgrna-eptb-bot	AAAACAGAGCTTGCTTGCATGAAAT	reverse primer to clone Sp-Cas9 sgRNA targeting <i>C. rodentium</i> eptB into pENTR-TC9 golden gate cassette
cr-sgrna-18995-top	CACGGAAGCGCTGATCGAATTCGAG	forward primer to clone Sp-Cas9 sgRNA targeting <i>C. rodentium</i> E2R62_18995 into pENTR-TC9 golden gate cassette
cr-sgrna-18995-bot	AAAACCTCGAATTCGATCAGCGCTTC	reverse primer to clone Sp-Cas9 sgRNA targeting <i>C. rodentium</i> E2R62_18995 into pENTR-TC9 golden gate cassette
cr-sgrna-bcsg-top	CACGGTGGTGGTGACCGTATTTGTG	forward primer to clone Sp-Cas9 sgRNA targeting <i>C. rodentium</i> bcsG into pENTR-TC9 golden gate cassette
cr-sgrna-bcsg-bot	AAAACACAAATACGGTCACCACCAC	reverse primer to clone Sp-Cas9 sgRNA targeting <i>C. rodentium</i> bcsG into pENTR-TC9 golden gate cassette

cr-sgrna-glpG-top	CACGTGAGAAATGCATAAAGGCGTG	forward primer to clone Sp-Cas9 sgRNA targeting <i>C. rodentium</i> glpG into pENTR-TC9 golden gate cassette
cr-sgrna-glpG-bot	AAAACACGCCTTTATGCATTTCTCA	reverse primer to clone Sp-Cas9 sgRNA targeting <i>C. rodentium</i> glpG into pENTR-TC9 golden gate cassette

Appendix C

Copyright permission for Chapter 2 - no copyright permission required



The screenshot shows a web interface for RightsLink. At the top left is the CCC RightsLink logo. At the top right are links for Help and Live Chat. The main content area is divided into two sections. The first section, titled "Efficient inter-species conjugative transfer of a CRISPR nuclease for targeted bacterial killing", lists the author as Thomas A. Hamilton et al, the publication as Nature Communications, the publisher as Springer Nature, and the date as Oct 4, 2019. It also includes a copyright notice: "Copyright © 2019, The Author(s)". The second section, titled "Creative Commons", states that the article is distributed under a Creative Commons CC BY license, which permits unrestricted use, distribution, and reproduction in any medium, provided the original work is properly cited. It further notes that permission is not required to reuse the article and provides a link to Springer Nature for requests for permission for uses not listed.

CCC RightsLink

Help ▾ Live Chat

SPRINGER NATURE

Efficient inter-species conjugative transfer of a CRISPR nuclease for targeted bacterial killing

Author: Thomas A. Hamilton et al
Publication: Nature Communications
Publisher: Springer Nature
Date: Oct 4, 2019

Copyright © 2019, The Author(s)

Creative Commons

This is an open access article distributed under the terms of the [Creative Commons CC BY](#) license, which permits unrestricted use, distribution, and reproduction in any medium, provided the original work is properly cited.

You are not required to obtain permission to reuse this article.

To request permission for a type of use not listed, please contact [Springer Nature](#)

© 2023 Copyright - All Rights Reserved | [Copyright Clearance Center, Inc.](#) | [Privacy statement](#) | [Data Security and Privacy](#)
| [For California Residents](#) | [Terms and Conditions](#) Comments? We would like to hear from you. E-mail us at customer@copyright.com

Figure C.1: Proof of copyright permission not being required for chapter 2.

Thomas A. Hamilton

Education

PhD Candidate, Biochemistry, 2017-present
Western University, London, Ontario

Bachelor of Medical Science, Honors Specialization in Biochemistry and Cell Biology, 2013-2017
Western University, London, Ontario

Publications

Thomas A Hamilton, Benjamin R Joris, Arina Shrestha, Tyler S Browne, Emma Allen-Vercoe, Sébastien Rodrigue, Bogumil J Karas, Gregory B Gloor, and David R Edgell. Functionalizing uncharacterized conjugative systems from metagenomic data for targeted delivery of a CRISPR nuclease. (In Preparation), 2023.

Thomas A Hamilton, Gregory M Pellegrino, Jasmine A Therrien, Dalton T Ham, Peter C Bartlett, Bogumil J Karas, Gregory B Gloor, and David R Edgell. Efficient inter-species conjugative transfer of a CRISPR nuclease for targeted bacterial killing. *Nature Communications*, 10:4544, 2019.

Jason M Wolfs, **Thomas A Hamilton**, Jeremy T Lant, Marcon Laforet, Jenny Zhang, Louisa M Salemi, Gregory B Gloor, Caroline Schild-Poulter, and David R Edgell. Biasing genome-editing events toward precise length deletions with an RNA-guided TevCas9 dual nuclease. *Proceedings of the National Academy of Sciences*, 113(52):14988–14993, 2016.

Posters and Presentations

De novo construction of bacterial conjugative systems identified from metagenomic datasets as platforms for synthetic biology. Synthetic Biology: Engineering Evolution, and Design (SEED) Conference, Arlington, Virginia. 2022 (poster)

Efficient inter-species conjugative transfer of a CRISPR nuclease for targeted bacterial elimination. Annual Conference of the Canadian Society of Microbiology, Sherbrooke, Quebec. 2019 (poster)

Efficient inter-species conjugative transfer of a CRISPR nuclease for targeted bacterial elimination. Synthetic Biology Symposium Conference, Waterloo, Ontario. 2019 (poster)

Bacterial sex and death: what it can do for your microbes. Maud L Menton Memorial Symposium, London, Ontario. 2019 (oral presentation)

A CRISPR-based system to modulate microbial populations. Synthetic Biology Symposium, London, Ontario. 2018 (poster)

Awards and Honors

Award	Value	Level	Location of Tenure	Period Held
Canadian Graduate Scholarship - Doctoral (CGS D)	\$35,000	National	Western University	2021/05-2022/04
NSERC Postgraduate Scholarship - Doctoral (PGS D)	\$42,000	National	Western University	2019/05-2021/04
Ontario Graduate Scholarship	\$15,000	Provincial	Western University	declined
Ontario Graduate Scholarship	\$15,000	Provincial	Western University	2018/05-2019/04
Graduate Biochemistry Program Entrance Scholarship	\$10,000	Institutional	Western University	2017/09-2018/08
Rossiter Award	\$100 (book prize)	Institutional	Western University	2017/06
Dean's Honor List	-	Institutional	Western University	2013/09-2017/05

Teaching Experience

Teaching Assistantships

Biochemistry 4410A, Western University 2017
 Biochemistry 4410A, Western University 2018
 Biochemistry 4410A, Western University 2019
